

# Final Report

DSE Spring 2017

## Velo-E-Raptor

Group 08

M.C. Dhondt	4274318
J.W. van Gelder	4229215
F.R. Scholtens	4359224
G.J.H.A. Verkerk	4303172
P. Volkov	4160762
R.R. Vossebeld	4277287
J.A. Vreeken	4268547
J. Weigand	4295811
E. de Winkel	4284003
R.K. van der Zwaard	4290690





# Final Report

DSE Spring 2017

Velo-E-Raptor

by

Group 08

**Project duration:** April 24, 2017 – July 6, 2017  
**Tutor:** Ir. J. A. Melkert  
**Coaches:** Ir. M. Coppola  
Ir. T. J Berdowski

**Date:** 04/07/2017  
**Version:** 2  
**Quality Assurance:** Mariska Dhondt, Rogier Vosseveld



# Preface

This report is the work of ten enthusiastic students, currently finishing up the Bachelor's degree programme in Aerospace Engineering at Delft University of Technology. The goal of this report is to give the reader an overview of the steps that were taken to make a detailed design of one final concept of the Design Synthesis Exercise project 8: The Velo-E-Raptor.

We would like to express our gratitude to our project coordinators, Ir. Joris Melkert and Ir. Ronald van Gent, as well as our project coaches, Ir. M. Coppola, Ir. T.J. Berdowski, Ir. W. Hu, Ir. J. van Kuijk, the teaching assistants, the DSE committee and the supporting system engineering staff, for their expertise and advice.

*Group 08*  
*Delft, June 2017*



# Contents

<b>Summary and Final Design Overview</b>	<b>ix</b>
<b>List of Abbreviations</b>	<b>xv</b>
<b>List of Symbols</b>	<b>xvii</b>
<b>1 Introduction</b>	<b>1</b>
<b>2 Detailed Design Approach</b>	<b>3</b>
2.1 Design Choices . . . . .	3
2.2 Sensitivity Analysis . . . . .	3
2.3 Iteration . . . . .	3
<b>3 Design Choices</b>	<b>5</b>
3.1 Propeller Location . . . . .	5
3.2 Pilot Position . . . . .	8
3.3 Tail Configuration . . . . .	9
3.4 Control System . . . . .	10
3.5 Landing Gear . . . . .	11
3.6 Flaps . . . . .	12
<b>4 Aerodynamics</b>	<b>13</b>
4.1 Literature Study . . . . .	13
4.1.1 Flow Interference . . . . .	13
4.1.2 Airfoil Parameters . . . . .	14
4.1.3 Maximum Lift and Stalling . . . . .	15
4.1.4 Winglets . . . . .	15
4.2 Approach . . . . .	16
4.2.1 Zero-Lift Drag Coefficient . . . . .	16
4.2.2 XFOIL 6.9 . . . . .	17
4.2.3 XFLR5 v6.38 & Athena Vortex Lattice 3.36 . . . . .	17
4.3 Results . . . . .	18
4.3.1 Airfoil Selection . . . . .	18
4.3.2 Wing Parameters . . . . .	19
4.3.3 Wing Twist and Winglet . . . . .	20
4.3.4 Zero-Lift Drag Coefficient . . . . .	20
4.3.5 Aerodynamic Forces & Coefficients . . . . .	21
4.4 Verification and Validation . . . . .	22
4.4.1 Zero-Lift Drag Coefficient . . . . .	22
4.4.2 Software . . . . .	23

4.5	Conclusion . . . . .	24
4.6	Project Design and Development Logic . . . . .	25
4.6.1	Computational Fluid Dynamics . . . . .	25
4.6.2	Aerodynamic Optimization . . . . .	25
4.6.3	Other Aerodynamic Effects . . . . .	26
<b>5</b>	<b>Performance and Power</b>	<b>31</b>
5.1	Approach . . . . .	31
5.1.1	Propeller . . . . .	31
5.1.2	Power System . . . . .	34
5.1.3	Performance . . . . .	35
5.2	Results. . . . .	36
5.2.1	Propeller . . . . .	36
5.2.2	Power system . . . . .	39
5.2.3	Performance . . . . .	41
5.3	Power Allocation and Electrical Block Diagram . . . . .	43
5.4	Verification and Validation. . . . .	45
5.4.1	Verification. . . . .	45
5.4.2	Validation. . . . .	45
5.5	Conclusion . . . . .	47
5.6	Project Development and Design Logic . . . . .	47
<b>6</b>	<b>Stability</b>	<b>49</b>
6.1	Approach . . . . .	49
6.1.1	Program Selection . . . . .	49
6.1.2	Modelling the Aircraft . . . . .	50
6.1.3	Stability Analysis . . . . .	50
6.1.4	Control Surfaces. . . . .	51
6.1.5	Stability and Control Derivatives. . . . .	52
6.2	Results. . . . .	52
6.3	Verification and Validation. . . . .	54
6.4	Conclusion . . . . .	56
6.5	Project Design and Development Logic . . . . .	56
6.5.1	Wind Tunnel Testing . . . . .	56
6.5.2	Control Surfaces. . . . .	56
<b>7</b>	<b>Control System</b>	<b>57</b>
7.1	Pilot Control Mechanism. . . . .	57
7.2	Sensors . . . . .	58
7.3	Control System. . . . .	59
7.3.1	Literature Study . . . . .	59
7.3.2	Approach . . . . .	59
7.3.3	Flight Computer. . . . .	60
7.3.4	Results . . . . .	61
7.3.5	Verification and Validation . . . . .	62
7.3.6	Flight Envelope Protection . . . . .	62
7.3.7	Flight Modes . . . . .	63

7.3.8	Conclusion . . . . .	63
7.4	Failure Modes . . . . .	64
7.5	Hardware . . . . .	65
7.6	Project Design and Development Logic . . . . .	66
<b>8</b>	<b>Structures</b>	<b>67</b>
8.1	Approach . . . . .	67
8.2	Assumptions . . . . .	71
8.3	Material Selection . . . . .	71
8.3.1	Frame . . . . .	71
8.3.2	Sail. . . . .	71
8.4	Results. . . . .	72
8.4.1	Wing Analysis . . . . .	72
8.4.2	Tail Analysis . . . . .	74
8.4.3	Landing Gear Analysis . . . . .	74
8.4.4	Mass Estimation. . . . .	75
8.5	Verification and Validation. . . . .	76
8.5.1	Verification. . . . .	76
8.5.2	Validation. . . . .	77
8.6	Production . . . . .	78
8.6.1	Part Manufacturing. . . . .	78
8.6.2	Assembly . . . . .	79
8.7	Conclusion . . . . .	81
8.8	Project Design and Development Logic . . . . .	81
<b>9</b>	<b>Operations</b>	<b>83</b>
9.1	Lay-out . . . . .	83
9.1.1	Pilot Attachment to Aircraft . . . . .	83
9.1.2	Body Support . . . . .	83
9.1.3	Helmet . . . . .	85
9.1.4	Control . . . . .	85
9.1.5	Flight Instrumentation. . . . .	85
9.1.6	Pedal System. . . . .	87
9.1.7	Safety Equipment. . . . .	87
9.2	Flight Procedures . . . . .	88
9.2.1	Pilot Training . . . . .	88
9.2.2	Takeoff . . . . .	88
9.3	Conclusion . . . . .	88
9.4	Project Design and Development Logic . . . . .	89
<b>10</b>	<b>Sustainability</b>	<b>91</b>
10.1	Design . . . . .	91
10.2	Production . . . . .	91
10.3	Lifetime . . . . .	92
10.4	End-of-Life . . . . .	93
10.5	Conclusion . . . . .	94

<b>11 Sensitivity Analysis</b>	<b>95</b>
11.1 Weight . . . . .	95
11.2 Stability . . . . .	95
<b>12 Market Analysis</b>	<b>97</b>
12.1 Stakeholder Analysis . . . . .	97
12.2 Customer Segment . . . . .	98
12.3 Market Size and Product Cost . . . . .	99
12.4 Customer Needs . . . . .	101
12.5 Target Consumer Cost . . . . .	101
12.6 SWOT analysis . . . . .	102
<b>13 RAMS</b>	<b>103</b>
13.1 Reliability . . . . .	103
13.1.1 FMECA . . . . .	103
13.1.2 Compensating Provisions . . . . .	104
13.2 Availability . . . . .	105
13.3 Maintainability . . . . .	106
13.3.1 Maintainability of the Design . . . . .	106
13.3.2 Maintenance Plan . . . . .	108
13.4 Safety . . . . .	109
13.4.1 Functional Hazards . . . . .	109
13.4.2 Additional Hazards . . . . .	111
<b>14 Cost estimation</b>	<b>113</b>
14.1 Material and Component Cost . . . . .	113
14.2 Labor Cost . . . . .	115
14.3 Total Cost . . . . .	117
<b>15 Technical Risk Assessment</b>	<b>119</b>
15.1 General Analysis Procedure . . . . .	119
15.2 Risk Management Methods . . . . .	119
<b>16 Compliance Matrix</b>	<b>123</b>
<b>17 Conclusion and Recommendations</b>	<b>131</b>
<b>Bibliography</b>	<b>133</b>
<b>A</b>	<b>137</b>
<b>Appendix A: Project Design and Development Logic</b>	<b>137</b>
<b>Appendix B: Failure Mode Effect &amp; Criticality Analysis</b>	<b>141</b>
<b>Appendix C: Work Division</b>	<b>142</b>

# Summary and Final Design Overview

The Velo-E-Raptor Design Synthesis Exercise project has the following mission: "Design an electrically assisted, human powered and sustainable method of flight that is accessible and safe for entertainment and sports usage". After the "Bird" concept was chosen in the midterm-report, detailed design of this concept was performed [41].

First, all resulting design choices are explained to determine the final configuration of the aircraft. For every choice, a trade-off was done where all departments investigated the consequences of certain options. The decision was made to position the pilot on top of the wing, with the cycling system below the wing. A fly-by-wire control system is chosen to control the aircraft. Two propellers will be used which are located on the leading edge for propulsion. After the final configuration was decided upon, every technical department ran a separate analysis of this concept.

For the aerodynamic analysis, studies were performed to model all sources of drag on the Velo-E-Raptor configuration. Furthermore, XFLR5 and AVL were used to model the planform, which produced results of aerodynamic performance that can serve as inputs for other departments. The planform has been optimized to meet the needs of other departments.

In the performance and power department, a custom design was made for a propeller that produces as little noise as possible. Even when designing for noise, the propulsion system still has enough power and battery capacity to perform all necessary manoeuvres, while staying lightweight. Furthermore, the performance parameters were calculated. The requirements for glide ratio and maximum speed are not met by a margin of 1.5, but the design team and customer are still satisfied with the performance.

The goal for stability and control analysis was to design an aircraft that is stable and controllable in all flight conditions. The aircraft is statically stable by a sufficient margin. Despite a very minor, negligible instability in spiral, all dynamic modes are stable and safe for flight. The aircraft's attitude is controlled electronically by the use of a flight computer, the software can be extended to implement a flight envelope protection and different flight modes. The aircraft is controllable with a two-axis control system, where a rudder is also present which acts automatically to counteract disturbances.

For the structural analysis, a computational model was created consisting of stress analysis calculations of all structural components. After optimization of the wing structure, all loading and weight requirements were satisfied while staying lightweight. In addition, a production plan was set up for the manufacturing of all different parts as well as an assembly plan.

From an operational perspective, the Velo-E-Raptor distinguishes itself from current (hang) gliders in attractiveness, ease of use, comfort and most of all safety. The "cool" user experi-

ence is achieved by the prone pilot position and intuitive control bar, while still being comfortable. The Head-Up-Display allows for better monitoring of the flight conditions and is the main contribution to the ease of use of the Velo-E-Raptor. Most importantly, many measures have been taken to ensure the safety of the pilot and the aircraft, resulting in a fail-safe system during prescribed operations.

Besides technical analysis, a market analysis was performed. Potential stakeholders and customers were identified and their needs were investigated and taken into account to make a business model. The target cost of €83,300 has been estimated, which is the retail price at which the Velo-E-Raptor would be a profitable product.

Furthermore, sustainability plays an important role in the Velo-E-Raptor design. An electric propulsion system is used to provide thrust without emissions. Due to the proposed circular economy model, production of the aircraft will be done in an ecological way. All in all, 78 mass percentage of the materials used can be recycled. Compared to current (hang) gliders on the market, the Velo-E-Raptor is a sustainable product that is prepared for the future.

Finally the reliability, availability, maintainability and safety (RAMS) of the system have been investigated. The reliability of the system has been determined by performing a failure modes, effects and criticality analysis. For both availability and maintainability, extensive operation and maintenance plans have been developed to guarantee operations of the Velo-E-Raptor can always run as smoothly as possible and in the correct way. To ensure the safety of the pilot, a hazard analysis has been performed to specify the risks the pilot will be exposed to. From the RAMS analysis the risks of Velo-E-Raptor operations could be assessed and mitigated.

After all models were developed, the design could be iterated between different departments. The result is a design that meets all important safety, stability, sustainability and customer requirements, while maintaining a low weight. To reach this result several regulatory, performance and operations requirements are left unsatisfied as a compromise.

To finish the report, the project design and development logic have been worked out. Here, it is indicated what actions are required to make the Velo-E-Raptor a success after this report. By identifying all necessary actions that have to be taken until the aircraft is produced, the costs have been estimated to be €193,000. While the initial cost is still higher than the target cost, a large part consists of labour costs of future development. A profitable business model can be established in the long term when the Velo-E-Raptor design is finalized. Then, it can be produced on a bigger scale and costs are reduced significantly. In the next phases of the design, it should be further investigated how the product can be made profitable.

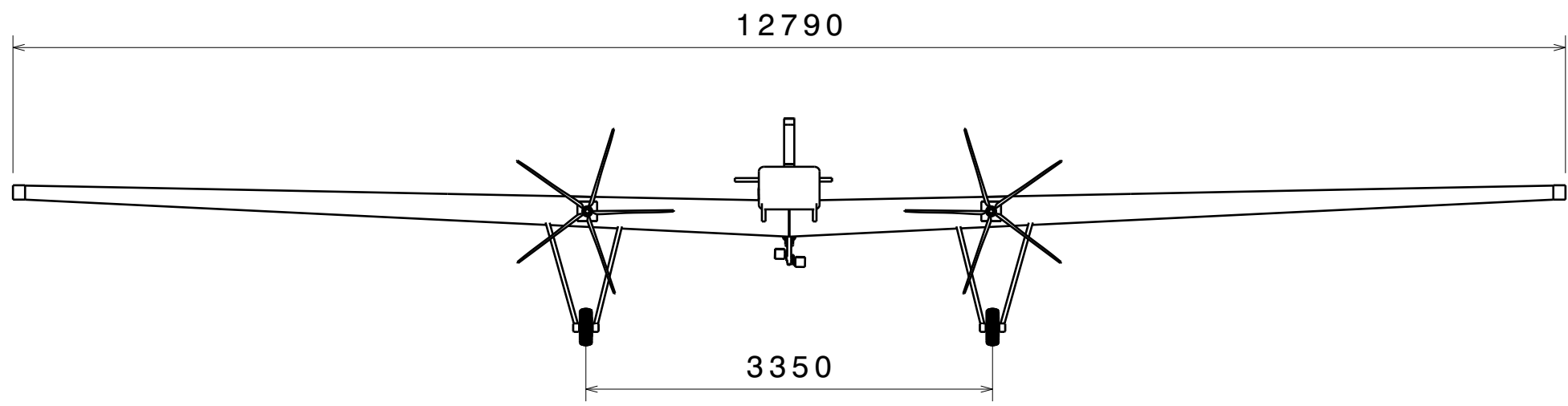
A number of recommendations can be made with respect to the design. Difficulties that arose in the design process were for a large part due to the pilot integration in the wing, which complicated the analysis process for aerodynamics as well as stability and control. Access to a wind tunnel to perform tests on interference and stability is therefore advisable, which can also be used to determine deformation, noise and flutter characteristics that were not yet quantified. Furthermore, additional design optimization to reduce weight, increase

the gliding ratio and decrease noise is advised. Moreover, an autopilot should be designed to increase safety even further.

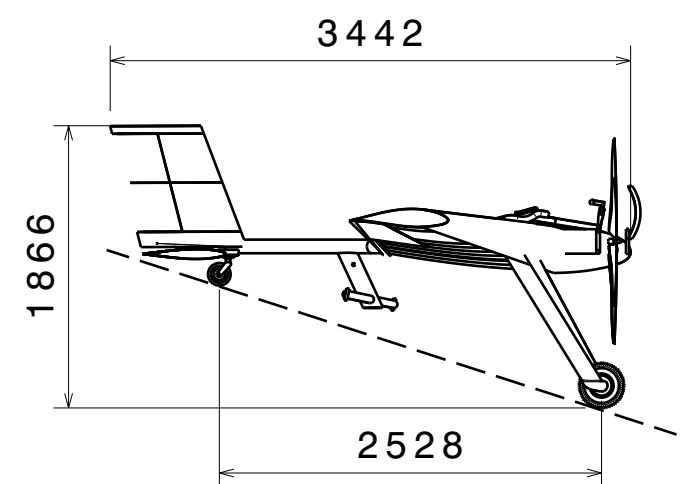
To provide an overview of the final design, in table 1 the main parameters of the final configuration are given for a pilot with a weight of 85 kg. To give a visual impression of the final configuration, a CATIA render and technical drawing of the final configuration are shown in figure on the next page. In figure 1, the hardware diagram is shown. The functional flow and functional breakdown of the Velo-E-Raptor operations have remained the same, and can be found in the baseline report [40, ch.1].

Table 1: The main parameters of the Velo-E-Raptor final configuration

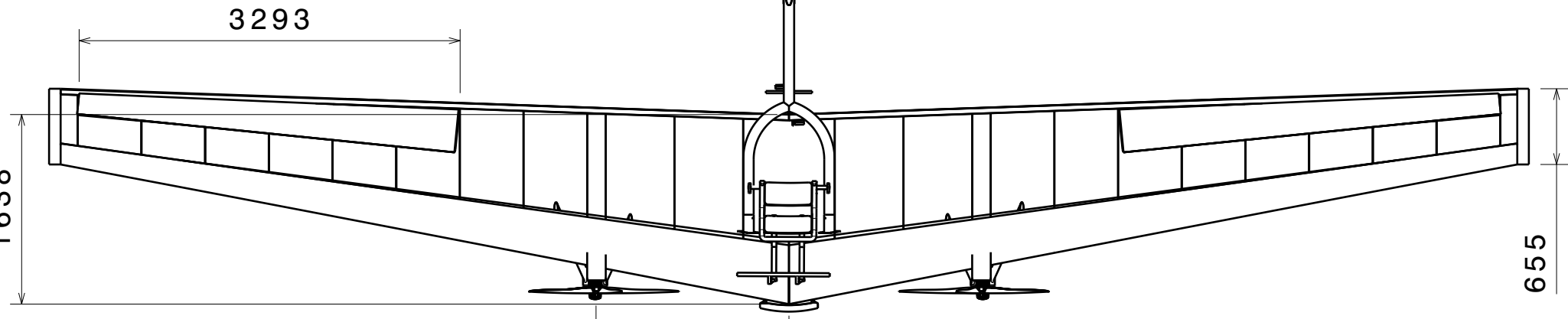
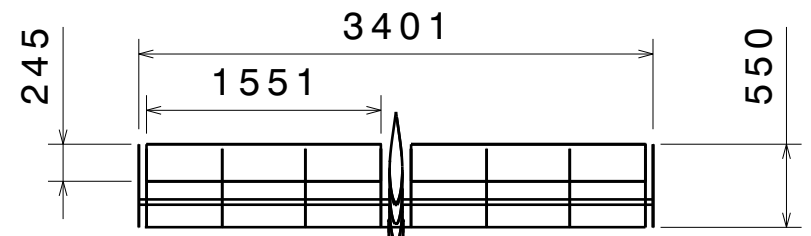
	Value	Unit
Empty weight	65.1	kg
Maximum takeoff weight	150.1	kg
Maximum gliding ratio	13.5	–
Stall speed	24.4	kts
Cruise speed	40.0	kts
Maximum speed	63.3	kts
Cruise lift coefficient	0.4	–
Maximum lift coefficient	1.1	–
Wing surface	13.9	m <sup>2</sup>
Wingspan	12.4	m
Aspect ratio	11.0	–
Taper ratio	0.4	–
Quarter-chord sweep	8.9	deg
Wingtip washout	4.0	deg
Dihedral	1.0	deg
Continuous power available	11.8	kW
Tail distance	2.1	m
Horizontal tail surface	1.9	m <sup>2</sup>
Vertical tail surface	0.5	m <sup>2</sup>



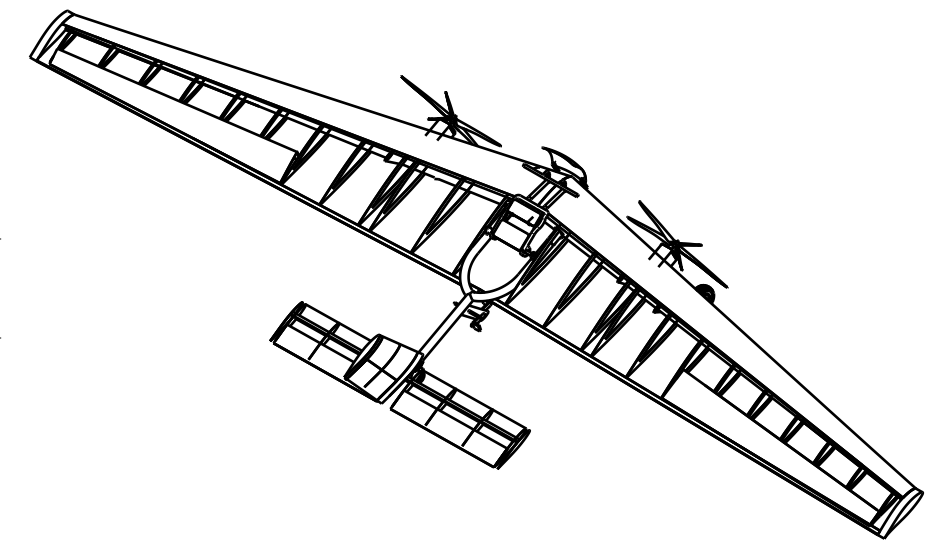
Front view  
Scale: 1:50



Side view  
Scale: 1:50



Top view  
Scale: 1:50



Isometric view  
Scale: 1:80

This drawing is our property. It can't be reproduced or communicated without our written agreement.		<b>Velo-E-Raptor</b>			
DRAWN BY <b>J. Weigand</b>		DATE 04/07/2017		DRAWING TITLE <b>Main sizing parameters</b>	
CHECKED BY <b>M.C. Dhondt</b>		DATE 04/07/2017			
DESIGNED BY <b>DSE group-08</b>		DATE 04/07/2017		SIZE <b>A3</b>	DRAWING NUMBER <b>1</b>
		SCALE <b>1:50</b>	WEIGHT (kg) <b>65.1</b>	SHEET <b>1/1</b>	REV <b>2</b>

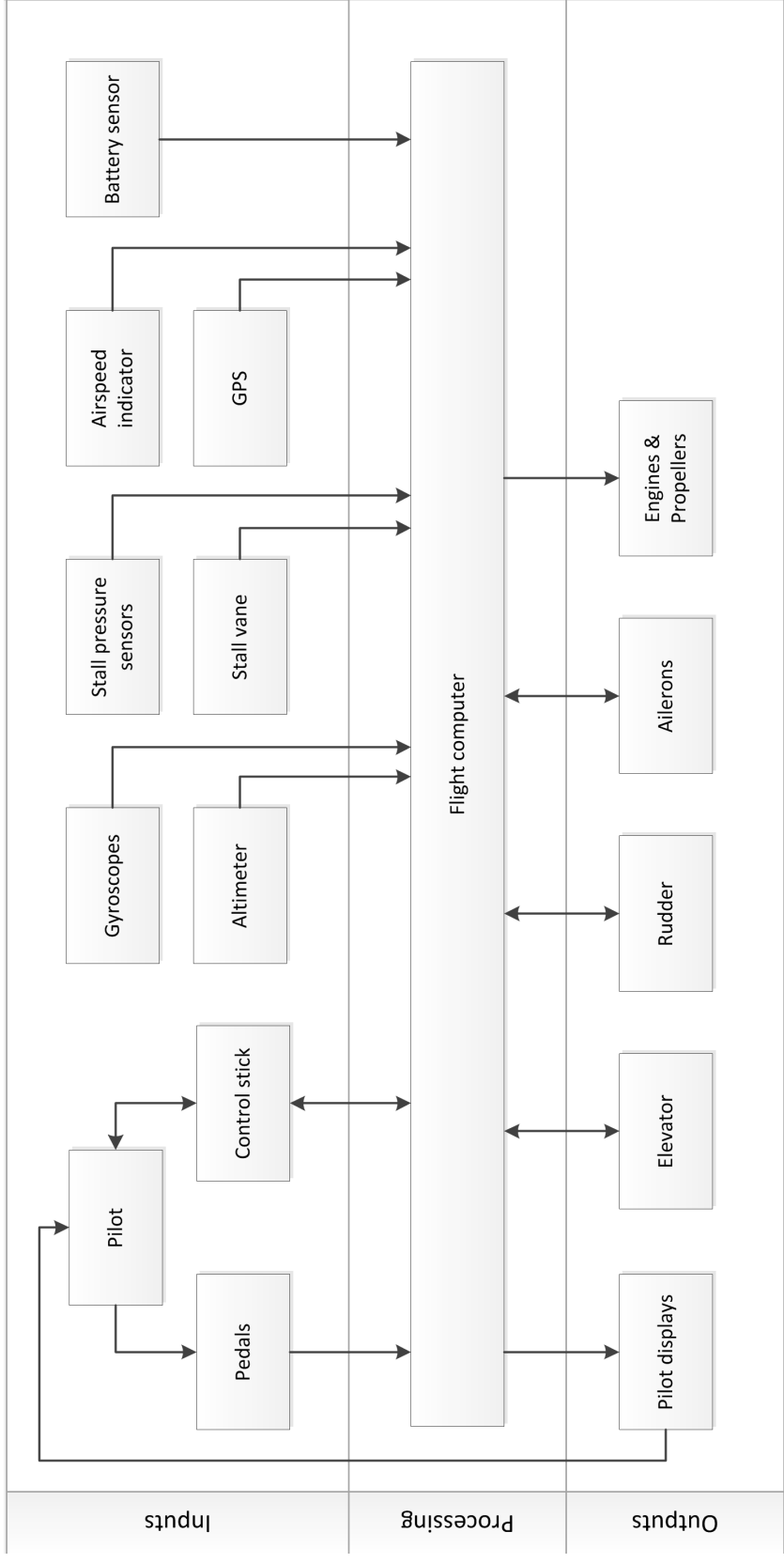


Figure 1: Hardware Diagram



# List of Abbreviations

Abbreviation	Description
A.o.A.	Angle of Attack
AVL	Athena Vortex Lattice
BC	Battery capacity
BEM	Blade Element Momentum Theory
CFRP	Carbon Fiber Reinforced Polymer
CFD	Computational Fluid Dynamics
c.g.	Center of Gravity
DEP	Distributed Electrical Propulsion
DOT	Design Option Tree
DSE	Design Synthesis Exercise
EPRIB	Emergency Position Radio Indicator Beacon
EPS	Expanded Polystyrene
FBW	Fly By Wire
FFD	Functional Flow Diagram
FLPHG	Foot Launched Powered Hang Glider
GUI	Graphical user interface
HG	Hang Glider
HUD	Head-Up-Display
LCO	Lithium cobalt oxide
LFP	Lithium iron phosphate
LLM	Lifting Line Theory
LRI	Lift Reserve Indicator
LTO	Lithium titanate
MTOW	Maximum takeoff weight
MTWLW	Maximum takeoff weight less wing
NACA	National Advisory Committee for Aeronautics
RAMS	Reliability, Availability, Maintainability and Safety
RDT	Requirements Discovery Tree
RDT&E	Research Development Test & Evaluation
RPM	Revolutions per minute
S&C	Stability and Control
S.M.	Stability margin
SP	Sailplane
UA	Unconventional Aircraft
VER	Velo-E-Raptor
VLM	Vortex Lattice Method
V&V	Verification and Validation
WBS	Work Breakdown Structure
WFD	Work Flow Diagram



# List of Symbols

Symbol	Unit	Description
$A$	–	Aspect ratio
$A$	$m^2$	Propeller disk area
$A_i$	$m^2$	Drag area
$a$	–	Actual induction factor
$B$	–	Number of propeller blades
$b$	$m$	Wing span
$c$	$m$	Chord
$C_D$	–	Drag coefficient
$C_{D_0}$	–	Zero lift drag coefficient
$C_L$	–	Lift coefficient
$C_{l_\beta}$	–	Lateral stability derivative
$C_m$	–	Moment coefficient
$C_{m_{ac}}$	–	Moment coefficient about aerodynamic center
$C_{m_\alpha}$	–	$C_m$ -alpha slope
$C_{n_p}$	–	Lateral stability derivative
$C_{n_\beta}$	–	Lateral stability derivative
$C_T$	–	Thrust coefficient
$D$	$N$	Drag
$E$	$Pa$	Young's modulus
$e$	–	Oswald factor
$J$	–	Advance ratio
$L$	$N$	Lift
$l$	$m$	Length
$l_h$	$m$	tail arm
$m$	$kg$	Mass
$P$	$W$	Power
$P_a$	$W$	Power available
$P_r$	$W$	Power required
$RC$	$m/s$	Rate of Climb
$Re$	–	Reynolds number
$S$	$m^2$	Area
$T$	$N$	Thrust
$t$	$m$	Thickness
$V_{cruise}$	$m/s$	Cruise speed
$V_{max}$	$m/s$	Maximum speed
$V_s$	$m/s$	Stall speed
$W/P$	$N/w$	Power loading
$W/S$	$N/m^2$	Wing loading
$W$	$N$	Weight
$\alpha$	$deg$	Angle of attack
$\beta$	$deg$	Angle of sideslip
$\rho$	$kg/m^3$	Density



# Introduction

Electrical amplification of human power is a technology that is evolving rapidly. Amplifying human power opens up a range of opportunities for electrically powered vehicles. Implementing such a power system into an aircraft has not been examined yet. This gave birth to the idea to design an electrically assisted human powered aircraft.

To be able to be used as a new form of air sports the aircraft shall attract a wide variety of people. Since it has always been a dream of mankind to fly like a bird, this was chosen as a starting point for the design of the Velo-E-Raptor. Combining this with the electric amplification of human power this led to the following mission: "design an electrically assisted, human powered and sustainable method of flight that is accessible and safe for entertainment and sports usage".

The purpose of the Velo-E-Raptor Design Synthesis Exercise is to design an aircraft that fulfills this mission. To do this, the mission statement was translated into a set of requirements [40]. During the baseline and midterm phase different conceptual designs have been examined. Trade-offs have been performed to compare the different concepts resulting in one conceptual design, referred to as the "Bird" concept.

The purpose of this report is to provide a detailed analysis of the final design. The detailed analysis is performed by five technical departments: Aerodynamics, Performance and Power, Stability and Control, Structures and Operations. In an iterative process the design is finalized, after which the reliability, availability, maintainability and safety (RAMS) analysis is done. Also a cost estimation is performed to be able to check the requirements on cost.

First, in chapter 2 the approach taken for the detailed design phase is further elaborated on. Several design choices on the final configuration are explained in chapter 3. Next, in chapters 4 to 9 the technical analysis per department can be found. Sustainability of the Velo-E-Raptor is discussed in chapter 10. Next, the sensitivity of the design for a change in system parameters is discussed in chapter 11. The sensitivity analysis is followed by a market analysis in chapter 12 and RAMS analysis in chapter 13. The target cost set in the market analysis is compared to the total cost of the Velo-E-Raptor in chapter 14. Lastly, the risks of this project are analyzed and discussed in chapter 15. To conclude, requirement compliance is treated in chapter 16, discussed in chapter 17. A further note to the readers with respect to the footnotes is that these have been consulted within the timeframe: April 24, 2017 - July 4, 2017.



# 2

## Detailed Design Approach

As explained in the midterm report [41, ch.11], the group decided to approach the detailed design differently than before, both in project organization and system engineering. In this chapter, the approach to the detailed design process will be briefly explained to define the structure of the remainder of the report.

### 2.1. Design Choices

When moving from conceptual to detailed design of the current Velo-E-Raptor concept, there were still choices to be made about the configuration. In order to eliminate uncertainties, several design choices were introduced early in the final design process. For every choice, the consequences of multiple options were investigated by every relevant department, and a trade-off was done. The process and result of every trade-off can be found in chapter 3.

### 2.2. Sensitivity Analysis

When all departments chose a method for computing certain outputs, a sensitivity analysis could be performed. The sensitivity analysis was performed on all methods used, to test how sensitive the outputs were to certain inputs, and obtain knowledge of how parameters interact with each other. From this, the feasibility and certain risks could be obtained.

The sensitivity analysis was performed in the following steps. First, the most critical inputs and outputs for every model were obtained. Secondly, the inputs were varied separately, and the change in outputs were determined. Finally, for every output it was determined when the design becomes unfeasible. From the combination of these steps, the sensitivity of the Velo-E-Raptor design to certain inputs were determined and the risks that the design would become unfeasible was assessed. The results are described in chapter 11.

### 2.3. Iteration

Due to the nature of aircraft design, many parameters are relevant for multiple departments. Therefore, after all technical departments finished their analysis, iterations needed to take place.

To assess what inputs and outputs are exchanged between departments, an  $N^2$  chart was made with parameters. The  $N^2$  chart can be found in table 2.1. Here, the outputs can be

found on the horizontal line and the inputs on the vertical line. With this tool, every department could determine what outputs were expected from them, and a planning was made for the iterations. The operations and sustainability departments were not included, as they did not have any computational models that required iterating after different inputs were given. Instead they provided inputs for the departments that did not require frequent iterating.

This  $N^2$  chart indicates the parameters that were iterated initially. Other inputs were set to be constant during iterations. When a feasible design could not be found after finishing the iteration, other solutions had to be found by varying the inputs that were chosen to be constant at first.

Table 2.1: Parameter iteration  $N^2$  chart

Aerodynamics	Zero-lift drag coefficient Maximum lift coefficient	Airfoils	Lift distribution Drag distribution Moment distribution Airfoils
Wing area Propeller dimensions	Power and Performance	Wing area Power system weight & balance Cruise lift coefficient	Wing area
Trim angle of attack Tail dimensions		Stability & Control	Sweep Tail dimensions Tail length
Landing gear dimensions	Weight	Structure weight & balance	Structures & Materials

# 3

## Design Choices

During the trade-off in the midterm report, the Velo-E-Raptor was a concept with very few details known about the detailed configuration. In figure 3.1 can be seen what the aircraft looked like at that point in time. For detailed analysis, several decisions had to be made about the specific subsystems that were not yet touched during the midterm. This chapter aims to describe the decisions made by the design team.

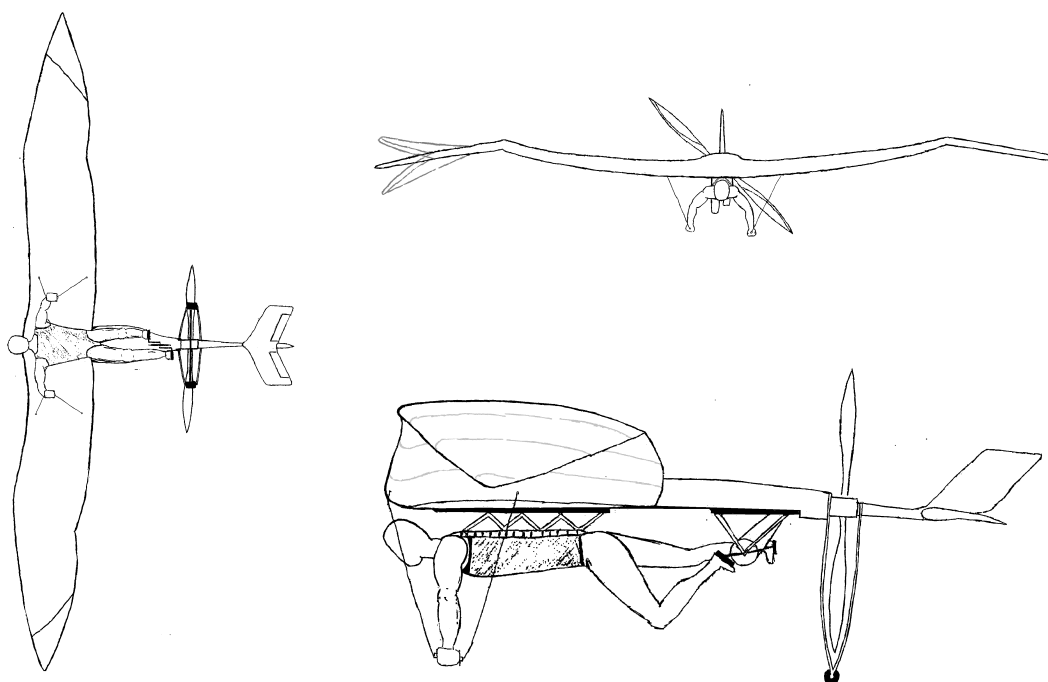


Figure 3.1: The Velo-E-Raptor configuration at the start of the detailed design phase [41]

### 3.1. Propeller Location

An important design choice is the propeller configuration. There are four possible locations for the propeller and depending on the location it is decided to have one or more, but an even amount of, propellers. The different configurations can be seen in figure 3.2. The first configuration has only one propeller which is located in front of the tail surfaces. The second configuration has two or more propellers which are located on the leading edge of

both wings. The third configuration has one propeller which is located above the wing. The fourth configuration has two or more propellers which are located on the trailing edge of both wings.

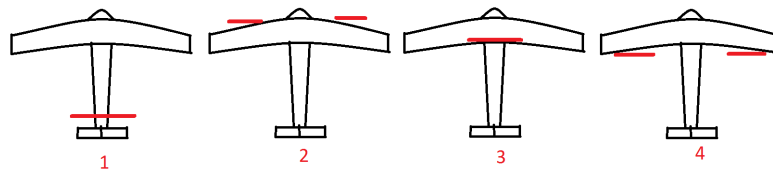


Figure 3.2: Different propeller configurations

A trade-off is performed for the different configurations. The result of the trade-off can be seen in table 3.1. There are seven aspects on which the different design choices are judged. These aspects are: propeller efficiency, propeller weight, noise, aerodynamics, structural weight, center of gravity location and stability and control. Each aspect is judged as negative (-), neutral (0) or positive (+). These scores are shown in the trade-off matrix as red, blue or green respectively.

Table 3.1: Trade-off table for different propeller configurations

	Configuration 1	Configuration 2	Configuration 3	Configuration 4
Propeller efficiency	-	+	0	0
	Higher disc loading In turbulent flow	Low disc loading In free flow	Higher disc loading In free flow	Low disc loading In turbulent flow
Propeller weight	0	-	0	-
	Single propeller	Two propellers	Single propeller	Two propellers
Noise	-	+	-	0
	High disc loading	Low disc loading	High disc loading	Low disc loading
	High tip speed	Low tip speed	High tip speed	Low tip speed
	In turbulent flow	In free flow	In free flow	In turbulent flow
Aerodynamics	0	+	0	0
	No upwash benefits	Upwash benefits	No upwash benefits	No upwash benefits
Structural weight	-	0	0	-
	Protective structure	Protective structure	No protective structure	Protective structure
	Complex structure	No support structure	Support structure	Support structure
Center of gravity	-	0	0	0
	C.G. more aft	C.G. close to pilot	C.G. close to pilot	C.G. close to pilot
Stability and control	-	0	-	0
	C.G. more aft	C.G. in front	C.G. in the middle	C.G. in the middle
	Rotational flow on tail	No rotational flow on tail	No rotational flow on tail	No rotational flow on tail
	No a-symmetrical thrust	A-symmetrical thrust	No a-symmetrical thrust	A-symmetrical thrust
	No pitch moment	No pitch moment	Pitch moment	No pitch moment

### Propeller Efficiency

To increase the propeller efficiency the disc loading of the propeller should be decreased. Because the radius of the propeller is a limiting factor, it is more convenient to use more propellers in order to decrease the disc loading. Another way to achieve a higher efficiency is to place the propeller in the free stream airflow instead of a turbulent airflow. A turbulent airflow will interfere with the flow around the propeller's airfoil decreasing its efficiency.

### Propeller Weight

Using more than one propeller will be heavier than using a single propeller. Even though

the propellers can be smaller when using more propellers, more propellers result in a higher weight.

### **Noise**

In order to reduce noise levels produced by the propeller the disc loading and tip speed should to decreased. Therefore, using more propellers is more convenient than using one propeller. Another method to decrease noise levels is to place the propeller in a free airflow rather than a turbulent airflow because the interference between the propeller blades and the turbulent airflow will cause a significant amount of noise.

### **Aerodynamics**

Propellers cause upwash and downwash on each side due to the blades rotating up or down with respect to the wing. Having one propeller only, these effects occur on opposite sides of vertical plane of the aircraft, resulting in an asymmetric lift distribution. Having more than one propeller rotating in opposite direction will result in a symmetric lift distribution. When both are rotating inboard up at the leading edge of the wing, the root of the wing will feel upwash which is beneficial for lift generation. When placing the propellers behind another object, wing or pilot, its wake will interfere with the propeller intake, reducing its efficiency [52].

### **Structural Weight**

When the propeller is on the end of the tail or on the wings (especially when placed on the wingtips) a structure is needed to protect it from hitting the ground. This protective structure adds weight. Having a propeller on top of the aircraft or on the trailing edge of the wing will require a support structure which will also add weight. When the propeller is placed on the leading edge of the wing or on the tail, the spar of the wing or the tail can be used as the supporting structure which will be beneficial for saving weight. Placing the propeller on the tail will require a relatively heavy complex structure increasing the weight.

### **Center of Gravity**

To make it easier for the pilot to lift the aircraft it is convenient to have a center of gravity as close to the pilot as possible. Having a center of gravity more to the aft of the aircraft will make it hard to lift the tail off the ground. When the propellers are placed far from the root, it will be hard to balance the aircraft.

### **Stability and Control**

To increase the stability of the aircraft the center of gravity of the aircraft should be located such that the stability margin is large [30]. Therefore, it is more convenient to place the propellers on the front of the aircraft rather than on the back. It is not convenient to have a single propeller in front of the tail surfaces. This is because the rotating propeller will produce a rotating airflow in the same direction of the propeller. This rotational flow will cause an aerodynamic force on the vertical tail. To counter this, the vertical tail needs a rudder.

Using more than one, but an even amount of propellers, counter rotating propellers will solve this problem. Having more propellers may, however, cause stability problems in case of a single motor failure. When one of the motors fails, the aircraft experiences asymmetrical

thrust. This can be solved by adding a rudder, shutting off the other motor or adding more propellers to increase the redundancy. Having a propeller on top of the aircraft will cause a pitch down moment when delivering thrust and a pitch up moment due to drag, when the engines are not working. These moments will have a negative effect on the stability of the aircraft.

To conclude, it was found that more propellers placed on the leading edge of the wing is the most convenient position to place the propeller. The option of four or more propellers was investigated as well, but this would add too much structural weight. This is further explained in chapter 5.

## **3.2. Pilot Position**

The position of the pilot influences the overall configuration of the aircraft, as well as the operations needed to take off, land and control the aircraft. The critical function with respect to the pilot position is the transition that the pilot has to make from a (running) takeoff position to the in-flight position and vice versa for landing. The first time the pilot position and transition was discussed two options were identified. After one iteration it was found that for both options not all requirements could be met that were set on the position by the different technical departments. Therefore it was decided to add a third pilot position that is derived from the design of the Flying Wing, one of concepts that was considered during the conceptual design phase [41]. To see which pilot position and transition is desirable a trade-off on the pilot position is performed. The trade-off criteria used are discussed below.

### **Controllability**

To ensure safe takeoff and landing, the pilot needs full attention for controlling the aircraft during flight phases. The requirement this sets on the transition is that the pilot must be able to control the aircraft in both takeoff and flight position. The actions needed to effect transition must not distract the pilot from controlling the aircraft.

### **Ergonomics**

During takeoff and landing the pilot should be able to carry part of the weight of the aircraft. The pilot position determines how the pilot has to carry these loads. To minimize the risk of injury two things should be avoided: firstly that Carrying loads with a bent back can cause severe injuries. Instead loads should be carried by the lower body which implies that the pilot has to be able to stand straight during takeoff and landing<sup>1</sup>. Of course, with respect to ergonomics it would be optimal if the pilot does not have to carry any weight.

### **Drag**

To reduce drag the pilot position should be as prone as possible, as a higher pilot inclination increases the frontal area of the pilot with respect to the airflow.

### **Complexity transition mechanism**

The transition mechanism should be as simple as possible. Firstly to reduce weight and secondly because complexity has a negative effect on the reliability of such a system. It was

---

<sup>1</sup>[https://www.newcastle.edu.au/\\_\\_data/assets/pdf\\_file/0015/82014/manual-handling-information.pdf](https://www.newcastle.edu.au/__data/assets/pdf_file/0015/82014/manual-handling-information.pdf)

found that the bigger the transition is that has to be made (i.e. the higher the rotation point of the pilot, the bigger the transition) the more complex the transition system will become.

### Center of gravity shift

The transition of the pilot will cause the c.g. of the pilot and thus of the aircraft to shift. For the stability of the aircraft this c.g. shift is an unwanted effect and should thus be minimized. In the best case scenario the pilot rotates around its own c.g. Also a c.g. position close to the neutral point of the wing is favorable.

Table 3.2: Trade-off table for pilot position

	Configuration 1	Configuration 2	Configuration 3
Controllability	<b>0</b>	<b>-</b>	<b>+</b>
	Wing a.o.a. sensitive to body movement	Control of transition mechanism needed	Easy and quick transition
Ergonomics	<b>-</b>	<b>+</b>	<b>+</b>
	Bent position	Straight position	Straight position
Drag	<b>-</b>	<b>0</b>	<b>0</b>
	Larger inclination of pilot		
Transition mechanism	<b>+</b>	<b>-</b>	<b>+</b>
	Simple mechanism: only transition of legs needed	Complex mechanism: rotation pilot around shoulders	Simple mechanism: transition around c.g. of pilot
C.g. shift	<b>0</b>	<b>-</b>	<b>+</b>
	C.g. due to leg transition	Large c.g. shift due to rotation around shoulders	Rotation point in c.g. pilot

### 3.3. Tail Configuration

An aircraft can have different tail configurations and also different control surfaces. The examined configurations consist of single horizontal planes attached at different heights of the vertical tail or V-tail types, in which the vertical and horizontal plane are combined. The V-tail has the advantage that it has less interference drag [66] that it causes at the connections of the surfaces because of the airflow influence of the surfaces is combined and causing a high airflow and respectively more drag, but has more complicated controls, as each control in one direction interferes with another direction or axis. As the area has to be the same, the V-tail does not have many advantages compared to a conventional tail. The most common reason to use a V-tail is to avoid wakes and propeller wash. As the controls are complex and every deflection causes multiple reactions to the attitude of the aircraft, it was decided that a conventional tail, consisting of a vertical and horizontal stabilizer, is the best option.

As a conventional tail has been chosen, the learning of the use of the rudder remains for the pilots, but many pilots have trouble understand the proper use of the rudder <sup>2</sup>. The rudder is mainly used for adverse yaw, crosswind landings, asymmetric power conditions and spin recovery. [65] Novice Velo-E-Raptor pilots will have to be able to fly the aircraft after a one week course. As the rudder is not used much and the landing will happen always against the wind direction on a field, the rudder is not necessary for landing. For adverse yaw during turns there will be a rudder that will be controlled by the flight computer but not by the pilot. Therefore the pilot will have a two-axis control to ensure easier control than three-axis control.

### **3.4. Control System**

With respect to the control of the aircraft it had to be decided whether a mechanical control system or a Fly-By-Wire (FBW) control system would be used. FBW is the generally accepted term for flight control systems which use computers to process the flight control inputs and send corresponding electrical signals to the flight control surface actuators <sup>3</sup>.

Currently only mechanical control is used for ultralight aircraft. However, fly-by-wire can offer improvements. To be able to compare the two systems a literature study is performed that allows for a trade-off of the two systems.

#### **Fly-By-Wire Control System**

The advantages of fly-by-wire systems were first recognized by military aircraft designers that were looking for effective means to control a highly maneuverable aircraft. It was found that aircraft with relaxed static stability can be made flyable by computer intervention. Nowadays fly-by-wire has become the standard for commercial aircraft as well. Airbus even uses their FBW technology as one of their competitive advantages over other manufacturers <sup>4</sup>.

FBW has become very popular over the last decades for a couple of reasons. Compared to a mechanical system the FBW system can result in structural weight savings by the replacement of mechanical control cables. The biggest advantage of FBW is the greater precision in controlling and the possibility of the computer to control the aircraft. By doing so the aircraft can be protected from exceeding flight-envelope limitations. Also, one could fly closer to its aerodynamic limits without running the risk of exceeding stall limits.

#### **Mechanical Control System**

One of the main reasons to choose mechanical control for ultralight aircraft is because FBW systems have never been implemented on aircraft of the size as the Velo-E-Raptor before. The need for FBW systems has been less urgent than for fighter or commercial aviation aircraft; such aircraft do not necessarily need to have relaxed stability. Also structural savings are limited and may even be canceled out by extra weight of redundant control systems.

---

<sup>2</sup><http://www.planeandpilotmag.com/article/whats-the-rudders-real-purpose/#.WVDTilGxW0j>

<sup>3</sup><https://www.skybrary.aero/index.php/Fly-By-Wire>

<sup>4</sup><http://www.airbus.com/innovation/proven-concepts/in-design/fly-by-wire/>

### **Trade-Off**

The trade-off for a FBW or mechanical control system comes down to the question whether it is preferred to choose for a conventional control system that is a "safe decision" in terms of risk management or to choose for a systems that has numerous advantages, especially with respect to safety. When choosing a FBW system, flying can be made much safer for the pilot because he can be protected against exceeding flight envelope limitations. Implementing a FBW system is the change that is needed to make the aircraft safer than any ultralight aircraft currently on the market. Since this design choice introduces higher complexity and therefore higher risk to the design of the Velo-E-Raptor, special attention will be devoted to designing the control systems. This is further elaborated upon in chapter 7.

## **3.5. Landing Gear**

For the landing gear design choice, four options have been considered. These options are listed below:

1. No landing gear
2. Landing gear in front of the pilot
3. Landing gear behind the pilot
4. Landing gear both in front and behind the pilot

Option 4 was selected, because of the high mass of the aircraft. Since the aircraft mass is 65.1 kg it is uncomfortable for the pilot to carry during takeoff and even dangerous to carry during landing. Therefore, the aircraft mass has to be carried by support wheels.

The center of gravity location of the aircraft is approximately at the same location as the center of gravity (c.g.) location of the pilot. Due to these c.g. locations it is not possible with one or two wheels to carry some of the aircraft mass. Therefore it was decided to use a three wheel landing gear with wheels under each propeller (in front of the pilot) and one wheel under the tail. This way the aircraft mass is supported by the landing gears but the pilot still carries his own weight such that he or she still can run and push or pull the aircraft during takeoff and landing. In chapter 8, figures 9.1(b) and 9.4(a) the landing gear is shown.

For safety reasons it was decided to use landing gears both in front of and behind the pilot that fully support the weight of the aircraft. This allows for emergency landings without the input from the pilot. Besides, during foot-landing high impact loads can be encountered by the pilot, which are currently considered to be too dangerous. This was discussed with the costumer, who said that safety is the driving requirement and should be met by all means. However, regulations will not consider the Velo-E-Raptor as a foot-launched aerial vehicle, as it can takeoff without the use of legs. More information about the regulations can be found in the baseline report [40] and the midterm report [41]. A disadvantage of this tail wheel configuration is that it is prone to nose over but this risk is reduced by using relatively large (30 cm diameter) frontal landing wheels and the distance between the c.g. and the frontal landing gear is maximized.

### 3.6. Flaps

For takeoff and landing conditions, the addition of flaps was considered for the detailed design. A short study was done on the types of flaps that could be applied to the Velo-E-Raptor [12][67]. Due to the flexible skin being spanned around the entire airfoil, complex flap designs such as slotted flaps were not feasible for the Velo-E-Raptor. If flaps were used, three options were considered:

- The trailing edge could be pulled down by a cable deforming the trailing edge.
- The trailing edge could be pulled down locally by hinges in the ribs.
- The flexible skin could be removed and a rigid wing structure could be used locally at the location of the flaps, similar to the ailerons.

One problem that every option introduces is additional weight. Flaps would need actuators and taking redundancy into account, this would add 1.2 kg if the same actuators are used as the ailerons. Besides, additional structure is necessary to support flaps and actuators, especially in the third option.

A second problem is complexity. The fly-by-wire system would have to incorporate flaps into the equation. Therefore, additional risk is introduced: they could not be operated properly or fail at some point, making it impossible to land if flaps are required to produce enough lift during landing.

For these reasons, flaps will not be used for the Velo-E-Raptor. The wing surface will have to increase to satisfy lift conditions during landing, but the increase in weight is estimated to be less than a series of flaps and actuators, and the simplicity of not having flaps agrees with the Velo-E-Raptor mission of making the operation of the aircraft as easy as possible.

# 4

## Aerodynamics

### 4.1. Literature Study

#### 4.1.1. Flow Interference

##### Interference drag

In section 4.2.1, zero-lift drag of all separate aircraft components will be estimated. For the total aircraft, additional drag will be present. Interference drag is caused by boundary layers of multiple bodies interacting with each other [66]. Therefore, interference drag is usually caused by joints between bodies, or the wake of one body colliding with another.

Because of the shape of a person, separation of the boundary layer is likely to occur [7]. Therefore, for the wing section where the pilot is positioned, boundary layer interference will be present and the airflow around the wing will be disrupted. No analytical methods are known to estimate interference drag due to a pilot. Therefore there is uncertainty about the effects of interference on the aerodynamic coefficients. In order to account for interference in detailed design, the following precautions are taken:

- For conventional aircraft, interference increases the  $C_{D_0}$  by 4% [56]. A lot of interference is expected in the airflow around the Velo-E-Raptor relative to conventional aircraft, so an increase in  $C_{D_0}$  of 10% will be taken to account for interference drag. If in a later stage the interference drag proves to be higher, fairings will have to be designed to reduce the interference drag below 10%.
- The wing planform section where the pilot is positioned is assumed to produce no lift. The remaining wing area will have to produce enough lift for all operations. This precaution is taken to ensure that regardless of any airflow interference, the Velo-E-Raptor will always produce enough lift. This is comparable to conventional aircraft with a fuselage at the wing root, where the fuselage also interferes with the lift distribution.
- Sharp corners have to be avoided for joints in the structure, as well as the region between pilot and wing. Fairings will have to be designed where sharp corners cannot be avoided.

##### Pilot wake

After the design choice, made in section 3.2, to put the upper body of the pilot on top of

the wing, an additional study was performed on whether the airflow around the pilot would interfere with the tail surfaces.

In this position, the pilot is comparable to a bicycle racer. In this sport, aerodynamics has already been studied thoroughly [7]. The key measure to reduce drag is to prevent separation and keep the flow attached to the human body as long as possible. Besides reducing drag, preventing separation of the airflow ensures the tail is not disturbed by vortices produced by the pilot. Due to wing downwash, the legs and cycling system do not influence the tail surfaces, even at high angles of attack, as they are located below the wing. This conclusion can be validated by current hang gliders with tail configurations<sup>1 2</sup>, of which the stability is proven in flight with the pilot located below the wing.

From this study, two recommendations can be done for detailed design:

- The helmet and harness of the pilot shall be optimized for smoothness and be as streamlined as possible to minimize drag and prevent separation of the boundary layer for as long as possible, comparable to the equipment in bicycle racing. This is further discussed in section 4.6.2.
- For tail design, a long tail arm and large span for the surfaces is recommended, to prevent the wake of the pilot influencing the tail effectiveness. This is taken into account in the tail design in chapter 6.

To investigate the effects of both interference drag and pilot wake in detail, Computational Fluid Dynamics (CFD) can be used to model the pilot in the wing and investigate the effectiveness of the tail. The DSE project does however not have the time and resources for CFD, and therefore this analysis has not been carried out during the project. This will be further explained in section 4.6.1.

#### **4.1.2. Airfoil Parameters**

One of the most important design choices to be made is the selection of the airfoil. To determine the effect of a variation of airfoil parameters, a literature study was performed on airfoils of the NACA 4-, 5- and 6-digit series [12]. In this section the findings are reported that were used for the airfoil selection.

An increase of thickness ratio of an airfoil leads to an increase of the lift curve slope, as well as increasing the  $C_{l_{max}}$  (until a t/c of about 15% for NACA 63 airfoil series with a camber of 3%) [67, sec. 2-9, 4-16]. An increase in camber leads again to an increase in maximum lift coefficient. However, once the thickness is increased to the extent that it leads to a flow separation, naturally, the  $C_L$  drastically decreases. Increasing the nose radius however generally leads to an increase of the lift slope and stall angle [67, sec 2-8]. For the optimal nose radius, the stall angle is the most important factor to take into account. It is also dependent on surface roughness, Reynolds number and Mach number. For low Reynolds numbers, below 1,000,000, it was found that sharper leading edges are beneficial and for higher Reynolds

---

<sup>1</sup><http://www.a-i-r-usa.com>

<sup>2</sup>[http://www.aeros.com.ua/structure/hg/tail\\_en.php](http://www.aeros.com.ua/structure/hg/tail_en.php)

number a larger noise radius would be preferred.

Applying camber to an airfoil decreases the suction peak observed in symmetrical airfoils, to get a more even pressure distribution. Moving the camber location more aft decreases the angle of attack for zero-lift, but increases the magnitude of  $C_{m0}$ . For sailplanes thick airfoils with high camber are often used [12].

### 4.1.3. Maximum Lift and Stalling

The maximum lift of a wing depends on the airfoil selected, the flight conditions, planform design and the high-lift devices installed. In addition, interference effects have to be considered. More important is the stall behavior, as an abrupt stall should be avoided at all cost. Physically, stall can take three forms. Either it originates at the leading edge, suddenly, by means of a bubble burst, or more gradually with a laminar separation bubble, where the flow reattaches again. The sudden type is known as "short bubble type", and should be avoided at all cost, due to the sudden loss in lift and negative shift in pitching moment. The second form, also known as "long bubble type" is preferred due to its gradual behavior, but remains hard to predict. The third mode is trailing edge stall. Due to gradual growth of the turbulent boundary layer near the trailing edge, turbulent separation follows. This separation progressively moves forward with increasing angle of attack, causing that part of the airfoil to stall in a relatively predictable manner. For thick airfoils ( $t/c > 0.15$ ), this type of stall is often observed. It should be noted, that although these distinct varieties can be distinguished, a combination of them can also occur [37] [67].

Considering the planform, the most important shape parameter is the washout. It is important that the tip section incidence angle is lower than that of the root section, to make sure that the tip stalls at a later stage than the root section. This way the controllability of the aircraft in post-stall conditions can be ensured. Furthermore, different airfoils have been selected for the tip and root, to ensure a good stall performance. However, these choices are highly dependent on the flight conditions, as airfoils have different behaviour at different Reynolds numbers.

### 4.1.4. Winglets

A study was performed to investigate if winglets would be beneficial to add to the Velo-E-Raptor planform. While existing hang gliders usually do not have winglets, there are some on the market <sup>3</sup>, and sailplanes have adapted winglets on a large scale. Winglets seem to provide an improvement of a few percent in drag [57]. Besides, winglets reduce wing twist and provide additional yaw stability [17], resulting in more favorable spin characteristics.

A downside of winglet design is that if not done correctly, the winglets will not improve aerodynamic performance and only add drag and weight to the aircraft. Winglet design is a sensitive process dependent on many aircraft parameters and using existing winglet designs on the Velo-E-Raptor has a high probability of harming the aircraft performance [57]. Detailed design of the winglet planform is necessary to improve the performance of the design.

---

<sup>3</sup><https://www.willswing.com/wills-wing-winglets-qa-2/>

In section 4.3.3, a preliminary design is shown that is used to quantify possible improvements that can be made by implementing winglets. Since detailed optimization should take place before implementing them, the recommendation is made to investigate winglets further at a later stage, as explained in section 4.6.2.

## 4.2. Approach

### 4.2.1. Zero-Lift Drag Coefficient

For all parts of the aircraft exposed to airflow, an estimation of drag had to be made to enable the estimation of the aircraft's aerodynamic drag reliably. The parameter that can be estimated for each part is the drag area ( $A_i$ ), which is defined as the frontal area of the part ( $S_i$ ) with respect to the airflow, multiplied by a drag coefficient ( $C_{D0i}$ ) which is dependent of the shape of the part. The drag area of one component can be divided by the wing reference area, to find its contribution to the zero lift drag coefficient with respect to the aircraft. Finally, the contributions of all components can be summed up to find the total aircraft zero lift drag coefficient ( $C_{D0}$ ).

$$C_{D0} = \sum \left( \frac{A_i}{S_{ref}} \right) = \sum \left( \frac{S_i \cdot C_{D0i}}{S_{ref}} \right) \quad (4.1)$$

For an estimation of the pilot including harness, experimental results were used [14]. Data from wind tunnel experiments are taken where the drag area for a large variety of pilots and equipment was measured. The hang glider structure is also included in the experiment. Harnesses produced today are more aerodynamically efficient than the ones used in the experiment. Therefore the drag area might be slightly overestimated. Additional wind tunnel experiments were found about the drag area of various bicycle configurations [7], which is comparable to the position the pilot will be in.

For cylindrical shapes, an estimation of the drag area is based on frontal area with respect to airflow and a two-dimensional drag coefficient of 1.2 [56][66]. When this method is used for struts, streamlined shapes such as airfoils can be used instead of a circular cross-section, the drag coefficient can be reduced to 0.35.

For the landing gear wheels, a similar method is used as the cylindrical shapes. Instead, a drag coefficient of 0.3 will be used for regular wheels. The coefficient can be reduced to 0.15 if wheel fairings are applied [56].

When the Velo-E-Raptor is gliding and the propulsion system is turned off, the propeller blades will produce drag as well. A rough estimation of the added drag during this condition was found by approximating the drag area of the blade areas at a certain inclination [66].

Finally, the  $C_{D0}$  of the wing and tail can be added as well. The methods for determining the aerodynamic coefficients of the wing and tail are discussed in section 4.2.3.

After analyzing all different parts, other sources of drag might be unaccounted for in the estimation above. Therefore, a safety factor of 20% will be added to the total  $C_{D0}$  [56]. Com-

bined with the safety factor for additional interference drag as discussed in section 4.1.1, a total safety factor of 30% will be used for further calculations.

### 4.2.2. XFOIL 6.9

#### Description

The program XFOIL 6.9 (developed between 1986 and 2001) is a useful tool in designing and analyzing subcritical airfoils, especially at low Reynolds numbers [53]. The program can determine the pressure distribution and lift and drag coefficients just beyond  $C_{L_{max}}$ . It makes use of viscous analysis for the flow around the airfoil, where the boundary layer is modelled with the dissipation integral (described in detail in [55]). A global Newton method is used for the computation. Considering transition from laminar to turbulent flow, the program includes forced or free transition options, as well as allowing transitional separation bubbles [54]. For the transition of the flow from laminar to turbulent, it makes use of the  $e^9$  method [50]. The profile drag is calculated using the Squire-Young formula, which has been numerically validated in [23]. A Karman-Tsien compressibility correction is applied for accurate compressibility correction. The program allows for full inverse airfoil design, where altering desired output is translated to a new airfoil geometry.

#### Limitations

The program is based on incompressible analysis, Mach numbers of higher than 0.7 should not be exceeded. However, as the flight speeds of the Velo-E-Raptor will not reach above Mach 0.1, this is not a problem.

In XFOIL, the wake trajectory is determined using inviscid methods, to give a significant decrease in computation time. The error that arises with this only becomes significant near stall and therefore it is acceptable for use in the attached flow regime [54]. Especially at large angles of attack, the results should therefore be interpreted with care.

#### Usage

XFOIL has been used to compute the  $C_L$ - $\alpha$ ,  $C_D$ - $\alpha$  and drag polar of the airfoils selected for the design. The curves for these were computed for Reynolds numbers between the lowest and highest Reynolds numbers that occur during the three dimensional analysis in XFLR5 & AVL (see section 4.3).

### 4.2.3. XFLR5 v6.38 & Athena Vortex Lattice 3.36

#### Description

The program AVL 3.36 (Athena Vortex Lattice), developed by Drela et al.<sup>4</sup>, has been used to perform an aerodynamic analysis on the planform design to determine its lift and drag properties. It has been in development since 1988 and is widely used for aerodynamic analysis, for example in [10], [27] and [62]. A more recent developed program of the same kind is XFLR5. Both programs are based on the use of a vortex lattice method (VLM), which models the lifting surfaces as a thin sheet of discrete horseshoe vortices and numerically computes the lift and induced drag, and related aerodynamic coefficients and derivatives. XFLR5 also comes with additional algorithms: LLT (lifting line theory), 3D Panel and a VLM algorithm

---

<sup>4</sup><http://web.mit.edu/drela/Public/web/avl/>

that makes use of quadrilateral vortices. Viscous drag is extrapolated from the XFOIL analysis, to get an estimation for the viscous effects that are neglected in a VLM analysis. Next to aerodynamic analysis, also flight-dynamic analyses with specified mass properties can be performed with these programs.

### **Limitations**

Since the programs use a vortex-lattice method, it is best suited for thin airfoils at low angles of attack as the influence of thickness and viscosity is neglected. Modelling slender fuselages and nacelles with source and doublet filaments is also possible, where results are consistent with slender-body theory [19]. Furthermore, AVL assumes a quasi-steady flow, neglecting for example the Von Karmen effect [48, p. 231-232]. The resulting forces are calculated using the Kutta Joukowski relation. The classical Prandtl-Glauert transformation is used to correct for compressibility effects, which ensure that the program can be used for Mach numbers up to 0.6 which is well above the upper limit of the flight envelope. In the linearization process, errors are generated when it is applied to thick surfaces or when large velocity perturbations of the freestream velocity occur. However, for the design purposes, these errors are assumed to be very small.

### **Usage**

XFLR5 and AVL were the primary tools for the aerodynamic and stability analyses performed during the design. The program gives a detailed output for lift, drag and moment properties, for the range of angles of attack and the specified flight conditions. Additionally, the Stability and Control department made use of the stability functionalities of the programs, which yields the eigenmodes and stability derivatives. The outputs for aerodynamic loading were then communicated to the Structures and Materials department, as well as the Performance and Propulsion department.

## **4.3. Results**

### **4.3.1. Airfoil Selection**

First, from literature a selection from the different NACA series was made based on the description in [12, p. 238-239] and from the results of the literature study as described in section 4.1.2. Since the NACA 4-digit series generally have high-drag properties and NACA 5-digit series have adverse stall characteristics for low Reynolds numbers, the NACA 6-digit series was chosen for the airfoil selection process. These series are known for their low profile drag (in laminar flow conditions), and for thicker cambered sections the maximum lift and docile stall is similar to that of the 4-digit series. Furthermore, these series have been tested extensively and differences between varieties could be easily compared. The geometry parameter selection followed. Camber was chosen such that the design  $C_l$  is met. The location of maximum camber was chosen to be rather aft, since this results in a gradual stall, but a lower  $C_{l_{max}}$ . The thickness ratio is chosen to be on the thick side of the spectrum ( $t/c=18\%$ ), to ensure a trailing-edge stall and to have structural advantages. For the comparison of airfoils, the experimental two-dimensional data have been taken from [43], and served together with XFOIL analyses as the basis for the airfoil selection.

The most important selection for stall characteristics was that of the tip section. For this section, a NACA 63<sub>3</sub>-618 airfoil was chosen because it has excellent stall characteristics. The minimum drag value for this airfoil lies at 0.005, which can be achieved for lift coefficients between 0.2 and 1.0. A note should be made that this is due to the "laminar drag bucket" which is often observed, but that propeller interference or skin deformation can lead to a turbulent interaction, and a slight increase of the drag coefficient at low angles of attack (of about 0.001). Furthermore, it is capable of achieving a  $C_l$  of 1.4 (at  $\alpha = 9^\circ$  or higher). That is why this airfoil has been chosen to be placed at the tip, so that stalling is highly unlikely to occur. However, the pitching moment about the aerodynamic center is about -0.1, which is relatively high compared to other airfoils from the series. In order that the aircraft remains controllable, the total pitching moment of the main wing was decreased by selecting a different root section airfoil. Since the Reynolds number at the root is significantly higher, NACA 5-series airfoils were considered as well, resulting in a NACA 23018 selection for the root. This airfoil is capable of achieving a  $C_l$  of 1.4, while having a  $C_{m_{ac}}$  of zero due to symmetry and an optimal drag coefficient of 0.007 in the range of  $C_l$  between -0.1 and 0.5, ideal for cruise.

The results of the XFOIL analysis performed on these airfoils can be found in section 4.3.5, for the minimum and maximum Reynolds numbers encountered in flight.

### 4.3.2. Wing Parameters

For the determination of the wing parameters, a constant trade-off between stability and aerodynamic performance had to be made. In the Stability and Control chapter, the processes for the determination of dihedral and sweep are discussed. The wing twist has to be selected to optimize lift distribution and stall performance. It improves the stall performance by delaying the tip stall and therefore ensuring controllability on the onset of stall. Furthermore, a more equal distribution of lift along the span could be obtained this way, since the tip section inherently produces more lift due to its camber.

#### Tail Parameters

Another important consideration to make when designing for good stall characteristics are the tail parameters. The tail is used for controllability, and the function of it has to be ensured beyond stall, in order to be able to recover from stall. The position of the tail with respect to the wing is one of the main parameters. From [12, p. 51-52], it is found that when the tail is placed at the same height as that of the main wing, the aircraft remains very stable beyond the stall angle, making sure that the aircraft remains controllable. For the tail airfoil, the NACA 63<sub>3</sub>-018 has been selected. This airfoil comes with a good lifting performance (a  $C_{l_{max}}$  of 1.2), ensuring a good performance and allowing for a smaller horizontal tail surface, reducing weight. The stall performance of this airfoil is similar of the NACA 63<sub>3</sub>-618 airfoil, which makes sure that the aircraft is not likely to stall.

#### Taper

Ideally, the taper ratio for small aircraft is as low as possible [12]. A lower taper ratio has structural and stall benefits. The minimum taper ratio is usually limited by the control surface dimensions. The ideal taper ratio for induced drag is 0.4, as it most closely resembles the elliptical lift distribution. For a first iteration, where little is known yet about control surfaces, 0.4 will be used as taper ratio for the Velo-E-Raptor. If any changes in planform dimensions are desired, the taper ratio will be revised.

### 4.3.3. Wing Twist and Winglet

As described in section 4.1.3, a washout is included in the design to enhance the stall performance and spanwise lift distribution. The value for twist was iterated until the lift distribution resembled that of an elliptical distribution, for a minimal induced drag coefficient. The lift distribution at cruise, as shown in figure 4.1, was obtained. This resulted in a  $4^\circ$  washout. This measure, together with the airfoil selection will ensure that no stall shall occur at the tip, and controllability can be maintained even when the root section has stalled.

Another investigation was done on the implementation of winglets to the design. Using a VLM analysis, after an iterative process, the implementation of a winglet resulted in a decrease of induced drag coefficient above an angle of attack of  $2^\circ$  for the same amount of total wing area (a top view of this planform can be seen in figure 4.2). This decrease was quantified to be 6.1% for an angle of attack of  $10^\circ$ , which can significantly increase the performance during landing and takeoff. Moreover, a drag decrease of 0.005 at  $\alpha_{\text{cruise}}$  was found. However, at angles below  $2.0^\circ$ , a slight increase in drag coefficient arises (0.0025 at  $\alpha$  equal to zero). Application of winglets to the horizontal tail did not result in a performance amelioration, most likely due to the interaction with the wing wake and relatively low lift-induced drag. Before implementation into the design can occur, a more detailed (stability) analysis has to be performed.

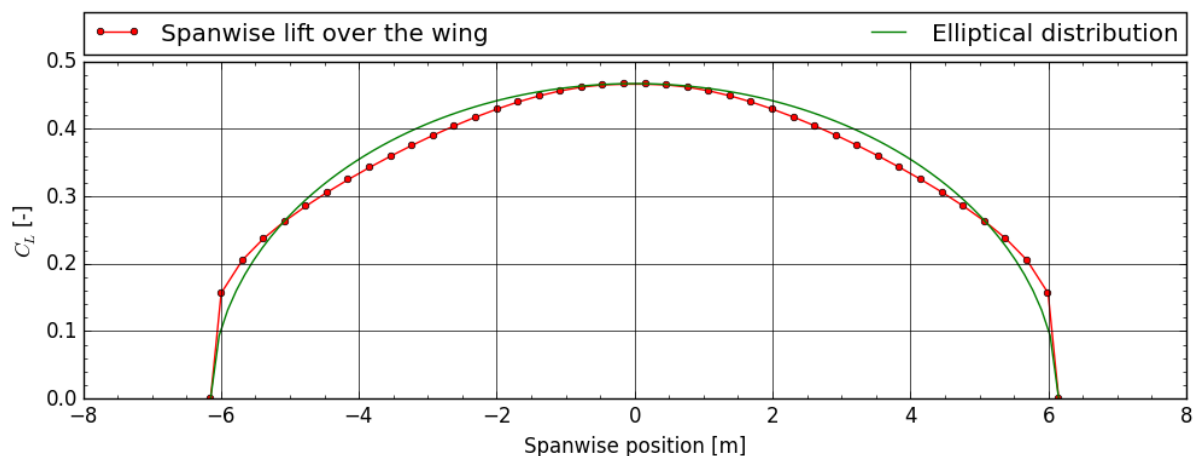


Figure 4.1: The spanwise lift distribution of the Velo-E-Raptor in cruise, compared to an elliptical distribution.

### 4.3.4. Zero-Lift Drag Coefficient

In this subsection, the results of the method described in section 4.2.1 are shown. In table 4.1, the zero-lift drag coefficients of all various components can be found. In table 4.2, the total values can be found in different configurations, including the 30% safety margin.

The choice was made to use streamlined struts in the final design, as it decreases the total clean configuration  $C_{D_0}$  by 30% and had structural benefits as well due to the elongated cross-section. The landing gears are not retractable. No fairings were designed for the wheels as the difference is negligible. During takeoff and landing configuration, the standing

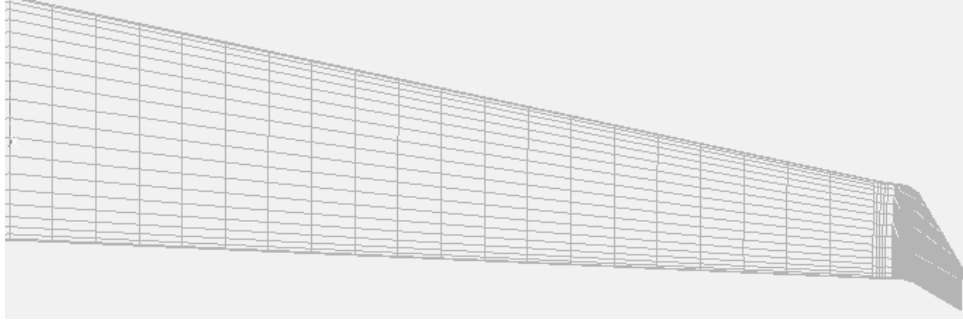


Figure 4.2: Velo-E-Raptor wing including the winglet design.

Table 4.1:  $C_{D_0}$  of separate components based on the wing reference area

Component	Pilot (prone)	Pilot (standing)	Planform	Wheels	Struts	Stopped propellers
$C_{D_0}$ [-]	0.0180	0.0303	0.0082	0.0010	0.0040	0.0020

Table 4.2:  $C_{D_0}$  of different aircraft configurations

Configuration	clean	takeoff	landing	gliding
$C_{D_0}$ [-]	0.0401	0.0560	0.0587	0.0427

pilot  $C_{D_0}$  is used. During the landing and gliding configuration, the propellers are stopped and produce drag as well.

### 4.3.5. Aerodynamic Forces & Coefficients

To start off, the chosen airfoils were analyzed in the range of Reynolds numbers that apply during flight. These values can be found in table 4.3, together with the flight speeds. The results of the XFOIL analysis can be seen in figure 4.3 for the minimum and maximum Reynolds numbers. The value of the Reynolds number has been determined using its definition with the section chord length as characteristic length  $l$ , the speed equal to the flight speed and the sea level kinematic viscosity of  $1.46 \cdot 10^{-5}$  [61, p. 20]. The Karman-Tsien compressibility factor was not used, since a quick calculation following its definition indicated that for the Mach number at cruise, 0.06, a correction of approximately one per mille applies [48]. The results of XFOIL were then used for the analysis done with XFLR5.

In the XFLR5 analysis, a pilot weight of 75 kg was taken, as well as point masses for most components of the aircraft, as provided by other departments. For this analysis, the results can be found in figure 4.4 and table 4.4. The values for flight speed, angle of attack,  $C_L$ ,  $C_{D_{planform}}$  were obtained from the XFLR5 analysis. The  $C_{D_{total}}$  was obtained by adding the  $C_{D_0}$  components from section 4.2.1 to the calculated values from XFLR5. The resulting  $L/D$  for cruise is 8.57, which uses the  $C_{D_0}$  values from section 4.2.1. One can also see that the drag values for stall are relatively low, which is due to the underestimation of the drag coefficient for these highly viscous flight phases (and the 2D extrapolation of viscous drag cannot give accurate results. Furthermore, the results of XFLR5 are accepted up till an angle of attack of  $12^\circ$ , which is well below the onset of stall in the 2D case, which is even later in the 3D

case due to sweep. At this angle of attack, the maximum lift coefficient is 1.1. For the lifting performance during landing, the section of the wing where the pilot is placed was assumed to produce zero lift. The tail section produces sufficient lift to compensate for the losses in lift in the main wing during landing.

Table 4.3: Reynolds numbers for planform sections during takeoff, cruise and landing

Flight phase	Takeoff	Cruise	Landing	Stall
Flight speed [m/s]	15.33	20.57	15.14	12.67
Reynolds number wing root	$1.69 \cdot 10^6$	$2.27 \cdot 10^6$	$1.67 \cdot 10^6$	$1.40 \cdot 10^6$
Reynolds number wing tip	$6.76 \cdot 10^5$	$9.07 \cdot 10^5$	$6.67 \cdot 10^5$	$5.59 \cdot 10^5$
Reynolds number elevator (MAC)	$5.77 \cdot 10^5$	$7.74 \cdot 10^5$	$5.70 \cdot 10^5$	$4.77 \cdot 10^5$
Reynolds number fin (MAC)	$4.72 \cdot 10^5$	$6.34 \cdot 10^5$	$4.66 \cdot 10^5$	$3.90 \cdot 10^5$

Table 4.4: Overview of the aerodynamic coefficients for the Velo-E-Raptor

Flight phase	Takeoff	Cruise	Landing	Stall	Unit
Flight speed	15.3	20.6	15.1	12.1	m/s
Angle of attack	6.53	3.36	6.70	11.00	deg
$C_L$	0.68	0.38	0.70	1.10	–
$C_{D_{\text{planform}}}$	0.023	0.012	0.024	0.049	–
$C_{D_{\text{total}}}$	0.069	0.044	0.072	0.110	–

## 4.4. Verification and Validation

### 4.4.1. Zero-Lift Drag Coefficient

#### Verification

The method used to find the zero-lift drag coefficient is found by summing up the drag areas of different aircraft components, as can be seen in equation (4.1). The input parameters were thoroughly checked, and the drag areas of each component was separately verified by carrying out the calculations by hand. Any errors found were taken out and the results match.

#### Validation

Experimental data of the zero-lift drag coefficients of hang gliders or comparable aircraft is unfortunately not available. The methods used for the different components can however be validated.

The  $C_{D_0}$  inputs applied by the method are used by multiple sources [62][66][56][7]. The pilot drag area is found by comparing multiple wind tunnel experiments [66][7], and no computational methods are used that need to be validated. The theoretical drag area estimation for struts, landing gears and cables is validated using wind tunnel experiments [66].

The stopped propeller drag area estimation is based on empirical propeller data [66]. Admittedly there can still be errors when using this estimation, but it was only used to provide

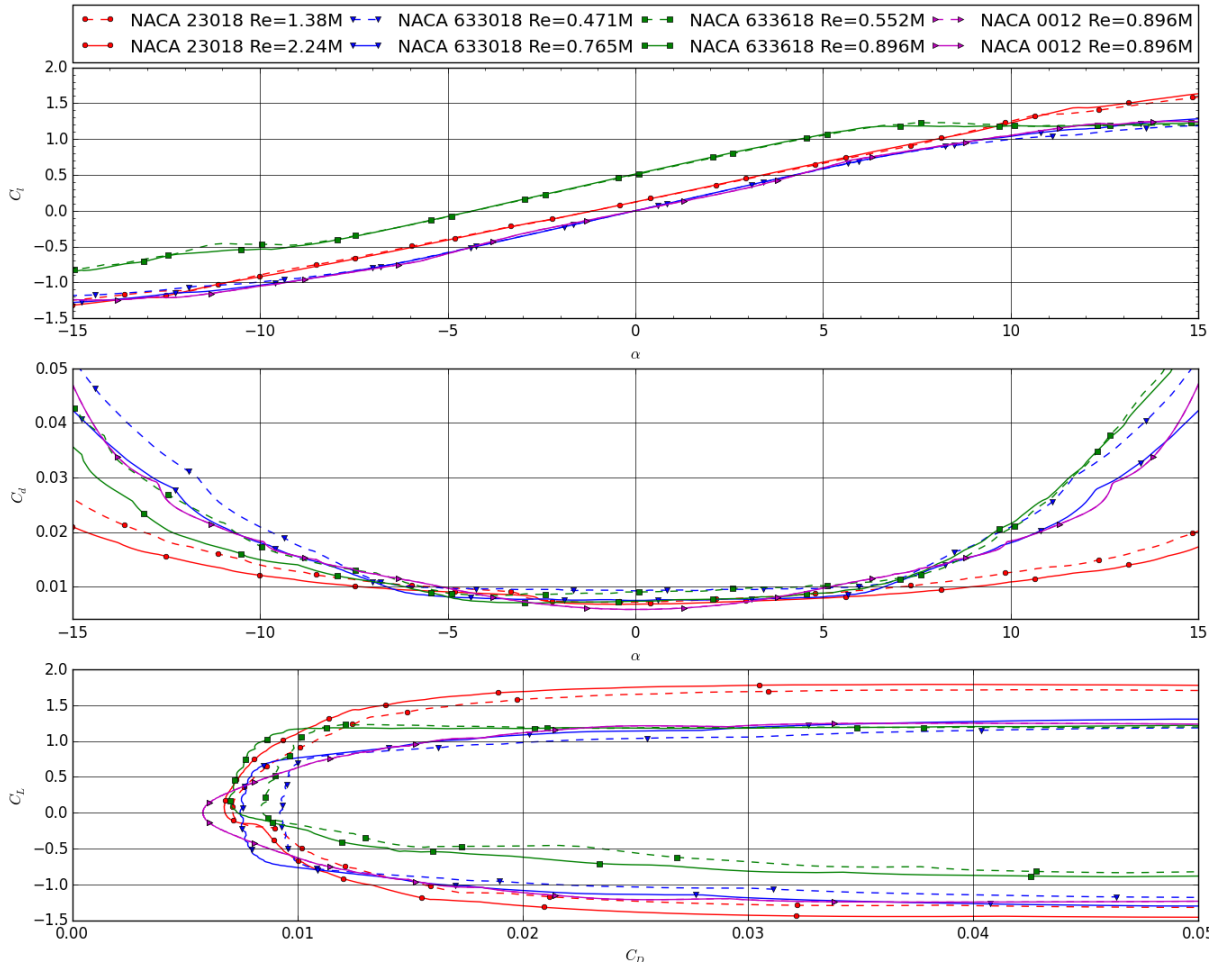


Figure 4.3: Lift and drag performance for the airfoils selected from the XFOIL analysis, at minimum and maximum Reynolds numbers

a first estimation of what the drag would be while gliding and no other calculations depend on this value.

For the unaccounted sources of drag and interference drag, the safety factor was taken from aircraft reference data compared to the method [56]. The possible error in this safety margin is unknown, but the safety factor was chosen to be on the higher end, because an underestimation of drag would be unfavorable if it ends up to be higher in further design changes.

#### 4.4.2. Software

Since the aforementioned programs have their limitations and inaccuracies in the output, quantifying the error in the results becomes very important. The XFOIL results were validated by comparison to experimental data from [43]. From this, the error margin was determined. Verification for XFLR5 was done by running the same configuration in AVL and by comparing the results, the correct implementation of the vortex lattice theory could be checked. For validation, test data was used with similar Reynolds numbers and flight velocity.

### Validation XFOIL

The results from XFOIL were validated by comparing experimental results from [43] to the results obtained by evaluating the airfoils chosen for the wing root- and tip section, as well as the horizontal tail section in XFOIL. The Reynolds numbers for the analysis were matched with the ones used in the windtunnel tests,  $3 \cdot 10^6$  and  $6 \cdot 10^6$ . The results of this comparison can be seen in figure 4.5.

### Verification XFLR5

The verification of the quadrilateral Vortex Lattice Method (VLM2) was done by doing a comparative analysis using the Lifting Line Theory (LLT), horseshoe Vortex Lattice Method (VLM1). Furthermore, the results from the viscous estimation were obtained by comparing the results to an inviscid VLM2 analysis. These results can be found in figure 4.6. As can be seen, little difference exists between the VLM1 and VLM2 analysis, indicating that these methods have been correctly implemented. The differences between VLM2 and LLT comes from neglecting the tail contribution in LLT. Therefore, the negative lift contribution and increase in drag from the drag become visible. The inviscid method used shows the contribution of drag due to the tail. The inviscid VLM2 method, compared to the viscous analysis (including extrapolated viscous drag data from XFOIL), shows the calculated viscous drag component. The lift performance results are very similar for all methods.

Furthermore, a comparative analysis was performed in AVL, by modelling the same model in the same flight conditions (setting flight velocities equal). An inviscid analysis was performed, to compare the results from the VLM method, comparing  $\alpha$ ,  $C_{Di}$  and  $C_L$ . The results for the different flight phases are listed in table 4.5. As can be seen, the lift and drag performance is very similar. The absolute deviation of angle of attack where these values are obtained does not exceed 0.17, which is acceptably close.

	XFLR5			AVL		
	$\alpha$ [°]	$C_L$ [-]	$C_{Di}$ [-]	$\alpha$ [°]	$C_L$ [-]	$C_{Di}$ [-]
Takeoff (15.33 m/s)	6.53	0.6828	0.0135	6.38	0.6827	0.0145
Cruise (20.57 m/s)	3.36	0.380	0.0041	3.19	0.379	0.0045
Landing (15.14 m/s)	6.70	0.699	0.0142	6.56	0.700	0.0152
Stall (12.67 m/s)	9.90	1.0005	0.0293	9.75	0.9995	0.0311

Table 4.5: Comparative values obtained from XFLR5 and AVL data

## 4.5. Conclusion

The goal of the aerodynamics department is to provide reliable planform parameters for other departments to use as inputs. The result of the aerodynamic analysis provides sufficiently accurate results for other models to build on. The planform is optimized to meet all the needs of other departments and satisfy as many requirements as possible.

While the aerodynamic performance of the Velo-E-Raptor is slightly worse than current hang gliders, this is caused by the many additional sources of drag of the Velo-E-Raptor con-

figuration. This is a compromise on aerodynamics, but the addition of a propulsion system will ensure the overall performance of the design will meet the mission needs.

## **4.6. Project Design and Development Logic**

In this section a brief explanation will be given on the post-DSE activities of the aerodynamics department. All planned activities can be observed in appendix A , where an indication of time and resource allocation is given.

### **4.6.1. Computational Fluid Dynamics**

Computational Fluid Dynamics (CFD) is the most accurate and reliable way of modelling an aircraft and determining its aerodynamic performance. Instead of only modelling a basic planform, in CFD a detailed simulation can be made of the airflow interacting with different parts and subsystems, including matters such as pilot interference or flow separation that could not be modeled with the software described in section 4.2.3.

The Velo-E-Raptor is however a very complex object, and making a model and a mesh would be too time and resource intensive to be done during the short time span of the DSE project. For accurate results close to realistic flight conditions, it is recommended that a simulation is done in CFD during future development.

### **4.6.2. Aerodynamic Optimization**

After detailed design is finished, the aircraft can be optimized for aerodynamic efficiency. While the final configuration of the Velo-E-Raptor described in this report will be able to operate, the optimization of aerodynamics will result in an increase of glide ratio and decrease of power required.

The improvements will result in an increase in weight and complexity. Therefore, for every separate optimization a consideration will need to be done between the better performance and added risk and weight, while always making sure the weight requirement is never exceeded. The aerodynamics of the following subsystems can be improved upon:

- Fairings can be designed for landing wheels and structural joints exposed to the airflow.
- While struts already use a streamlined cross-sectional shape, the shape could be optimized by for instance using airfoils.
- The landing gears could be made retractable, resulting in less drag during flight.
- The propeller blades could be made foldable in the direction of the airflow, resulting in less drag when gliding with the engines turned off.
- Winglets could be designed for the wingtips, resulting in a reduction in induced drag.
- The pilot equipment and instrumentation can be made streamlined.

### **4.6.3. Other Aerodynamic Effects**

#### **Aerodynamic vibrations**

A study was also performed on flutter effects caused by aerodynamic vibrations. Determining flutter characteristics usually requires complicated computational models, and reliable estimations cannot be calculated analytically. Aircraft are usually certified for flutter by performing wind tunnel or flight test experiments [18].

For the final configuration the theoretical maximum airspeed of the Velo-E-Raptor is 10 knots higher than the never-exceed speed of existing hang gliders. This never-exceed speed is defined that flutter is not a problem as long as the pilots maintain operating limits [39]. When a prototype of the Velo-E-Raptor is built, the flutter characteristics of the Velo-E-Raptor can be investigated further to test the limits of the design, and a never-exceed speed of the final configuration can be determined.

#### **Wing Deformation**

In the current analysis, no flexibility of lifting surfaces was taken into account. To increase the accuracy of the results, the effect of deformation during flight should be considered and compensated for.

#### **Propeller Wake**

For the propeller position design choice in section 3.1, the effect of the propellers on the wing planform was investigated. While it was determined that the effect on the total lift would be positive [52], the difference in lift distribution cannot be calculated accurately at this stage. Besides, the altered lift distributions could have an effect on structural or performance calculations. Finally, due to separated flow from the propeller blades hitting the planform, additional drag could be produced. All effects could be further investigated in detail by studying the wake of the propellers using CFD or experiments.

#### **Noise of Wings**

In general, noise produced by a propeller aircraft originates mostly from the propeller blades due to their high tip velocities. However, also at the trailing edge of the wings, turbulent flow interaction of the vortices create noise. From [59], [6], improvements can be made by including a (combed) serrated trailing edge, which is thought to ameliorate the streamlines at the trailing edge. However, this is not yet included in the design, but moved to the post DSE phase. This is done since the noise generated by the wings is relatively low when compared to the noise generation of the propeller blades.

#### **Stall Detection and Stall Strip**

Another design aspect that will have to be considered in the post-DSE phase, is a stall strip. This element ensures that the stall characteristics be laterally symmetrical. However, since the determination of the location and length of this strip is highly experimental in nature, this cannot be performed during conceptual design. Furthermore, there is the need to implement stall detectors and a warning system.

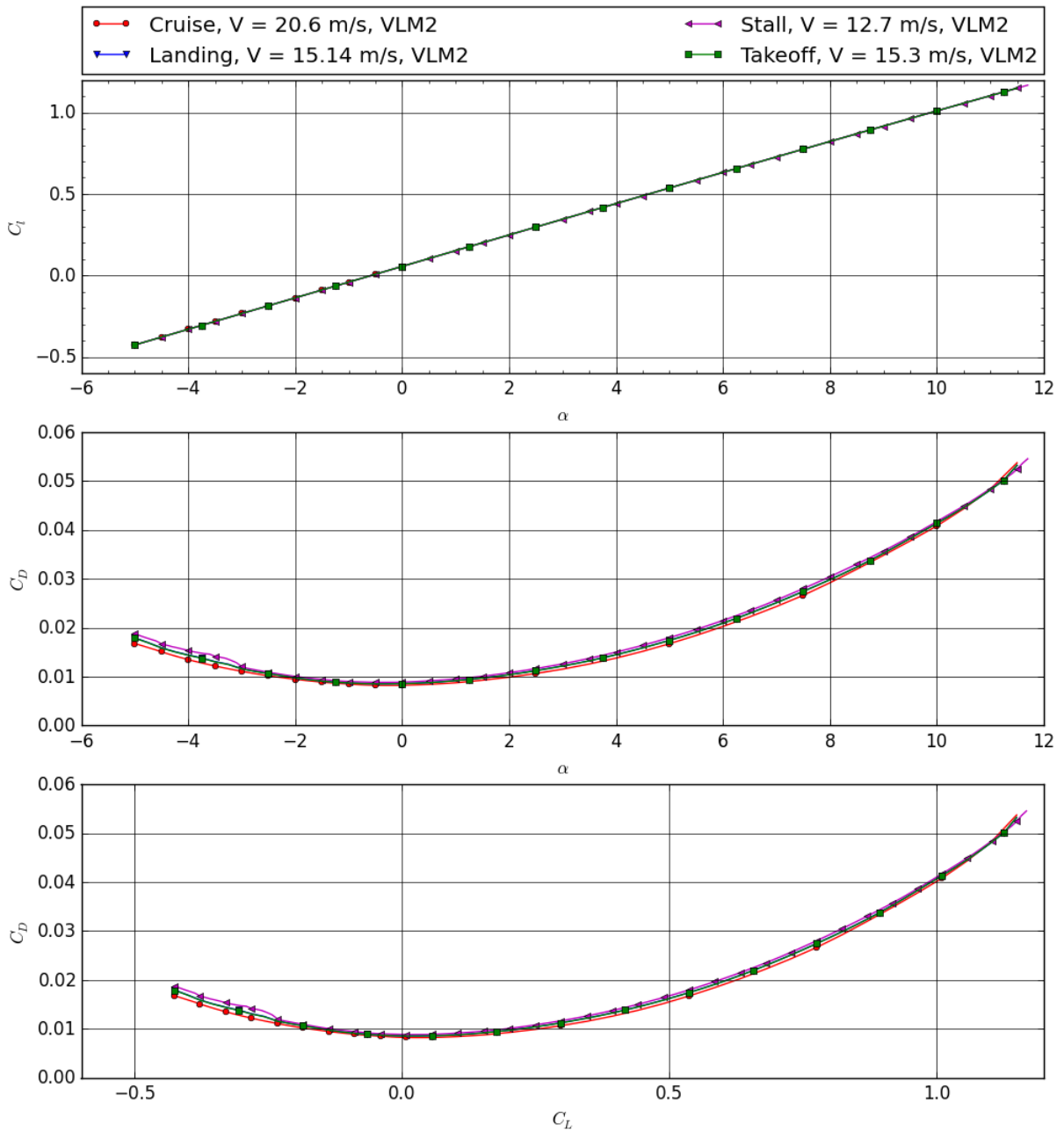
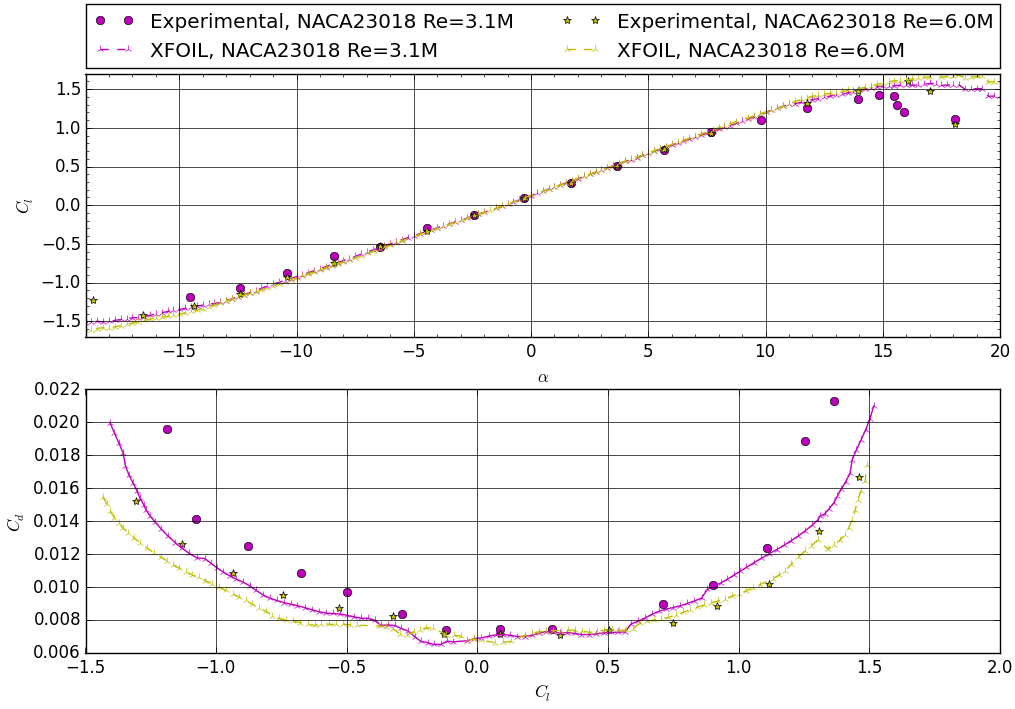
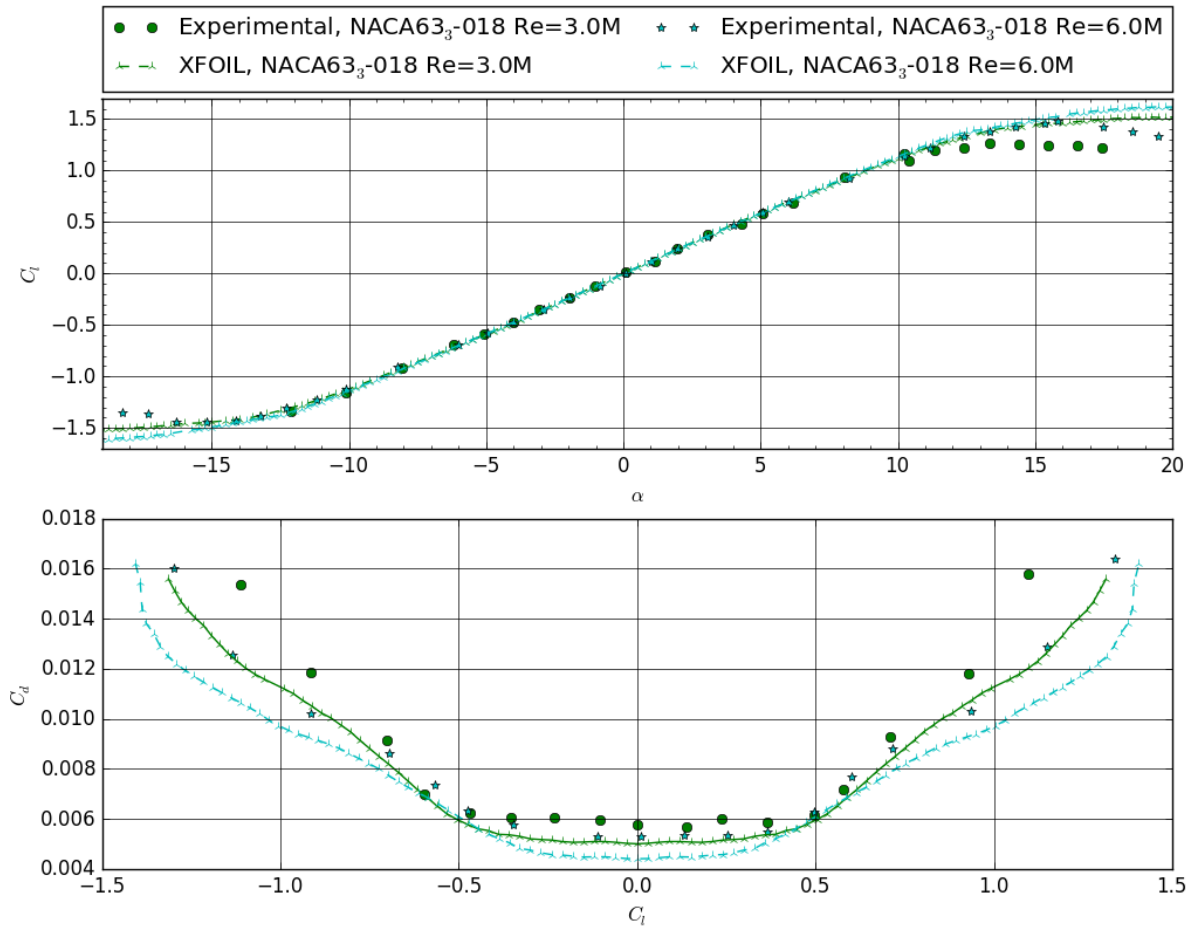


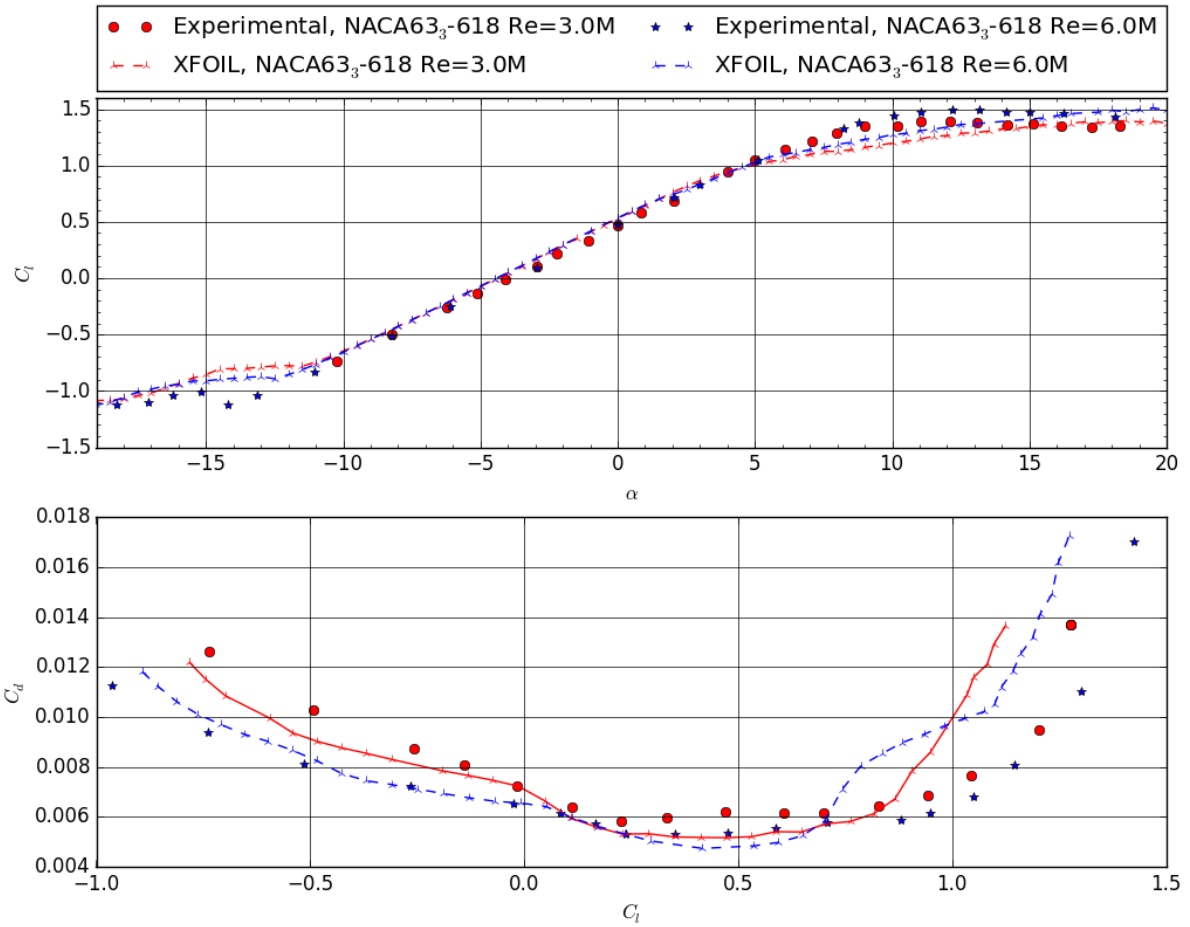
Figure 4.4: Lift and drag performance of the planform (wing and tail) resulting from the XFLR5 VLM2 analysis, at takeoff (15.3 m/s), cruise (20.6 m/s), landing (15.1 m/s) and stall (12.7 m/s)



(a) NACA 23018



(b) NACA 633018



(c) NACA 633618

Figure 4.5: Comparison between experimental data and computed data from XFOIL for the airfoils used in the aircraft design.

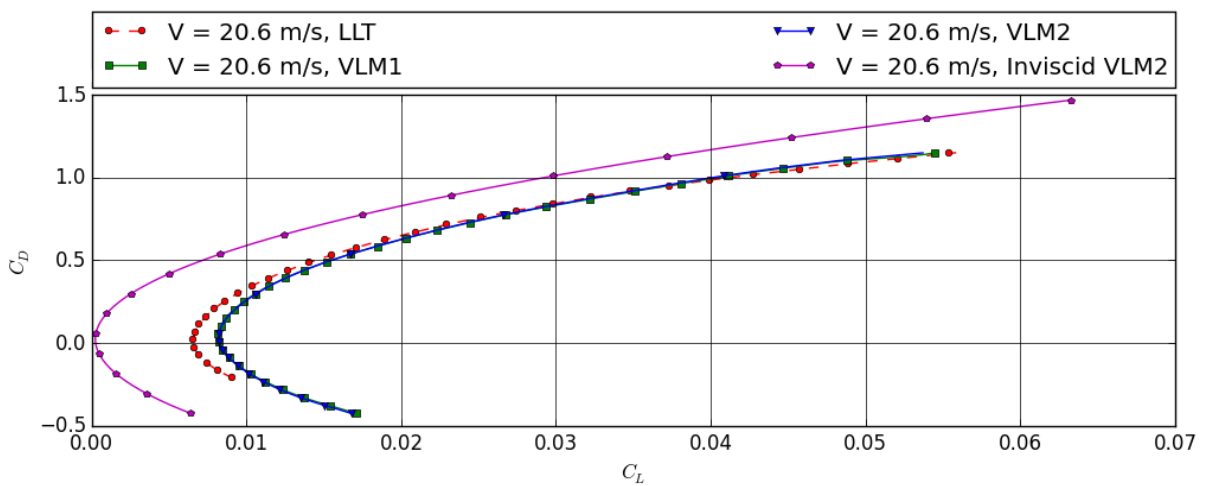


Figure 4.6: Lift and drag performance of the planform during cruise, compared between LLT, VLM1, VLM2 and Inviscid VLM2 methods.



# 5

## Performance and Power

### 5.1. Approach

For the detailed design phase, the performance and power of the aircraft was further examined. The design for the power part will be split into two separate parts. The first part consists of the design of the propeller and second part of the design of the integrated pedal system, including the engine and the battery. For the performance part all the performance parameters will be calculated.

#### 5.1.1. Propeller

For the propeller design, a choice had to be made between designing a new propeller or using a suitable existing propeller. A study was performed on the performance of existing propellers and it was found that there are no suitable propellers for the specific case of the Velo-E-Raptor, due to the noise requirement. There are propellers available that are designed for low noise, but these propellers operate at higher flight velocities and are therefore outside the scope of the Velo-E-Raptor<sup>1 2 3</sup>. To design a new propeller, multiple design choices had to be made. These will be explained below.

#### Number of Propellers

Before the propeller can be designed first the number of propellers had to be determined. Three options were considered: two or four propellers, or having distributed electrical propulsion (DEP). Adding more propellers adds weight, because more propellers and motors are added. Although the propellers and motors cause for a bending relief on the spar, more support structure is needed. So having more than two propellers is not beneficial to reduce the weight of the aircraft. However, adding more propellers will increase efficiency, because the disc loading of the propellers will decrease, as a larger total disc area can be created [28]. Also more propellers means more of the accelerated air will flow over the wings increasing lift. When more propellers are added on the leading edge of the wing, they have to be placed closer to the wingtip. This will make it harder for the pilot to balance and handle the aircraft on the ground. Also more protective structure is needed to keep these propellers from hitting the ground.

---

<sup>1</sup><https://whirlwindpropellers.com/airboats/shop/razor-x/>

<sup>2</sup><http://www.dtic.mil/dtic/tr/fulltext/u2/779773.pdf>

<sup>3</sup><http://www.up.ac.za/media/shared/Legacy/sitefiles/file/44/2163/8121/innovate2/inn2bl6263.pdf>

The main advantage with DEP is the fact that the wing size can be designed for cruise flight, instead of takeoff and landing [34]. The increased airflow over the wing, due to DEP, will increase the lift enough to meet the takeoff requirement even with a smaller wing. When the aircraft is in cruise flight the DEP shuts off and only the propellers on the wingtip will provide thrust. This means either the propellers, except for the propellers on the wingtip, have to be foldable or will significantly increase drag when switched off. Because the Velo-E-Raptor needs to be able to glide, having smaller wings than conventional hang gliders is not beneficial.

### Number of Blades

Another design parameter is the number of propeller blades. Increasing the amount of propeller blades has a positive effect on noise levels, but a negative effect on the efficiency. When the number of blades is increased the loading per blade is decreased, hence lower pressure difference between the front and the back of the blade [49]. A lower pressure difference will result in a lower noise level. When having more than one blade the blades will interfere with each other. This interference will make the propeller less efficient.

### Propeller Radius

One design parameter which improves noise levels as well as efficiency is disc loading. A lower disc loading will result in less noise, as there is less pressure difference. Furthermore, a lower disc loading means a relatively large amount of air is accelerated a small amount, which is more efficient than a small amount of air which is accelerated a large amount [28]. Because the aircraft should be as quiet as possible during the cruise phase, the cruise speed is used for determining the disc loading.

To determine the radius of the propeller, use was made of the blade element momentum (BEM) theory. This method estimates, using the conservation of momentum, energy, and mass, the thrust that a propeller will produce. From this theory, the optimal twist and chord could be determined. To do this, 2D airfoil data will be used and corrected with the Prandtl tip corrections for 3D effects.

The first parameter that needs to be calculated is the thrust coefficient  $C_T$ . This value was estimated using equation (5.1). The  $C_T$  was optimized for low noise and is only dependent on the amount of blades (B) [4].

$$C_T = 0.1\sqrt{B} \quad (5.1)$$

From the  $C_T$  value, the radius of the disk can be found. This is calculated using equation (5.2). As the propeller was optimized for optimum performance during cruise, the design thrust of the propeller is known. Therefore, the disk area of the propeller can be calculated. From the disk area, the radius of the propeller can be found [58].

$$T = \frac{1}{2}\rho V_{cruise}^2 C_T A \quad (5.2)$$

### **Tip Speed**

The tip speed of the propeller blades is an important design parameter, especially when looking at noise levels. The tip speed of a propeller is dependent of the radius of the propeller and the rotational speed. The efficiency of a propeller is practically unaffected by tip speeds up to the transonic regime. When the tip speed exceeds about a Mach number of 0.85, the flow over the blades partially become supersonic and cause a shock wave which can separate the flow. This separation will decrease the efficiency of the propeller drastically and should be avoided [42].

When looking at noise levels, an increase of tip speed will cause an increase in noise levels. Especially when the tip speed exceeds the critical Mach number. The same shock waves that causes the efficiency to drop will create a significant amount of noise and should be avoided [8]. Because noise levels become lower with lower tip speeds, it is beneficial to keep the tip speeds as low as possible [42].

### **Airfoil**

For the airfoil selection, it is important to select an airfoil that is optimized for the Reynolds number in which the propeller will operate. Furthermore, it is desirable to have an airfoil that has a large range of angle of attacks for which a good performance is achieved, as the propeller has to work in multiple speed regimes.

### **Propeller Twist and Chord**

The first step to calculate the twist and chord was to calculate the desired axial induction factor. This factor is a ratio between the speed of the incoming and outgoing flow. The axial induction factor could be determined using equation (5.3). As can be seen the optimal axial induction factor is only dependent on the thrust coefficient  $C_T$  [58].

$$a = \frac{1 - \sqrt{1 - C_T}}{2} \quad (5.3)$$

When the radius of the disk was calculated, the chord and twist for each blade element were calculated. This resulted in a calculated axial induction factor, from which the chord and twist could again be calculated. When the calculated axial induction factor converged to the desired axial induction factor, the chord and twist were saved and the chord and twist of the next blade element were determined.

When all the local lift and drag values were determined, these values were converted to the local thrust and torque of the propeller. These values for all the segments were summed and multiplied by the number of blades. This gave the total thrust and power usage of the propeller and the total efficiency could be calculated

### **Off Design Efficiency**

For the designed geometry of the blade, also the the efficiencies of the off-design rational speeds needed to be calculated, as the propeller also needs to operate in other speed regimes than the cruise speed. Therefore, a plot will be made that show how the propeller behaves in the off-design speed regimes.

## **Material**

A suitable material of the propeller had to be chosen, that is able to withstand all the force on the propeller and is lightweight. The three different materials that will be considered are oak wood, aluminum and Carbon Fiber Reinforced Plastic (CFRP). Furthermore, the attachment of the blades to the hub was considered.

## **Noise**

Because the noise requirement is a driving requirement, the main focus of the propeller design is to make it as quiet as possible. Furthermore, due to the weight and performance requirements, a balance has to be found between efficiency and noise. It was found that the design options which would improve noise levels had a negative effect on the efficiency of the propeller [72]. After the propeller was designed, the noise of the propeller was analyzed. For this analysis the method described in [4] is used. It should be noted that this approach does not include the interference noise with the wing, therefore the total noise from the propeller will be higher than that was calculated.

### **5.1.2. Power System**

After the propeller is designed, this propeller can be integrated into a full power producing system. This system includes a pedal system, battery, engine and the propellers. These components need to be connected to each other and a control system has to regulate the system.

#### **Pedal Mechanism**

First, a decision had to be made on how the power output of the pilot is converted to the power output of the aircraft. This can be done in several ways. It is possible to connect the pedals mechanically to the propeller and amplify this to reach the desired output. A second way is to add a dynamo to the pedals that will charge the battery. Lastly, just a power measuring instrument could be connected to the pedals. In this case the power output of the pilot will not be used or stored, but only as input for throttle control.

#### **Battery**

After determining how to convert the power output from the pilot to the power output of the aircraft, the engine and battery can be chosen. From the performance part, the required power output and battery capacity of the aircraft is known. With these values, a battery with the correct characteristic can be chosen. For the battery the most important parameter is the battery capacity in combination with the energy density, therefore this parameter dominated the battery selection.

Because of the harsh weight requirement, using lead acid batteries is not an option, because these would make the aircraft simply too heavy. Therefore a more modern lithium-ion battery is used, which has a higher energy density. There are different kinds of lithium-ion batteries of which lithium cobalt oxide, lithium iron phosphate and lithium titanate are of interest for the Velo-E-Raptor.

Lithium cobalt oxide (LCO) batteries have a high energy density between 150 and 200 Wh/kg. These batteries are not expensive as they are used in every day items such as laptops and cell

phones and they have an average cycle life of about 600 to 1,000 cycles<sup>4</sup>. Because the LCO batteries looked for are optimized for reliability and cycle life instead of energy density a cycle life of 1,000 will be considered. The disadvantage of these batteries is the fact that they need to be carefully designed for this aircraft because these batteries are more sensitive to have a thermal runaway than the other types. In case of a penetration by sharp object, for example a nail, the temperature will rise but a thermal runaway will not occur [33].

Lithium iron phosphate (LFP) batteries have a moderate energy density between 90 and 120 Wh/kg. They are more thermally stable and less prone to a thermal runaway than lithium cobalt oxide batteries and more tolerant to abuse. In case of a penetration by a sharp object, for example a nail, the battery will have a slight increase of temperature but like the LCO battery no thermal runaway will occur [31]. The batteries have a good cycle life of 1,500 cycles but it is essential to make sure the batteries get contaminated with dirt and especially moisture. If these get contaminated with moisture a cycle life of 50 can be expected.

Lithium titanate (LTO) batteries have a relatively low energy density between 70 and 80 Wh/kg. Although the energy density is low they can be charged faster than the other lithium-ion battery types. The cycle life of these batteries is 3,000 to 7,000 cycles which is high but the cost of these batteries are substantially higher compared to LCO and LFP batteries. Like LFP batteries they are thermally stable and less prone to a thermal runaway<sup>5</sup> [26]. Even in case of a penetration, like the LCO and LFP batteries, no thermal runaway will occur [16].

### **Throttle**

For the throttle control, an intuitive way of setting the throttle setting needs to be found. The way this is done is mostly focused on making the throttle control as intuitive and lightweight as possible

### **Motor**

An off-the-self motor will be used, as there are multiple electric motors available on the market that fulfill the requirements for the Velo-E-Raptor.

## **5.1.3. Performance**

The performance parameters of the aircraft were calculated using an analytical method. These methods include Raymer and Ruijgrok methods. [38] [9]. Some input values are needed to calculate the performance parameters. These values were taken from the requirements, or calculated in the aerodynamics department in chapter 4 and the stability and control department in chapters 6 and 7. These values can be found in table 5.1. From these parameters and the flight envelope, the performance parameters could be calculated.

---

<sup>4</sup>[https://batteryuniversity.com/learn/article/types\\_of\\_lithium\\_ion](https://batteryuniversity.com/learn/article/types_of_lithium_ion)

<sup>5</sup>[http://batteryuniversity.com/learn/article/types\\_of\\_lithium\\_ion](http://batteryuniversity.com/learn/article/types_of_lithium_ion)

Table 5.1: Input values from other departments

	Value	Unit
Max. lift coefficient	1.1	–
Zero lift drag	0.0401	–
Mass	65.1	kg
Aspect ratio	11	–
Oswald factor	0.85	–

## 5.2. Results

### 5.2.1. Propeller

#### Number of Propellers

The choice between two and four blades was done first. The extra weight, protective structures and the difficult balancing of the aircraft did not weigh up to the better efficiency, as the weight is the most limiting factor in the design of the Velo-E-Raptor. Therefore, two propellers are used.

#### Number of Blades

The Velo-E-Raptor will have propellers with five blades. A propeller with five blades has the best balance between noise and efficiency. Experimental data from research on propeller noise shows the relation between number of blades, noise levels and efficiency. The difference in the peak efficiency for a three, five, seven and nine bladed propellers is about 1%, however this is for the optimum tip speed of each propeller. When the tip speed is increased or decreased with 0.1 Mach it is shown that a three and five bladed propeller maintains a high efficiency and drop a maximum 1% while the efficiency of a seven nine bladed propeller will drop a significant 5% [2] [15]. Furthermore, it was found that other quiet aircraft, such as the Lockheed YO-3A quiet star also have five blades<sup>6</sup>.

Another advantage of having five blades is that five is an odd number. When the propeller is placed close to the leading edge of the wing and having an even amount of blades, the blades will interfere with the leading edge. Two of the blades will pass the leading edge at the same time creating noise. When the propeller has an odd number of blades this interference will be less, hence be more quiet [69].

#### Propeller Radius

The aircraft should be the quietest when it is closest to the ground. Because on average the ground in the Netherlands will be at approximately sea level, the air density used, will be  $1.225 \text{ kg/m}^3$ . Using the calculated thrust coefficient, which is equal to 0.223 for five blades, and using the needed thrust for cruise, the disc area and propeller radius were determined. The thrust for cruise is equal to 165 N. This results in a disc area of  $1.4 \text{ m}^2$  per propeller, and a propeller radius of 0.67 m.

<sup>6</sup>[http://barthworks.com/aviation/aviation\\_boeing\\_museum/2014\\_05\\_boeingmuseum09\\_yo\\_3a/2014\\_05\\_boeingmuseum09\\_yo\\_3a.htm](http://barthworks.com/aviation/aviation_boeing_museum/2014_05_boeingmuseum09_yo_3a/2014_05_boeingmuseum09_yo_3a.htm)

## Tip Speed

A tip speed of 0.2 Mach was chosen as a benchmark for the propeller. The tip speed of 0.2 Mach was chosen because the Lockheed YO-3A "Quiet Star" and modern wind turbines also use this tip speed as a benchmark due to noise requirements [58] [20]. Having a propeller radius of 0.67 m and a tip speed of Mach 0.2 results in a design RPM of 975. From the RPM, the advance ratio,  $J$ , of the propeller could be calculated. The design advance ratio is equal to 0.94.

## Airfoil

The propeller is designed to have a relatively low tip speed of 0.2 Mach. This means the flow going over the whole length of the propeller blade is slow and has low Reynolds numbers. For this reason it is important to have an airfoil which has good performance for these low Reynolds numbers. Therefore, the Clark-Y airfoil is used. This airfoil has a  $C_l/C_d$  that varies between 30 and 53 for Reynolds numbers between 50,000 and 100,000 [25]. Another airfoil that matches these performance is the RAF-6 but in order to get these performance it is critical to have the airfoil under an angle of attack of 3.5 degrees. When the angle of attack deviates from this optimum angle, the performance rapidly decreases. The Clark-Y has a larger range of angles for which it has good performance which is more beneficial <sup>7</sup>.

Another advantage of the Clark-Y is the fact that it is an old airfoil, which has been very popular especially during the second world war. Because of this there is a lot of experimental data available for this airfoil, which could be used for designing the propeller for the Velo-E-Raptor.

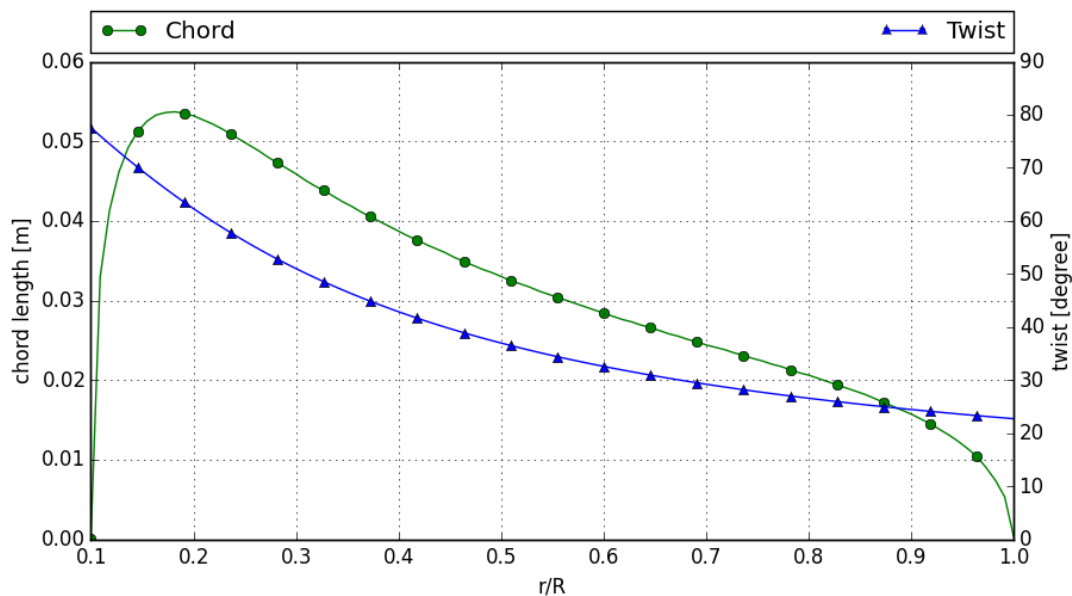


Figure 5.1: The chord length and twist of the propeller over the span of the blade

## Propeller Twist and Chord

As all the input parameters are determined, the chord length and the twist of each propeller

<sup>7</sup><http://airfoiltools.com/airfoil/details?airfoil=clarky-il>

could be determined. The results can be seen in figure 5.1. As can be seen in this picture, the chord length of the blades are relatively low compared to existing low noise propellers. This can be explained by the large amount, ten blades, used for the Velo-E-Raptor. To reach the desired thrust, the blades can have a small chord length, but still have a small disc loading.

### Off Design Speed Efficiency

The propeller is designed to work the most efficient at cruise speed, however the propeller has to work at other speed than the design speed. Therefore, the efficiency at other advance ratios is determined. The result of this analysis is presented in figure 5.2. The advance ratio is a ratio between the cruise speed and the rotational speed of the propeller. A larger advance ratio means a slow rotating propeller with respect to the flight speed. When the advance ratio of the propeller is lower than 0.25, the propeller will stall. As there is no reliable stall characteristic of the airfoil known, the efficiency for advance ratios lower than 0.25 could not be determined.

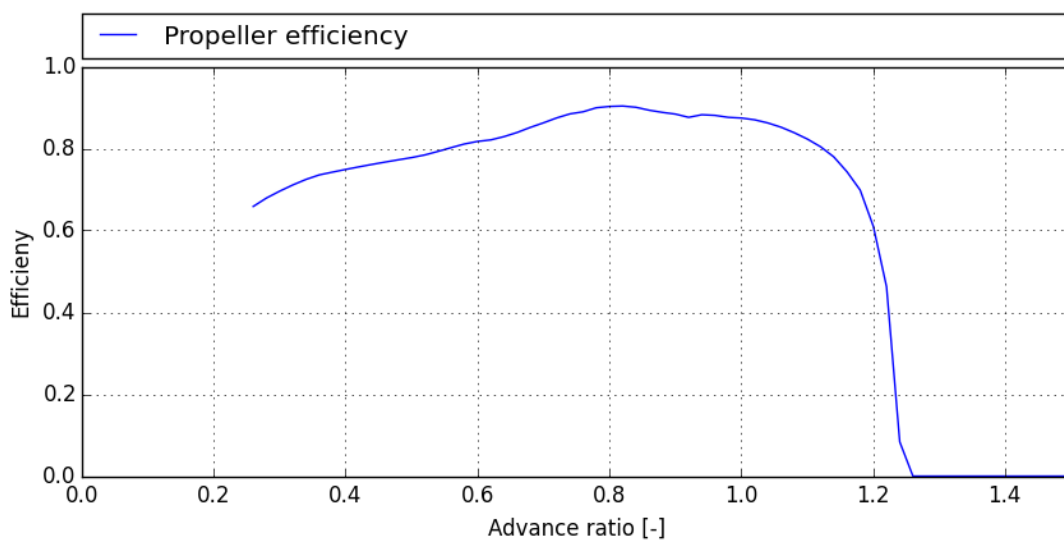


Figure 5.2: The efficiency versus advance ratio

### Material

The propeller will consist of five blades and a hub. The blades will be made from carbon fiber. This material is lightweight and strong. This reduces the weight of the propeller and makes sure the propeller can handle the aerodynamic forces. The hub will be made of aluminum. Aluminum is also a light weight material and is ideal to make complex shapes. Therefore a hub can be made that will allow the blades to be individually attached. This is beneficial for both the cost and ease of maintenance and sustainability because in case of damage only one blade has to be replaced.

### Noise

From [4, p. 173 - 188] the propeller noise, during the cruise phase of the aircraft, is calculated. To do this, the unsteady blade loading noise and the random noise production is evaluated. The steady blade loading is not taken into account. This turned out to be negligible as the sound pressure level of this loading is 20 db(A) lower than the other sound sources.

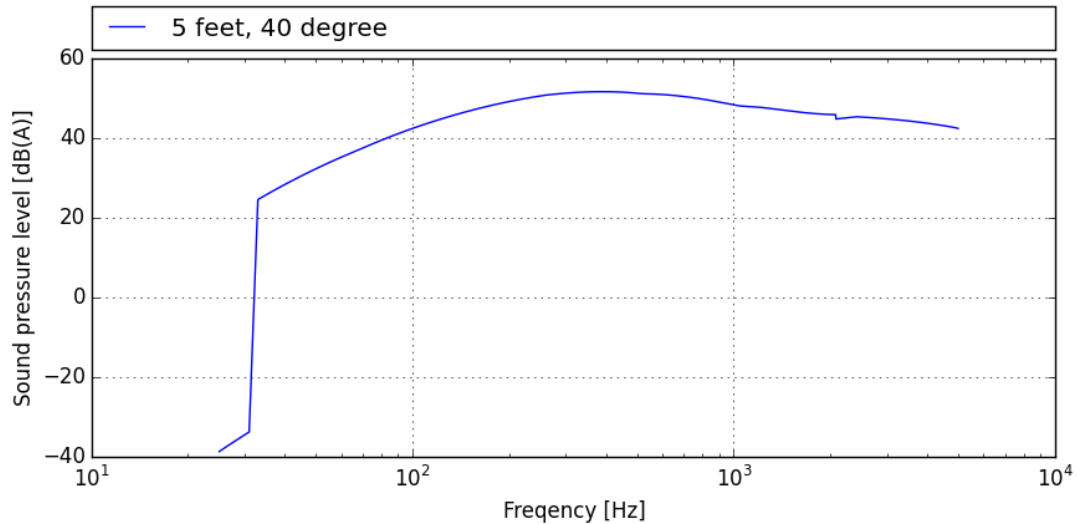


Figure 5.3: The sound produced by the propeller at different frequencies

After the sound pressure levels were calculated and added, an A-weighting was used to compensate for the relative loudness perceived by the human ear. The result of this can be seen in figure 5.3. The distance from the sound source is chosen to be 5 feet, as this is approximately the distance of the pilot from the propeller. The angle between observer and forward propeller axis is chosen to be 40 degrees, as this is the angle on which the highest sound levels are observed.

## 5.2.2. Power system

### Pedal Mechanism

The pedal mechanism does not directly power the propellers and is not directly connected to them. Especially because there are two propellers on the leading edge of each wing, connecting the pedal mechanism, would not be an efficient approach. Instead, the pedals are connected to a dynamo which will turn the rotational energy into electrical energy. This electrical energy is then stored inside the batteries from which it can be used to power the propellers. This approach will save weight, because no complex chain drive and support structure is needed. The throttle control will also be done using the pedals, as explained later in this section.

Another advantage of not being directly connected to the propellers is that in case of a pedal mechanism failure the propellers will not be affected because they can fully operate completely independent, as the only thing connecting them is an electrical wire. Also, it is safer for the pilot because he or she is not directly attached to two powerful electrical motors.

The pedal mechanism itself consists of bicycle pedals with toe clips connected to a crankset. The crankset is connected to the dynamo with a serpentine belt. Not only is a serpentine belt lighter than using a regular chain but also needs less maintenance and lubrication. Like on a bicycle the serpentine belt is connected in a certain gear ratio. The gear ratio can be changed to the pilots preference. This has to be changed before flight because due to weight requirements an in flight gear changing mechanism will add to much weight to the aircraft.

The location of the pedals will be adjustable, so pilots with different heights can move the pedals to their ideal spot. This will improve the accessibility and comfort.

Both the crankset and the dynamo are attached to the frame of the Velo-E-Raptor. The toe clips make sure the feet of the pilot stay on the pedals as long as the pilot wants to. This is especially helpful since the pilot is pedalling in a prone position, the pilot basically hang their feet into the pedals. It was not chosen to use clipless pedals because these require special kind of shoes, are harder to connect to during flight and are less intuitive to use.

### **Battery**

Because of the 70 kg weight requirement, the GSYUASA LSE serie lithium cobalt oxide batteries<sup>8</sup> are chosen for the Velo-E-Raptor. The requirement forces the batteries to have a minimum energy density of around 150 Wh/kg. The batteries are designed to have a good cycle life and be reliable as they are design for space applications. They have an energy density of 146 Wh/kg which is on the low end for LCO batteries but this is the case because they are designed to be safe instead of pushing the energy density. However, LCO batteries are generally thermally less stable, and much care has to be taken into designing the full battery system. A properly designed battery system will reduce the risk of overheating and a thermal runaway.

### **Throttle**

The throttle can be controlled on two ways. The first one is using the pedal mechanism and the second is the throttle control unit on the control bar.

The pedal mechanism is used to give the pilot an intuitive way to control the throttle. Like on a bicycle, when the pilot puts more effort into pedalling, the propellers will give more thrust. Because the pilot uses his legs during takeoff an alternative to the pedal mechanism is needed. This is the throttle control unit on the control bar. This way the pilot can control the throttle without pedalling or using his legs.

Both these throttle mechanism are connected to a throttle control computer. This computer gets throttle inputs converts them into an input signal for the electrical motors. This throttle control computer allows the pilot to select different modes and change settings. The pilot can select if he want to control the throttle with the pedals, the throttle control unit or a cruise control so the aircraft will maintain a selected airspeed. Also the pilot is be able to select the power amplification factor, the factor by which the input power of the pedal mechanism will be amplified by the electrical motors.

### **Motor**

The propellers are driven by two electrical motors, one for each propeller. The electrical motors used are two Hacker A150-8's<sup>9</sup>. These motors are design for large scale radio controlled aircraft and have a peak power of 9,000 Watt and a maximum RPM of 8,000. The electrical motors are located inside the wing behind the leading edge. In between the propeller and the motor a planetary gearbox is placed to reduce the high RPM of the motor to maximum

<sup>8</sup>[http://www.s399157097.onlinehome.us/SpecSheets/GSYuasa-LSE50\\_100\\_175.pdf](http://www.s399157097.onlinehome.us/SpecSheets/GSYuasa-LSE50_100_175.pdf)

<sup>9</sup><https://hackermotorusa.com/shop/hacker-brushless-motors/outrunners/a150-8/>

propeller RPM of 3674, as this is the highest possible RPM that could be reached in flight.

The peak power is the maximum power the motor can produce for only 15 seconds. After the 15 seconds, the motor will start to overheat. The motors have a continuous power of 5,920 W. This means the motors can not be overloaded during takeoff and the motor will never be pushed to the extreme. This will increase the durability and reliability of the motor. Also, because the motor is never pushed to its absolute limit there is a lower risk of overheating. Because the motor is located inside the wing there is no airflow which can cool the motor. Therefore each motor is water cooled. This way the motor can be cooled because the water is cooled with a small radiator placed on top of the wing.

Because the motors are placed inside the wing the noise produced by these motors will be damped and reduced. This is beneficial because the Velo-E-Raptor is designed to be as quiet as possible. Placing the electrical motors inside the wing will also protect the motors from the rain and dirt.

### **5.2.3. Performance**

To calculate the performance parameters, some assumptions had to be made. As the aircraft will be designed for the Dutch market, takeoff and landings are always performed at sea level. Furthermore, as there is no requirement for landing distance, this distance is set to 80 meters. Also, it was determined that the maximum load factor that the aircraft could sustain without losing altitude was 2. Finally, a safety factor was used for takeoff and landing speeds. Both the takeoff and landing lift coefficient was set to 10% below the maximum lift coefficient. Therefore, the takeoff and landing speeds are 1.21 times the stall speed. Using the maximum lift coefficient from chapter 4, this results in a takeoff and landing lift coefficient of 1.1.

#### **Wing Size and Required Power**

Using these assumptions, the results of this analysis could be calculated and can be found in figure 5.4. In this figure the most critical flight conditions were evaluated. It was found that the most critical flight conditions are the takeoff and landing, because of the short takeoff and landing distances. The feasible design region is marked with a light red color and the design point is marked with a bright red dot. This resulted in a wing loading of  $111.4 \text{ N/m}^2$  and a power loading of  $0.1224 \text{ N/W}$ . When the takeoff weight, as explained in section 8.4.4, were divided by these loadings, the wing size and minimum required power were calculated. These are the minimum values to fulfill all the desired flight operations and are equal to  $13.21 \text{ m}^2$  for the wing surface and  $12.03 \text{ kW}$  as the required power output.

#### **Design Speeds**

After the wing size and power estimations were performed, the optimal flight speed could be determined. To do this, the drag calculations from chapter 4 and wing geometry from chapter 6 were used. The maximum lift coefficient was used to calculate the stall speed. After the stall speed was determined, the drag and required power at each speed were calculated and presented in figure 5.5 and figure 5.6. From these diagrams, the maximum speed for powered, horizontal, steady and symmetric flight could be obtained. Furthermore, the speed for minimum drag and power and the corresponding drag and power required could be de-

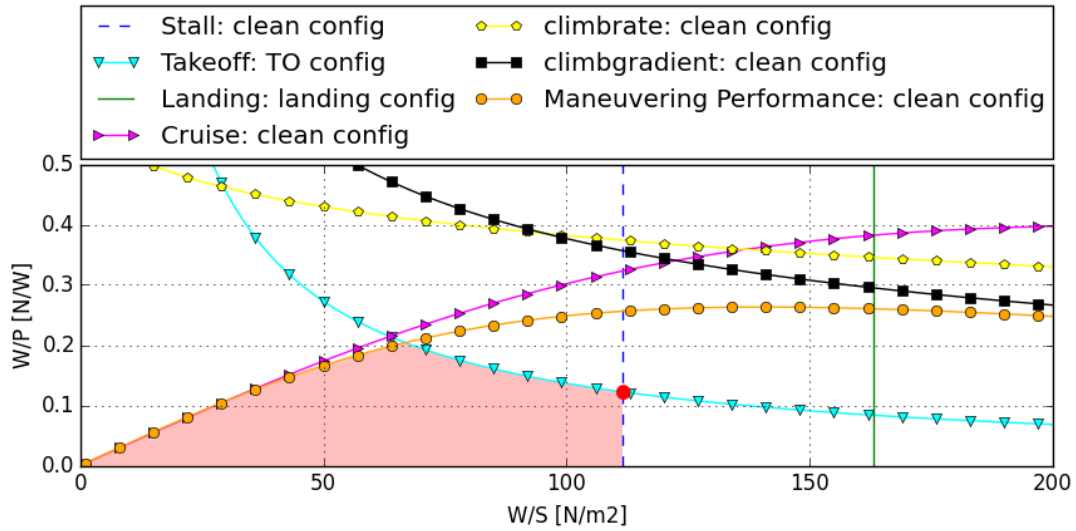


Figure 5.4: Wing loading versus power loading

terminated, these speeds are indicated with a vertical yellow dashed line. Moreover, the glide ratio at minimum drag speed was calculated. However, the flight speed for minimum power is below the stall speed and the minimum drag speed is within 1 m/s to the stall speed. As this could lead to very dangerous situations, it was decided that all the flight operations that preferably would be performed at minimum power and drag, are performed at 1.21 times the stall speed for a safety margin. All the result from this analysis can be found in table 5.2

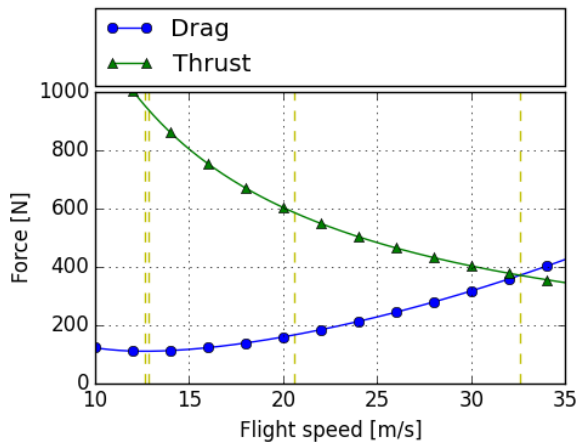


Figure 5.5: Force versus flight speed

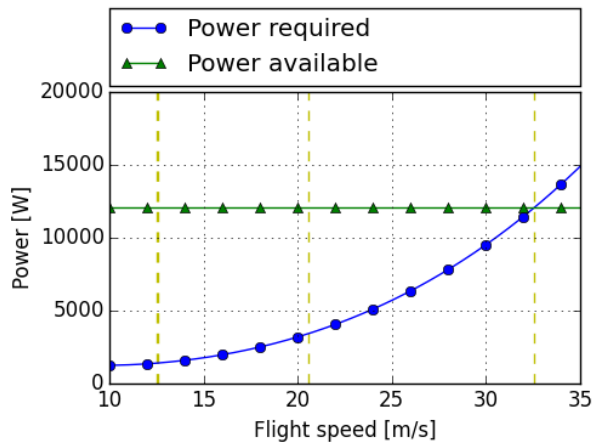


Figure 5.6: Power versus flight speed

### Turn Performance

The turn performance of the aircraft was evaluated after the symmetric case. From the maximum load factor it was determined that the maximum bank angle of the aircraft is 60 degrees. From the flight envelope, which can be found in figure 5.7, the minimum speed for which the load factor of 2 can be reached could be obtained. With this stall speed, the minimum turn radius can be found for a load factor of 2. Also the minimum speed to fly at the maximum load factor before structural damage occurs can be found at in the flight en-

Table 5.2: Performance Parameters

	Value	Unit
Stall speed	12.56	m/s
Maximum speed	32.59	m/s
Minimum drag speed	12.64	m/s
Minimum power required speed	9.607	m/s
Minimum drag	108.7	N
Minimum power	1206	W
Lift coefficient at min. drag	1.085	–
Lift coefficient at min. power	1.879	–
L/D at min drag	13.5	–

velope, as well as the maximum flight speed. The gust envelope can also be found in figure 5.7. However, due to the small weight of the Velo-E-Raptor and the low flight speeds, the gust envelope does not show load factor above 2. The results from the flight envelope and turn performance can be seen in table 5.3.

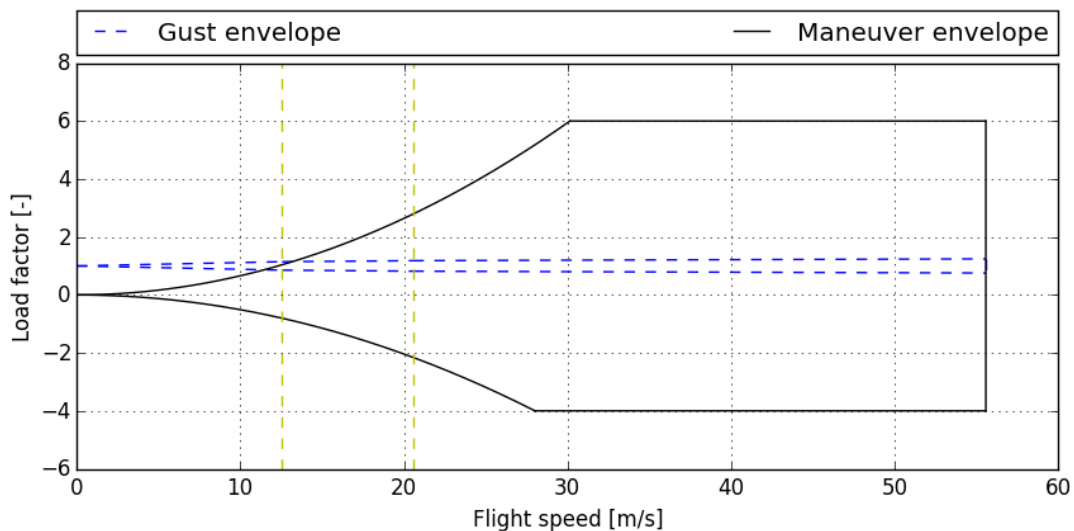


Figure 5.7: Flight envelope

### Climb Performance

Finally, the climb performance of the Velo-E-Raptor is calculated. Two parameters are determined for the climb performance: the power usage for a 1.3 m/s climb rate and the maximum possible climb rate. As mentioned before, these maneuvers will not be performed at the minimum power speed, but at 1.21 times the stall speed for safety reasons. The results of this analysis can be found in table 5.3.

## 5.3. Power Allocation and Electrical Block Diagram

As all the power consuming components of the Velo-E-Raptor were determined, the Power allocation could be made. In table 5.4 all the power consuming components are shown with

Table 5.3: Speeds and minimum turn radius at different load factors and climb performance

	Value	Unit
Min. speed @ load factor of 2	17.76	m/s
Min. speed @ load factor of 6	30.76	m/s
Minimum turn radius @ LF of 2	15.58	m/s
Minimum turn radius @ LF of 6	16.31	m/s
Power usage @ ROC 1.3 m/s	3653	W
Max. ROC	6.99	m/s

their corresponding power usage and the time they are used. If these values are multiplied, the required energy of that component could be calculated. When all the required energies of the components are added, a total of 0.979 kWh is needed. This is the minimum energy that needs to be stored in the batteries. For the propulsion battery, a capacity of 0.870 kWh is needed. To reach this, two batteries of 0.407 kWh and one battery of 0.204 kWh is used. The extra capacity makes sure that it is not only possible to cruise, but a climb could also be performed. The total mass of these batteries is 7.08 kg. For the non propulsive battery only a capacity of 0.1090 kWh is needed. One battery of 0.204 kWh and 1.50 kg is sufficient for this purpose. A summary of the batteries can be found in table 5.5.

Table 5.4: Energy consumption of all the components

	Amount	Power usage [kW]	Time usage [h]	Energy req. [kWh]
Engine - 30 min. cruise	2	1.7	0.5	0.870
Actuators	9	0.007	1.0	0.063
Computer	2	0.001	2.0	0.004
Instrumentation	2	0.003	2.0	0.012
Communication	1	0.015	2.0	0.030
Total power				0.979

Table 5.5: Energy capacity of all the batteries

	Min. energy [kWh]	Batteries used	Capacity [kWh]	Weight [kg]
Propulsion bat.	0.999	2 x 0.407 1 x 0.204	1.019	7.08
Non-propulsion bat.	0.109	1 x 0.204	0.204	1.50

As the batteries and the power consuming components are known, the electrical block diagram could be made. In figure 5.8 the electrical block diagram can be seen. In this diagram all the power consuming components and the batteries are depicted.

From the rotation of the pedals the generator will generate electrical energy for the battery that is connected to the engines. These engines will convert the electrical energy back to rotational energy. The second function of this battery is to be able to charge the battery that

is connected to all the non propulsive components, if this battery is drained. This is done because if these systems will run out of battery, the aircraft will not be controllable anymore. Therefore, this extra charging possibility makes sure a redundant system is created. The non-propulsive battery provide energy to all the non-propulsive components, such as the actuators of the control surfaces and the stick, the flight computer, instrumentations and the communications systems.

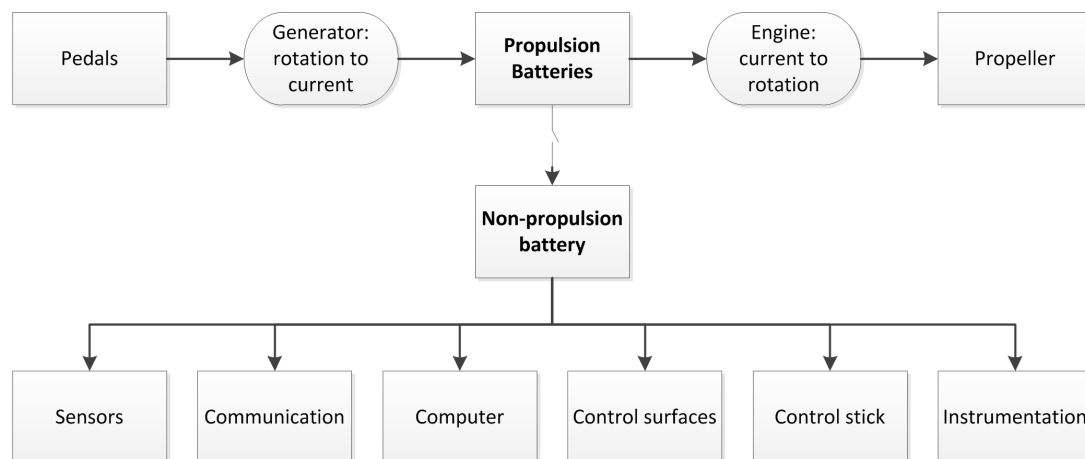


Figure 5.8: Electrical block diagram for the Velo-E-Raptor

## 5.4. Verification and Validation

### 5.4.1. Verification

#### Propeller

Besides a thorough check of the code that was written to calculate the propeller parameters and noise values, the results from the propeller optimization and efficiencies for the different advance ratios are compared. As the optimized propeller is used for the calculation for the different advance ratios, the highest efficiency in this analysis should occur at the advance ratio for which the propeller is designed. The design advance ratio for the chord and twist optimization case is 0.94, however from figure 5.2, it can be seen that the calculated optimal advance ratio is at 0.8. Though, the values of the efficiencies are the same. Therefore, it can be concluded that there is a possibility to optimize the code.

#### Performance

For the performance calculations, no simulations were performed. Only analytical equations from Raymer and Ruigrok were used. These equations were put in one Python script which calculated all the performance values at once. Using a unit check, the correctness of the inserted equations is checked and they all turned out to be correct.

### 5.4.2. Validation

#### Propeller

The total calculated efficiency of the propeller is 0.93. When comparing this to existing propellers, this number seems high, as 0.8 is a more common value for propellers. Especially,

as this propeller is optimized to minimize the noise and is not optimized to reach the maximum possible efficiency. This high efficiency could be explained by the methods that is chosen to calculate the performance of the propeller.

The propeller is designed using the BEM method. This method divides the propeller radially in a number of segments. On these segments the 2D lift and drag are calculated. As the 2D lift and drag is always a over estimation of a 3D case, these numbers are too positive. However, the method partially compensates for this overestimation by applying a tip and root correction. This correction assumes that no lift will be present at the tip and root due to the vortices that are present at the location. Though, not all the 3D effects are taken into account.

Furthermore, as the propeller rotates, airflow will not only pass the propeller in axial direction, but also in the radial direction. The BEM method does not take this velocity into account. Therefore, this assumption will also overestimate the efficiency of the propeller. Due to the overestimations of the program, it is chosen to use a propeller efficiency of 0.8, as this is a more realistic value.

The noise production of the propeller is compared with the noise production of the Lockheed YO-3A quiet star. It was found that the sound production of this aircraft is 54 dB(A) at a distance of 125 feet <sup>10</sup>. The results of the propeller prediction show a noise production of 51 dB(A) at 5 feet distance. This is significantly lower than the quiet star, but it should be noted that the interference noise and the noise from other parts of the aircraft are not taken into account in this analysis. Therefore, the noise of the total aircraft is underestimated and a the noise production of other components of the aircraft should be further investigated.

## **Performance**

To do the validation for the performance, the calculated performance parameters are compared to the performance parameters of existing hang gliders. The most complete parameter to compare is the glide ratio, as this parameters include a lot of other parameters, as it includes both the lift and the drag. When the glide ratios of other hang glider are evaluated, the calculated glide ratio is, with 13.5, on the the low side of found range. As current hang gliders can reach a glide ratio of 13 to 17 <sup>11</sup>. However, this relative low glide ratio can be explained by the fact that the pilot, propellers and the tail wings add some extra drag compared to more conventinal hangliders.

For the turn performance, the Velo-E-Raptor has a very comparable turn radius as other hang glider <sup>12</sup>. However, the climb performance is a bit high. This high climb performance can be explained due to the high power output of the propellers.

---

<sup>10</sup>[http://barthworks.com/aviation/aviation\\_boeing\\_museum/2014\\_05\\_boeingmuseum09\\_yo\\_3a/2014\\_05\\_boeingmuseum09\\_yo\\_3a.htm](http://barthworks.com/aviation/aviation_boeing_museum/2014_05_boeingmuseum09_yo_3a/2014_05_boeingmuseum09_yo_3a.htm)

<sup>11</sup>[http://www.hanggliding.org/wiki/A\\_Comparison\\_of\\_Hang\\_Gliding\\_to\\_Paragliding](http://www.hanggliding.org/wiki/A_Comparison_of_Hang_Gliding_to_Paragliding)

<sup>12</sup><https://www.ruppert-composite.ch/en/>

## **5.5. Conclusion**

The Performance and Power department designed a power system that is able to deliver enough power such that the Velo-E-Raptor can perform all its required maneuvers. A custom designed propeller was made, such that it produces as little noise as possible. However, this design could still be optimized to ensure the efficiency is higher and the noise could be calculated.

Besides the power system, the performance parameters of the Velo-E-Raptor were calculated and it was found that these parameters satisfy the needs of the project as well as the customer.

## **5.6. Project Development and Design Logic**

In this section a brief explanation will be given on the post-DSE activities of the Performance and Power department. All planned activities can be observed in appendix A, where an indication of time and resource allocation is given.

### **Design Detailed Battery System**

Not only the battery type is important for safety but also the layout of the full battery system. The way they are connected, how and where they are placed etc. Due to a lack of time and information during the DSE it was not possible to design this. To improve safety a further investigation has to be done on battery system management after the DSE.

### **Implement Safety Systems**

To further improve the safety of the Velo-E-Raptor multiple safety systems could be implemented into the design. A system can be made which detects propeller damage, for example by detecting vibrations caused by a broken propeller blade. The system will then automatically shut down both motors to avoid possible damage to aircraft and pilot. Or a system which detects damage on the motors because the internal resistance has changed or overheating of the motors or batteries and accordingly shuts down the motors. These kind of systems need to be further investigated after the DSE.

### **Quantify Noise and Optimize**

The design team put its bests effort to minimize the noise of the propeller. A first estimation of the propeller noise is performed. However, the total noise of the aircraft could not be quantified. Therefore, a way needs to be found to quantify the noise, without already building the propeller, as this could cost too much money. A way to estimate the noise, could be to make a complete CFD model that can estimate the pressure differences in the aircraft.

### **Design Energy Regeneration System**

When the propeller are not providing thrust, they are stopped. However, the kinetic and potential energy of the aircraft could be used to let the propellers spin. If they are used this way, they act like a windmill. The extra drag that is added by this system and the power output of the windmilling propeller should be investigated. If a great advantage is found, the system should be added to the Velo-E-Raptor.



# 6

## Stability

With safety as one of the most important requirements, stability and control is a key aspect of this design. From the requirements posed in the Baseline Report of this project [40], the goal is to design an aircraft that is both stable and controllable in all flight modes. As explained in section 3.4, this led to a system in which fly-by-wire controls ensure flight envelope protection. However, to make sure that the aircraft will be safe to fly even for inexperienced pilots, inherent stability is desirable. Because of this it was deemed necessary to first establish a stable aircraft, whose characteristics then functioned as an input for control. The complete control system will be treated in chapter 7.

### 6.1. Approach

For stability the initial design stage consisted of doing an in-depth literature study on the process of designing an aircraft to be stable, as well as the impact of certain design choices limited to Stability and Control (S&C). From this research a plan and schedule were made in collaboration with the system engineers and the other departments, leading to the final approach. It must be noted that the effect the pilot has on the design has not been fully taken into account in the analysis for stability. The complexity and unconventional nature of this configuration made it impossible to properly model this and no analytical methods sufficed either. This is a major simplification and it is not underestimated that this has an impact on the results. However due to limited time and resources, it has been made one of the top priorities in the post-DSE activities to determine these effects and compare the results to the model explained in the coming section.

#### 6.1.1. Program Selection

It was found that to do a proper stability analysis, finding reliable stability derivatives poses the biggest difficulty. No analytic or numerical methods exist that accurately describe these coefficients, as they are functions of the entire aircraft configuration and its response to disturbances. There are however different ways of estimating these values without doing extensive wind tunnel experiments. These include the well known, semi-empirical DATCOM method [64], as well as numerical tools such as CFD and the Vortex Lattice Method (VLM). After literary research it was decided that a combination of the programs XFLR5 and AVL provided the best means for doing a stability analysis. These are software packages that use the VLM method and allow for easy adjustment of parameters and a short computing time.



## Dynamic Stability

The dynamic stability analysis was done by looking at the eigenvalues of the eigenmodes and checking whether they were all negative and result in a damping ratio that allows for safe flight. A negative value indicates a dynamically stable and damped response to either pilot input or external disturbances. The vertical tail was sized such that the aircraft is laterally stable.

### 6.1.4. Control Surfaces

Once the aircraft was completely stable in cruise, the control surfaces were designed using mostly the AVL software package. The program allows the user to define control surfaces and see what deflection is needed to maintain a certain flight condition. First, as means of verification, it was checked whether the analysis done in XFLR5 for static stability was correct by modelling the final configuration including control surfaces in AVL. Constraints were set on the elevator deflection ( $\delta_e$ ) to provide zero pitching moment, and on the angle of attack ( $\alpha$ ) to provide the lifting coefficient expected at cruising velocity. Since the model was optimized for cruise and no pilot input, the expected output was a  $\delta_e$  of zero and an  $\alpha$  equal to the one found in XFLR5. When this was verified, different elevator and aileron configurations were tested to see if they were capable of providing the required pitch and roll rates when set to their maximum deflection angle. Important to note is that the assumption was made that these angular rates can be decoupled, resulting in only one control surface constraint at any moment.

The required pitch and roll rate were determined from literature as well as from team input. This resulted in a desired maximum roll rate of  $30^\circ/s$  ( $0.52 \text{ rad/s}$ ) and pitch rate of  $3^\circ/s$  ( $0.052 \text{ rad/s}$ ) [35]. These are relatively low angular rates for a light aircraft, however in line with the rest of the design they were chosen to improve the ease of use and safety of the Velo-E-Raptor. Furthermore, to make sure these rates can be reached in any flight phase, they were designed for takeoff and landing, where the velocity is lowest and the surfaces therefore less effective. The most important parameters that were changed in the process were spanwise length and percentage of the chord. Different maximum up and down deflections were set for the elevator and the ailerons. The elevator has a maximum deflection of  $20^\circ$  upwards and  $17^\circ$  downwards. The ailerons make use of differential deflection where the downward going aileron moves 0.75% of the way compared to the upward going surface. This is done to counter adverse yaw and results in a maximum upward deflection of  $35^\circ$  up and  $26^\circ$  down. With these deflections as constraints, the optimum configuration was then found iteratively.

Note that in order to analyze the control surfaces of a blended wing in AVL, an interpolated airfoil has to be used at the start of the control surface. This airfoil was created using the function INTE of XFOIL. This blend between the root and tip airfoil was found iteratively to be at an interpolation fraction of 0.15. This was checked by importing the airfoil into XFLR5 and comparing the  $C_m$ - $C_L$  curve to that of the aircraft with a completely blended wing. As can be seen in figure 6.2 it resembles the blended wing of XFLR5 as an approximation.

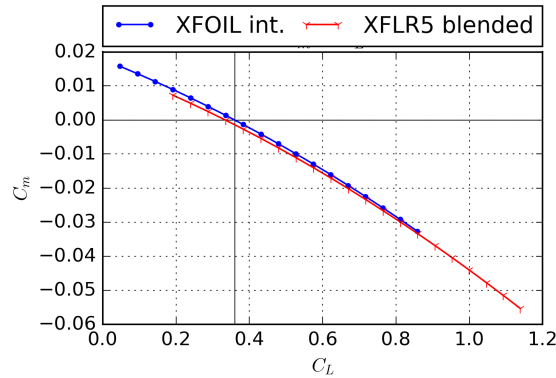


Figure 6.2: Results of  $C_m$ - $C_L$  for an interpolated airfoil between NACA 63<sub>3</sub>-618 and NACA 23018, as produced by XFLR5 and a manual interpolation, respectively

### 6.1.5. Stability and Control Derivatives

Having determined all the aircraft parameters this finally led to a set of stability and control derivatives and eigenvalues. To make sure that all the data recovered from these programs was reliable, a constant process of verification and validation was maintained. During the iterative process of refining the aircraft parameters, the results from both XFLR5 and AVL were compared. If any discrepancies existed they were analyzed and remedied before moving on to the next process phase. Since the control surfaces were designed using only AVL, this data was not verified as thoroughly. Though extra care was taken during validation it should be noted that this is something that can be improved in future research.

## 6.2. Results

As explained in the approach, the results and outputs expected for static stability were mostly certain aircraft parameters and the moment-lift curve. The final aircraft parameters, as seen in table 6.1 were found to give a stable aircraft. Figure 6.3(a) and figure 6.3(b) show the final  $C_m$ - $C_L$  and  $C_m$ - $\alpha$  curves for cruise, from which it can be seen that the aircraft is trimmed at an angle of attack of 3.3° and a  $C_L$  of 0.375, matching the requirements given by the Performance department. Furthermore it can be noted that a Stability Margin (S.M.) of 0.07 is relatively small<sup>1</sup>. This can be explained however by the small horizontal tail volume and the fact that the design pilot weight is more than the weight of the aircraft<sup>2</sup>[22]. The values for  $x_{c.g.}$  and  $x_{n.p.}$  should be taken as rough estimates using point loads, however they give a good initial estimate.

For the dynamic stability analysis, the eigenmode responses found are represented in table 6.2. Note that these are the responses as given by AVL, why this is will be further explained in section 6.3. From this table it can be seen that apart from the spiral mode, all modes have a negative eigenvalue and are therefore damped. The spiral instability is very minor and takes more than five minutes to double in amplitude. Also the aircraft will make

<sup>1</sup><https://ocw.mit.edu/courses/aeronautics-and-astronautics/16-01-unified-engineering-i-ii-iii-iv-fall-2005-spring-2006/systems-labs-06/spl8.pdf>

<sup>2</sup> <https://ocw.mit.edu/courses/aeronautics-and-astronautics/16-01-unified-engineering-i-ii-iii-iv-fall-2005-spring-2006/systems-labs-06/spl8.pdf>.

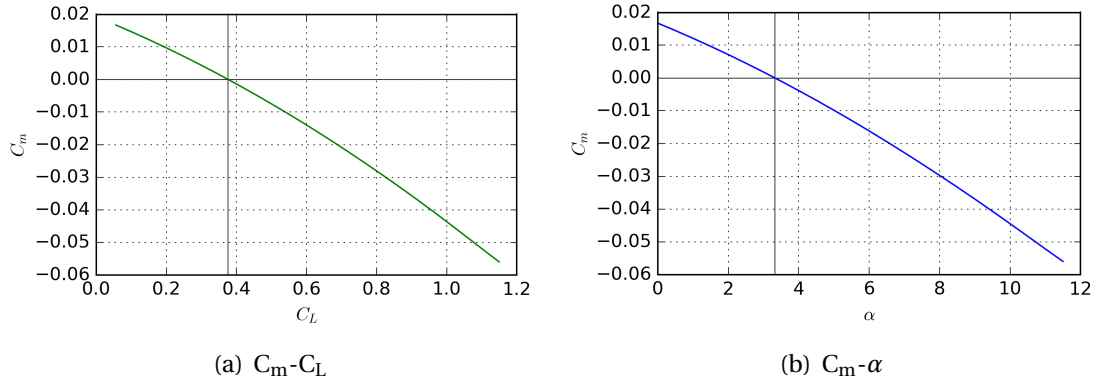


Figure 6.3: Moment curves of the final configuration

Table 6.1: Final aircraft parameters

	Value	Unit		Value	Unit
Sweep	9	°	Hor. tail volume coefficient	0.31	–
Dihedral	2.0	°	Ver. tail area	0.52	m <sup>2</sup>
Tail length	2.05	m	Ver. tail root chord	0.7	m
Hor. tail area	1.87	m <sup>2</sup>	Ver. tail tip chord	0.6	m
Hor. tail span	1.7	m	Ver> tail height	0.8	m
Hor. tail root chord	0.6	m	$x_{c.g.}/c$	0.869	–
Hor. tail tip chord	0.5	m	$x_{n.p.}/c$	0.800	–
Hor. tail inclination	-2.0	°	Stability Margin (S.M.)	0.07	–

use of a flight envelope system as explained in section 3.4, that can protect the pilot from entering a spiral. Another thing to notice is that despite the oscillatory nature of the dutch roll, the fly-by-wire system allows a yaw damper to function and counter this effect.

Table 6.2: Eigenmode analysis performed in AVL

	Eigenvalue [-]	Damping ratio [-]	Frequency [Hz]	$T_{1/2}$ [s]
Short period	$-6.72 \pm 3.31 i$	0.897	0.53	0.103
Phugoid	$-0.017 \pm 0.35 i$	0.049	0.06	40.76
Dutch roll	$-0.27 \pm 1.52 i$	0.172	0.24	2.612
Roll damping	$-16.27 \pm 0 i$	16.27	-	0.043
Spiral	$+0.002 \pm 0 i$	-0.002	-	-327.9

For the control surfaces the iterative process led to a control layout which can be seen from the CATIA drawings in the final design overview. Table 6.4 shows the dimensions and maximum deflection angles found.

Finally with all of the information gained previously, all stability and control derivatives were found. The most important ones are listed in table 6.4.

Table 6.3: Control surface dimensions.

Surface	Spanwise location [m]	x/c [-]	Max. Deflection Up [°]	Max. Deflection down [°]
Elevator	0.10 - 1.65	0.55	20	17
Ailerons	3.00 - 6.00	0.7	35	26

Table 6.4: Relevant stability and control derivatives

	Value		Value	Unit
$C_{L\alpha}$	5.481	$C_{Lq}$	7.076	$\text{rad}^{-1}$
$C_{m\alpha}$	-0.345	$C_{mq}$	-5.081	$\text{rad}^{-1}$
$C_{Y\beta}$	-0.076	$C_{lp}$	-0.538	$\text{rad}^{-1}$
$C_{m\delta_e}$	-0.458	$C_{l\delta_a}$	-0.802	$\text{rad}^{-1}$

Now that all important parameters have been defined, some comments can be made. First of all it is important to note that the control surfaces require large surface area's and deflections to initiate a certain turn rate. For the elevator this has mostly to do with the fact that the tail volume coefficient is small compared to conventional aircraft [22]. The reason for this is that due to the weight requirement a large empennage was simply not feasible. With an already small tail volume, the elevator is hence also less effective. For the ailerons the decision was made considering the fact that stability is of main importance for the current design goal. The inherent stability of the aircraft and consequent roll damping counteract the roll moment initiated by an aileron deflection. The team is aware that the designed control surfaces are larger than is typically expected. A more detailed analysis using for example wind tunnel tests is recommended.

### 6.3. Verification and Validation

While some of the verification and validation process of the stability analysis has already been explained, this section shall give a more complete overview. First of all, because of the iterative nature of the entire process, a lot of the verification and validation was done in parallel with the analysis itself. This was done to make sure that the process was correct and no time was wasted. Due to the fact that both XFLR5 and AVL were capable of similar analysis, a lot of the verification was done by cross-checking the results from these programs. Not only trim angle and lift coefficient were compared, but also stability derivatives, eigenvalues of the dynamic modes, neutral point location and more.

For validation these values were compared to data from the high-aspect ratio AS-W22 sailplane [5] where possible (marked by \* in the table) and a large range of conventional aircraft [30]. When a large difference existed between values found by XFLR5 and AVL, the derivatives from the latter were used for validation. This was decided because of the higher trustworthiness of this program compared to XFLR5. AVL is a program written for aircraft design by MIT and has been used in a wide variety of research articles as explained in section 6.1.1. Table 6.5 lists the most important parameters that were found using XFLR5, AVL and reference data. Note that some values such as the control derivatives can not be determined through XFLR5 and are therefore solely compared to the references. Unfortunately no other means

of verification was established but due to the decent correspondence to validation data it was accepted in this part of the project. Any future activities could use analytical methods or DATCOM to approximate these values as means of verification.

Table 6.5: Verification and validation data (\* = AS-W22 [5])

	AVL	XFLR5	Difference (%)	Reference data	Difference (%)	Unit
$\alpha_{trim}$	3.178	3.325	4.4	–	–	°
$x_{n.p.}/c$	0.869	0.864	0.6	–	–	rad <sup>-1</sup>
$C_{L\alpha}$	5.481	5.503	0.4	6.29*	12.9	rad <sup>-1</sup>
$C_{Lq}$	7.076	6.891	2.6	5.75*	18.7	rad <sup>-1</sup>
$C_{m\alpha}$	-0.345	-0.307	11.0	$-0.4 > C_{m\alpha} > -0.9$	–	rad <sup>-1</sup>
$C_{mq}$	-5.081	-5.173	1.8	$-5 > C_{mq} > -15$	–	rad <sup>-1</sup>
$C_{Y\beta}$	-0.076	-0.022	71.0	-0.28*	72.9	rad <sup>-1</sup>
$C_{lp}$	-0.538	-0.557	3.4	-0.73*	26.3	rad <sup>-1</sup>
$C_{m\delta_e}$	-0.802	n.a.	–	$-1.0 > C_{m\delta_e} > -2.0$	–	rad <sup>-1</sup>
$C_{l\delta_a}$	-0.458	n.a.	–	$-0.05 > C_{l\delta_a} > -0.2$	–	rad <sup>-1</sup>

It can be seen from table 6.5 that most of the verifiable values lie very close together and are in the same order of magnitude as the reference values. All values concerning longitudinal pitching moment are on the lower side of the spectrum compared to the reference data, but this can be explained by the low tail volume coefficient. Only  $C_{Y\beta}$  varies per program and does not comply with what can be expected. Despite thorough analysis no clear explanation for this was found. It should therefore be noted that any derivative with respect to side-slip might not be correct. Furthermore the value for  $C_{l\delta_a}$  is unusually large when compared to more conventional aircraft. This is in line with the large control surfaces but implies that extra care should be taken when testing the controls to make sure they function as expected. These are problems that should be treated in the post-DSE activities with high priority.

Table 6.6: Periodic dynamic response comparison for the Velo-E-Raptor (VER), a conventional Hang Glider and the AS-W22 Sailplane

	Damping ratio [–]			Frequency [Hz]		
	VER	Hang Glider	S-W22	VER	Hang Glider	S-W22
Short period	0.897	0.680	0.713	0.53	0.47	0.45
Phugoid	0.049	-0.078	-0.00033	0.06	0.18	0.05
Dutch roll	0.172	0.300	0.161	0.24	0.15	0.10

To make sure that the error margin on the stability derivatives does not provide too much of an error in aircraft dynamics, the characterizing values for the oscillatory eigenmodes were also compared to those of a conventional hang glider and the AS-W22 sailplane [70][5]. Due to the similarities the Velo-E-Raptor has with these types of aircraft similar dynamic responses can be expected. Table 6.6 shows that this is indeed the case and that despite the discrepancies for some of the derivatives the damping ratio and frequency of all aircraft are in the same order of magnitude.

## 6.4. Conclusion

From mission needs of the Velo-E-Raptor project, the goal for stability was to design an aircraft that is stable and controllable in all flight conditions. From the results it can be concluded that this goal has been achieved. The aircraft is statically stable by a sufficient margin. Despite a very minor, negligible instability in spiral, all dynamic modes are stable and safe for flight. Furthermore, by the way the control surfaces have been designed, even non-experienced pilots shall be able to fly the Velo-E-Raptor without extensive training.

It should be noted however that for accurate determination of the stability characteristics test data is needed. It is therefore recommended to critically assess any information taken from this analysis.

## 6.5. Project Design and Development Logic

### 6.5.1. Wind Tunnel Testing

It has become apparent that in order to do properly design an aircraft for stability, wind tunnel tests are a necessity. In the next phase of design, priority lies in using these tests to determine for example what the effect is of pilot interference on stability and control. Also, due to the non-rigid nature of the wing, warping of the structure due to either torsion or bending is very likely and the effects this might have on stability and controllability should be tested. In the design a dihedral of  $2^\circ$  is used though this might increase in flight due to the warping mentioned.

### 6.5.2. Control Surfaces

Due to the lack of proper verification and validation data on the control surface sizing, it is of key importance that these design parameters be checked for accuracy and whether they indeed adhere to the requirements posed. Also rudder dimensions have not yet been analyzed. The two-axis control system causes the rudder to only be controlled by the flight computer and control system and the design was therefore not prioritized in this stage of the project. This should be researched in combination with the derivative  $C_{Y\beta}$ . These are linked through the vertical tail surface size and require additional attention. Furthermore the ailerons shall be examined for their ability to function as spoilers during landing. When landing, a three point touch down is desirable but often difficult to perform. In the situation that the front landing gear touches the ground first, there is the possibility that the aircraft will takeoff again once the tail comes down. The main wing experiences a higher angle of attack and therefore gain lift, despite the pilot's intention to touch down. To counter this, the ailerons could both deflect upwards when touching down, losing lift in the process and generating extra drag to help the aircraft break. The effects this might have on stability and control should be examined in a coming design phase.

## Control System

The control system consists of several parts. The pilot gives an input, as mentioned in section 9.1.4, this signal goes to the flight computer together with the measurements of the sensors, the data will be processed and the signal of the desired deflections of the control surfaces will be sent to the actuators, which influence the attitude of the aircraft. In the coming parts the flight computer and the components will be described in more detail.

### 7.1. Pilot Control Mechanism

The pilot will be positioned on the wing and is supposed to get the feeling of a bird, as mentioned in section 9.1.1. To enhance this feeling for the pilot it is crucial to make a control system, such that the pilot can control the aircraft at any time. For this purpose the control mechanism will be part of the pilot attachment to the aircraft. A drawing of the control bar can be seen in figure 7.1.

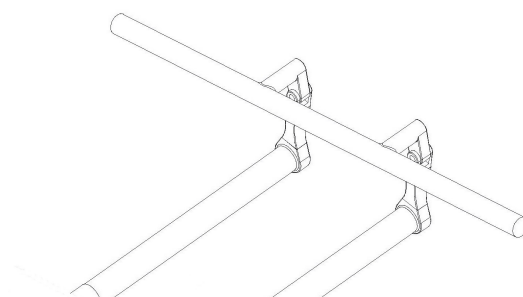


Figure 7.1: Control bar of the pilot

The control mechanism will be held in place by two bars for structural purposes and the control bar will be attached at two points, where the attachment can be moved similar to joysticks as well, such that the pilot can choose the control method for the aircraft using the bar or using the attachments as joysticks. Thanks to this construction the safety is increased by having two possibilities to control and having the possibility to control with one hand. It will also have a force feedback system to give the pilot information back through the control. This will be done with servos that are connected to the bars. By having two attachment points of the control bar there are two points of failure, such that the second joystick will serve as redundancy.

## 7.2. Sensors

Flight sensors are important for the pilot but also for the flight computer. The pressure sensors can cover several tasks depending on the location. Most measurements in an aircraft are performed by pressure measurements. There will be a number of pressure sensors on the Velo-E-Raptor. In a pitot tube it measures the airspeed, but the static pressure measurement can be used for altitude and vertical velocity measurements. On the wing it can function as a stall indicator by measuring the pressure on the upper wing surface and indicating, when separation occurs.

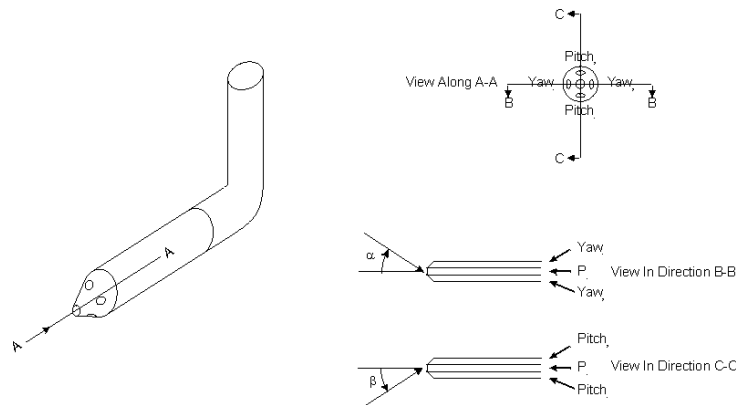


Figure 7.2: Five hole probe

Another location for pressure sensors is beneath the wing in an AoA probe, which uses two inlets at angles in different directions, which determine the angle of attack by using the difference of dynamic pressure. This indicator is widely used on aircraft as Dassault Falcons, Airbus A380 and many planes from Embraer <sup>1</sup>. This is a simplified version of a five hole probe, which is a pitot tube with four holes in 90° steps under an angle, as visualized in figure 7.2 <sup>2</sup>, which works with the difference in dynamic pressure as the AoA probe, but can determine the airflow vector in both directions as angle of attack and sideslip <sup>3</sup>. National Renewable Energy Laboratory was researching this device and it showed that the 5-hole probe delivers better results than a wind fin, which is used for weather measurements <sup>4</sup>. However, as it is not yet available on the market and a AoA probe is sufficient for the flight computer, the 5-hole probe is not taken into account at this stage.

Another stall indicator is a stall vane, which measures the direction at the lower surface at the wing directly after the leading edge. As soon as the flow from the lower surface goes to the upper surface over the leading edge, a small plate is pushed by the airflow, which triggers the sensor and by that also the stall warning. These will be attached at the leading edge, but outside of the influence of the propellers. For the angle of attack there is the AoA vane, which is a small free rotating wing attached to the outside wall of the aircraft, which is positioned

<sup>1</sup><https://www.pressreader.com/usa/flying/20170601/281732679404383>

<sup>2</sup><http://www-g.eng.cam.ac.uk/whittle/current-research/hph/pressure-probes/pressure-probes-fig-5.gif>

<sup>3</sup><https://www.grc.nasa.gov/www/k-12/airplane/tunp5h.html>

<sup>4</sup><http://www.nrel.gov/docs/legosti/old/22134.pdf>

around the leading edge or even further to the front and works as a fin for wind direction measurements, but there is no wall at the Velo-E-Raptor, where it could be attached, so this sensor will be not taken into account.

A magnetometer will provide the heading of the aircraft as a compass. The location of the aircraft can be determined by GPS, which is available for the pilot on the phone mentioned in section 9.1.5, but also the flight computer has a GPS receiver implemented for the flight computer. For redundancy it can also be used for altitude and vertical velocity measurements, but due to the accuracy, it should be used as a back-up.

The attitude will be determined by a three-axis gyro system, which measures the angular velocities. It will know the pitch rate, roll rate and yaw rate, which is important for the yaw damper. As the aircraft has no yaw control from the pilot, but does have an automatic yaw damper with a rudder, it is important to have good yaw rate measurements to counteract adverse yaw. Additionally accelerometers measure g-forces for the flight computer but also for structural reasons, but also with gravity the angles can be determined with three perpendicular accelerometers.

## **7.3. Control System**

### **7.3.1. Literature Study**

There are different parameters that the pilot can control. In aircraft there are three degrees of control: angle, angular velocity and angular acceleration. The easiest control for humans in general is to control velocity or for aircraft pitch, roll and yaw rate<sup>5</sup>. This control input can also be controlled in different ways namely in a open or closed loop, where in the closed loop the flight computer is monitoring the attitude of the aircraft to see if the desired behavior was achieved. Aircraft without fly-by-wire have an open loop, or a closed loop if the pilot is included in the control system as the controller. Therefore a pilot has more work with the controls, as he has to counteract oscillations and unwanted movements, which the closed loop can take over in a flight computer. With an electronic control the response can be adjusted and made smoother. To make the system safe, a level of redundancy of electronics has to be increased. The software can monitor the flight with a flight envelope protection, where it avoids the pilot entering flight conditions outside of the performance capabilities of the aircraft. For the feedback of the flight computer there are different sensors that can be used for the flight computer. These are explained in section 7.2.

### **7.3.2. Approach**

As the control system is an electronic system, there are different ways to design the controls. For this purpose a simplified model was made to analyze whether the aircraft is controllable with a fly-by-wire system. In order to analyze it, the simplified model with a feedback loop has been implemented in Simulink with a PID controller with the state-space from chapter 6. The tuning has been done manually, as there is not enough experience with control systems to use advanced tuning methods. First the tuning takes places with a P control,

---

<sup>5</sup>Ir. Dirk van Baelen, PhD Candidate at Control and Simulation, Faculty of Aerospace Engineering, TU Delft

where the I and D gains remain zero. As soon as the P control works, the tuning of the I and D is added. The result will show if the aircraft is controllable with a PID controller.

### 7.3.3. Flight Computer

The flight computer will use a PID controller for control along its three axis. The three controls are roll, pitch and yaw, where yaw will consist of only a yaw damper without an input from the pilot. As the surfaces and reactions are different for each axis, each PID controller will have different gains and has to be calibrated separately. As soon as the prototype of this control system will be working, it will be extended and optimized for smoother control.

A model of the software for the flight computer can be seen in figure 7.3. The inputs and outputs of this diagram correspond to the inputs and outputs of the flight computer for the control in figure 1. The input for pitch and roll from the pilot will be evaluated with the feedback data from the gyroscopes. The PID controller adjusts the signal and sends it to the servos, which translate the electrical signal to mechanical deflection, which influence the attitude of the aircraft.

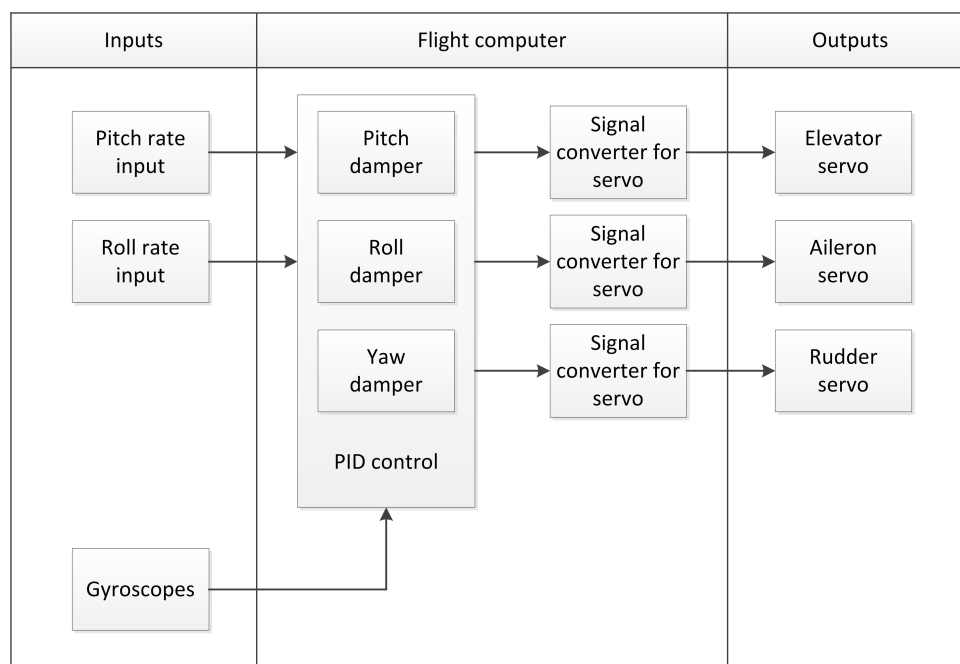


Figure 7.3: Data handling diagram for flight computer software

This model, which can be seen in figure 7.4, was simulated in Simulink. As the state-space of the aircraft can be assumed to be split into longitudinal and lateral movements, two models have been made. A PID control uses three gains:  $K_p$  for proportional,  $K_i$  for integral and  $K_d$  for differential control. These gains influence the signal and were analyzed and adjusted in the process. The gyro was neglected and the servo block was used as a time delay of 0.25 s for an electric servo. This value was extracted from the course AE4301 Automatic Flight Control System Design [13]. The model for lateral control had two separate loops. The loop for roll has the pilot input and a feedback loop from the state-space roll rate outcome back

to the input. The loop for yaw did not have an input, such that the feedback yaw rate from the state-space went directly to the PID control. Both loops were connected to the lateral state-space. The results will be discussed in section 7.3.4.

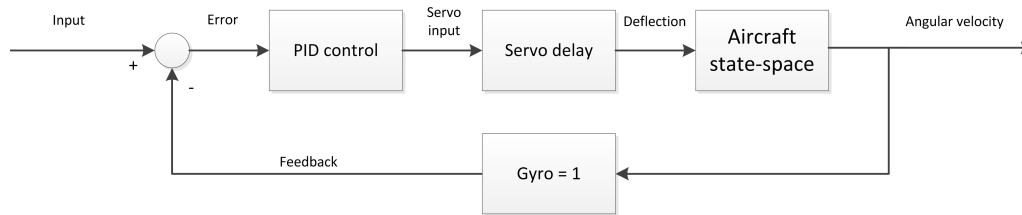


Figure 7.4: Model for PID control for simulation

### 7.3.4. Results

The results of the Simulink model showed that the aircraft is controllable. It shows the behavior of the aircraft with a certain input from the pilot. With a saturation block the designed maximum deflection of the control surfaces was used to make a realistic control. In longitudinal direction the state-space returns the horizontal velocity, angle of attack, pitch angle and pitch rate, where the input has to match the pitch rate. In lateral direction the outcome of the model are sideslip angle, bank angle, roll rate and yaw rate, where the roll rate has to match the pilot input and the yaw rate has to return back to zero after a change.

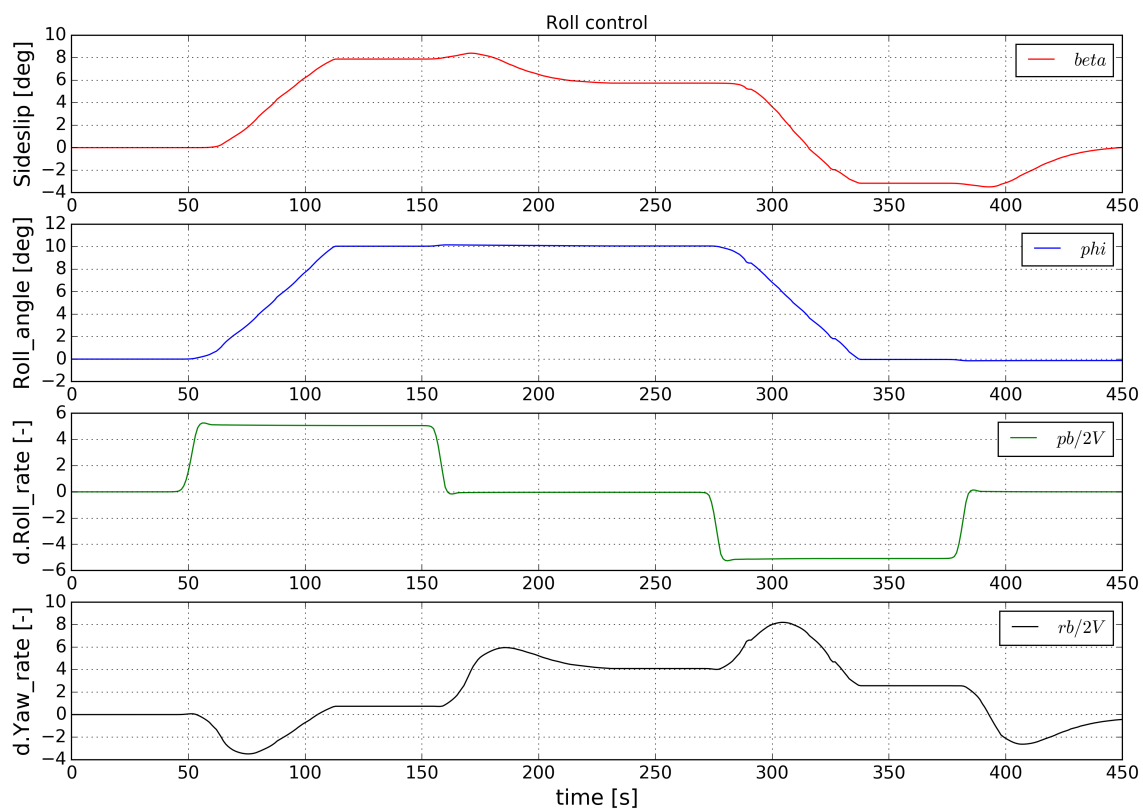


Figure 7.5: outcomes from the state-space in Simulink

In figure 7.5 the outcome of the model has been plotted after the gains were found, which make the control stable. The four graphs show the more important control, which is the lateral control, because the aircraft has to be controllable with a two-axis control system. Since the longitudinal control behaves as a conventional airplane, which fly with fly-by-wire, the lateral control is more important. The red graph in the first plot is the sideslip angle, which is caused by yaw. The second is the roll angle, which results from the roll that the pilots controls. The green graph ( $\frac{pb}{2V}$ ) in the third plot is the dimensionless roll rate, which the pilot controls, and the black graph in the forth plot ( $\frac{rb}{2V}$ ) is the dimensionless yaw rate.

Table 7.1: Gains for lateral control of the PID control

	$K_p$ [-]	$K_i$ [-]	$K_d$ [-]
Roll control	-15.0	-0.5	-0.4
Yaw control	2.0	0.05	0.2

As the third graph shows the roll rate, which is controlled by the pilot, which are step functions, the dimensionless roll rate output looks similar to a step function with slight overshoot and no steady-state error. The roll angle increases during the first input and decreases at the second input, as desired. During the input changes the dimensionless yaw rate changes and the rudder control counteracting the dimensionless yaw rate. This rudder control makes the sideslip staying constant, such that the vertical stabilizer decreases the sideslip again. On a later stage the yaw control will include the sideslip angle in a feedback loop to decrease the sideslip angle during flight maneuvers.

### 7.3.5. Verification and Validation

The derivatives for the state-space have been extracted from the results in chapter 6. The program that has transferred the stability and control derivatives was verified and validated in the project "Simulation, Verification and Validation", where flight data from the Cessna Citation II has been used to validate the program. Simulink is a verified and validated program [71].

In the stages of designing a model for control, the tuning happens with gain and phase margin plots and the time domain plots are used for verification that the tuning was successful. In this case the work has been done with the time domain plots and the results has shown that the controlled output is very close to the input step functions, which verify the model. The time domain used for the process can be seen in section 7.3.4.

### 7.3.6. Flight Envelope Protection

As the flight computer will handle the control of the aircraft, namely being in between the pilot and control surfaces, the signal processing can be used to make the flight safer, which is important, as the aircraft is designed to be flown by inexperienced pilots graduating after a one week course table 16.1 using a two-axis control. Therefore the flight computer will stop the pilot exceeding the flight envelope by first giving a warning visually and also audible but also mechanically in the force feedback control bar and blocking the pilot input to the control surfaces, as soon as the limit has been reached. The protection will prevent the

pilot entering stall, too steep dives and dangerous bank angles. As the aircraft can fly with up to 60° bank angle without losing altitude, the flight envelope protection will block a higher bank angle below the safe altitude. The dive will be blocked at the maximum airspeed by pitch up maneuver and if this maneuver does not recover the aircraft before the minimum parachute deployment altitude is reached, the rescue parachute will be deployed.

The flight envelope protection will work with the sensors and decide which action to take. If stall occurs the aircraft can pitch down, but below the safe altitude it should increase the thrust. The flight envelope protection will be also connected to the safety systems in order to keep the aircraft flying above the minimum parachute deployment altitude. Below the safe altitude the pilot gets a warning and the control will switch back to the safe flight mode for takeoff and landing. It will also check the data from the sensors, if the plane is flying or falling, such that the rescue parachute can be deployed in case the airplane falls and reaches minimum flight altitude.

### **7.3.7. Flight Modes**

The use of a flight computer gives the possibility for different control modes. For increasing the flying experience the pilot can have the option to change the flying behavior. For better pilot experience the pilot would like to have a more sensitive aircraft, so a flight mode can be used with higher gains, but the gains will be decreased again for landing to the takeoff settings below a certain altitude. Beginners will also learn flying with a less sensitive aircraft.

Another possibility can be to use different controllers for the pilot experience. Instead of using the PID control during flight, which makes the flying experience smooth, the pilot can choose to use only the proportional control without a feedback loop, which can bring the aircraft into oscillation and give a more extreme flight experience, where the pilot has to counteract the plane reactions himself, as the sports planes with mechanical control systems do.

### **7.3.8. Conclusion**

As the Simulink model analysis was performed, the model has shown that the aircraft is not just controllable but also controllable with the desired two-axis control. The parameters that can be controlled are pitch and roll, where the yaw rate reacted respectively during the turn and tried to counteract the adverse yaw. As the adverse yaw is the main reason for the use of rudder, the model showed that the rudder does not necessarily need to be controlled by the pilot, but the flight computer can take over the yaw control during the turns. As the landing is designed to be a field, the aircraft can land against wind direction, which also does not require the use of the rudder.

As the control system is performed electronically by the use of a flight computer, the software can be extended to implement a flight envelope protection and different flight modes. This is possible as the aircraft is controllable by usage of the flight computer and the extensions are part of the software.

## 7.4. Failure Modes

The aircraft will be using fly-by-wire controls and so this system has different kinds of failure modes. As it is a combination of electrical and mechanical control, there are more failure modes than in a purely mechanical control system. Three different categories of failure will be discussed: the failure of the fly-by-wire system, the controls of the pilot and the flight envelope protection which is a software failure.

### Fly-by-wire System

The fly-by-wire system consists of many components. The core of the system is the flight computer. If the computer crashes or does not function as desired, the aircraft is not controllable anymore. For that reason there will be a total of three computers. The redundancy is described in section 7.3. The other components of the fly-by-wire system are cables, connectors and actuators. Cables and connectors are responsible for transmitting a signal and if this part fails, the signal is not delivered to the actuator. The actuator deflects the control surface and if the actuator fails, there is no deflection. Therefore each control surface will have three actuators, where two are sufficient for the control surface. Each actuator will have its own cable to the flight computer, such that if any of these components fail, the redundancy will keep the aircraft controllable.

In order to increase the safety of flight there will be two computers running parallel. The active will process the data for flight and the other will be in stand-by. The stand-by mode will ensure that the switch can be performed within a short time, but do not use much electricity from the batteries. The first flight computer will use PID control and the second one a P control in case of flight conditions that can cause computation errors.

### Controls of the Pilot

The controls include two different aspects of failure: a software problem such as wrong gains or the flight computer being wrongly calibrated but also mechanical failure of the control bar and the force feedback actuators. The maintenance of the software has to be done by specialists, such that the probability of wrong calibration can be decreased. If the calibration is wrong, the takeoff should be aborted or in flight a safe landing has to be ensured. If a safe landing is not possible or too dangerous the rescue parachute has to be deployed above its minimum deployment altitude.

The mechanical failure of the controls means that the aircraft is not controllable, so an immediate deployment of the rescue parachute has to be the consequence or the takeoff has to be aborted. The failure of the actuators of the force feedback of the controls is a failure, which is difficult to sense for the pilot. The flight computer will detect a failure of the actuators due to change of electrical resistance and give the pilot a warning. If the pilot can fly without it, he can proceed with the flight, but due to a master alarm an immediate landing is advisable.

### Flight Envelope Protection

The flight envelope protection can fail in multiple modes. The hardware failure was described in the part fly-by-wire system. Another hardware failure are the sensors. Also the sensors have a level of redundancy. There are either multiple sensors of the same kind or

the parameter is measured by different sensors. This redundancy ensures a lower probability of failure. If one sensor fails, and returns a wrong value to the flight computer, the flight computer will trigger the master alarm and the aircraft has to land immediately. If the pilot warning system fails, but the flight envelope protection is still functional, the pilot can be confused, but will not enter dangerous flight conditions.

### **Multiple Failures**

If failure occurs in several systems or on all levels of redundancy an immediate deployment of the rescue parachute has to be triggered. For this reason the fly-by-wire system is designed to fly above a minimum altitude due to having the rescue parachute as a back-up, if too many systems fail. By the use of a rescue parachute system the aircraft can be made even safer than it already is designed to be.

## **7.5. Hardware**

The control system consists of different electronic parts, where there are sensors, the flight computer and actuators. The flight computer is the part, where all computations take place. It has to be powerful and it has to be easy to upgrade the software for extensions. A flight computer that is used on drones with the use sensors is the Erle-Brain 3<sup>6</sup>. This flight computer is a finished product, which has powerful hardware. It has also sensors integrated, but they are all located in the computer, so additional sensor have to be used, if the location is important.

The sensors are very important for the flight computer, but they also have to be lightweight and cost efficient in a sense that the aircraft remains affordable for the customers. There is a variety of pressure sensors, which are used in electronics<sup>7</sup>. A pitot tube can be found in aircraft shops, as pitot tubes are widely used and the most common way to measure airspeed<sup>8</sup>. Instead of making a system out of three gyros, it is easier to buy a three-axis gyro system off the shelf<sup>9</sup>. The cables in the aircraft have to be shielded against interference, so proper cables have to be used<sup>10</sup>. As the flight computer is located next to the battery, the cables are mainly used for the control mechanism, sensors and actuators.

Actuators for the control surfaces are an important part, which have to be reliable. To achieve fast and strong movements in combination with reliability the costs are higher than other servos<sup>11</sup>. In order to ensure the reliability of the actuators, each surface has three servos, where two are sufficient for the movement of the control surface, where the rudder uses only two servos. Using these amounts the Velo-E-Raptor will have 11 servos for control surfaces. As the control is a two-axis control, 4 servos are used for the force feedback, because the control bar has two attachment points. The other parts of the control system has always the same amount of components as the system for back-up as two flight computers, two

---

<sup>6</sup><https://erlerobotics.com/blog/product/erle-brain-3/>

<sup>7</sup><https://www.adafruit.com/product/2652>

<sup>8</sup><http://aircraftproducts.wicksaircraft.com/viewitems/pitots-venturi/12-vdc-heated-pitot-tube-and-hardware>

<sup>9</sup><http://www.chiefaircraft.com/bd-cortex.html>

<sup>10</sup><http://www.aircraftspruce.com/catalog/elpages/shieldwirez.php>

<sup>11</sup><https://www.servocity.com/hs-1100wp-servo>

sets of sensors (four pressure sensors, two pitot tubes and two gyro systems). Therefore also the length and amount of cables will result in 60 m of cables.

## **7.6. Project Design and Development Logic**

### **Control System**

The control system was simulated and analyzed in this chapter to see the possibility to control the Velo-E-Raptor with a fly-by-wire system. Therefore the development of this system is required to make a realistic model of it and work out the details. For this the full control system has to be developed. From that point the system can be optimized for flight comfort, which is desired for the pilot.

### **Certification of the flight computer**

Flight computers that fly nowadays in small aircraft are certified and safe, but they are also very expensive, big and heavy. They often have big steel casings, which prevents them to fit into the Velo-E-Raptor<sup>12</sup>. As the market for drones is growing and the flight computers for drones are developing to such a level that they can be made reliable, they also have to get certified to be able to be used for the Velo-E-Raptor. The certification makes the use of the flight computer be able to fly with a pilot on board and during the process weak parts of the computer and the code can be improved.

### **Velocity Vector Sensor**

The sensor for the velocity vector and thus the aircraft movement of the aircraft can be provided by the five hole probe. As there is no product of the 5-hole tube ready to buy, the sideslip angle cannot be determined easily. Therefore the five hole probe has to be built and calibrated for this aircraft. Only after this work the velocity vector can be measured in a good way.

### **Flight Modes**

The mentioned flight modes in section 7.3 create much room for new flight modes. By having some control engineers in the team many flight modes can be developed and by updating the software on the flight computer it will be cost efficient and easy for the customers.

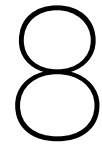
By developing the flight modes entertaining software can also be developed such as virtual checkpoints for races and virtual routes. These can also be implemented by updating the software, which will be a simple upgrade.

### **Autopilot**

Also by developing the software an autopilot can be implemented to cruise to a certain point, but also an auto pilot assisted takeoff and landing conditions can be established for beginners and bad weather conditions.

---

<sup>12</sup><http://www.centuryflight.com/products/systems/yaw-damper.html>



# Structures

## 8.1. Approach

The purpose of the Structural department is to design a structure that allows the design parameters chosen by different departments to be realized. In order to do this, first a detailed wing design was made. Next, the tail was analyzed and finally all the other structural components were designed for. The structure is designed for an ultimate load factor of 6, including a safety factor of 1.5 calculations are done using a load factor of 9. The load factor of 6 is standard in hang gliding and a safety factor of 1.5 is standard in aerospace applications <sup>1</sup>.

For each structural component a program was written in Python. These programs were subsequently verified by comparing the results with a simple stress analyses run by CATIA. After each program was verified, the parameters were optimized to minimize the weight of the structure. The optimization resulted in both a better understanding of which design options would be more beneficial than others and it resulted in a better mass estimation and center of gravity range which the other departments could use.

### Main Wing

In the program analyzing the stresses in the main wing, the type, dimension and location of the spar was determined. Also, the number and locations of the ribs were optimized. Furthermore, an analysis of the skin was done. Two stringers were used, one to maintain the shape of the leading edge and one for the trailing edge. Further stringers were not deemed necessary in the design. As skin buckling is reversible with a flexible skin it is not seen as a big problem. A further analysis of the need for stringers will be done in the post DSE phase. The stresses were calculated using methods described in the book Aircraft Structures by Megson [68]. The direct stresses were combined with the shear stresses using the von Mises stress criterion <sup>2</sup>.

To assess the outcome of the wing analysis, certain requirements were set. These requirements include the maximum wing deflection, the maximum rotation angle and the maximum airfoil deformation.

A maximum wing deflection of 1.4 m was chosen. This number resulted from looking at the maximum wing bending of the DG-1000 sailplane. This plane has a maximum wing deflec-

<sup>1</sup>[http://www.paraglidingforum.com/files/aw\\_specs\\_262.pdf](http://www.paraglidingforum.com/files/aw_specs_262.pdf)

<sup>2</sup><http://web.mae.ufl.edu/nkim/eas4200c/VonMisesCriterion.pdf>

tion of 2.3 m with a wingspan of 20 m<sup>3 4</sup>. To design for an equal decrease in performance due to wing deflection, the wing deflection was scaled linearly. The average deflection of the DG-1000 sailplane is 11.5 cm per meter span. The span of the Velo-E-Rapter is 12.3 m and therefore it was decided to stick to a maximum wing deflection of:  $0.115 \cdot 12.3 = 1.4$  m. This deflection will only occur at the ultimate load.

For the maximum wing rotation a value of 3° was chosen. This value was chosen in communication with the Stability and Control department

Also a requirement for the airfoil deformation was set. The maximum deformation of the (top) skin was set to be 1% of the chord length. This value was determined together with the Aerodynamics and Stability and Control department.

### Stringers

Two stringers are used in the leading and trailing edge of the main wing. These stringers prevent the skin from deforming at the trailing and leading edges. This will ensure less airfoil deformation due to which the wing will be more aerodynamically efficient.

### Ribs

The ribs were not analyzed in detail. This has to be done in the post DSE phase. For now, the ribs are approximated by 1 mm thick CFRP plates. In reality material could be saved using cutouts and material has to be added to make an edge where the rib touches the skin and spar. Two design options were considered here: producing the ribs as one piece and place them over the spar or producing the ribs in two pieces such that the spar can run all the way to the skin. These options can be seen in figures 8.1(a) and 8.1(b) respectively. The first option was selected as the ideal height of the spar at the tip would not be equal to the local airfoil thickness due to a minimum thickness of the spar. The airfoil deformation affects the aerodynamics of the aircraft. In case wind tunnel tests (appendix A) show that this effect causes the non-satisfaction of requirements, the second option must be selected.

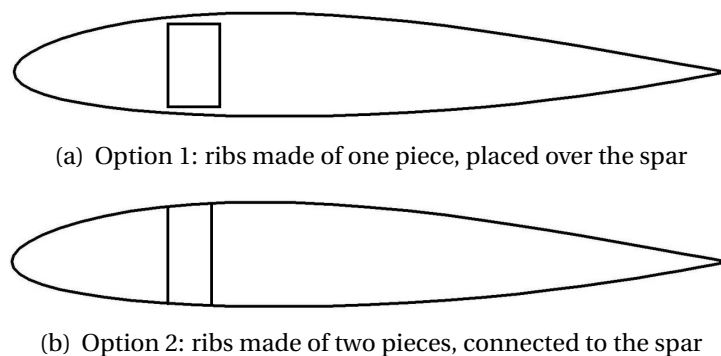


Figure 8.1: Rib options

<sup>3</sup><https://www.dg-flugzeugbau.de/en/library/testing-destruction-dg>

<sup>4</sup><https://www.dg-flugzeugbau.de/en/library/dg-sailplane-a>

## Tail

In the program for the tail, the tail dimensions, tail forces and maximum tail deflection were used as inputs. These parameters were then used to do a stress analysis and optimize the structural cross section to minimize weight.

For the tail stress analysis an approximation of the actual tail was done by calculating the tail as if it has the shape depicted in figure 8.2(a). In reality, however, a tail shape as depicted in figure 8.2(b) will be used for aesthetic reasons and for reducing weight.

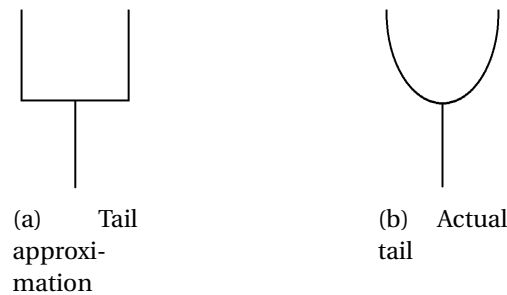


Figure 8.2: Tail layout

## Landing Gears

For the landing gears several options were considered and in figures 9.1(b) and 9.4(a) the two chosen designs are shown. Figure 9.4(a) shows one of the two front landing gears which has two functions: it relieves the pilot of the weight of the aircraft during takeoff and landing and at the same time it protects the propellers from touching the ground. The rear landing gear depicted in figure 9.1(b) has two functions too: it protects the tail from the ground and it relieves the weight of the aircraft.

## Optimization

To optimize the structure, different methods were used. All structures with the exception of the main wing were optimized by a simple looped process that finds the minimum weight. The amount of parameters defining the main wing were too large for these simpler methods of optimization and required a different optimization algorithm to reduce processing time significantly. The method used is a genetic algorithm.

A genetic algorithm imitates the genetic process applied to species living on planet earth. This is done by producing an initial generation that consist of individual chromosomes. Chromosomes consist of a list of variables that describe the structure of the wing. These variables are chosen initially at random between defined boundaries. Once all chromosomes in a generation are defined their fitness is calculated. Fitness is the criteria that describes the quality of a chromosome. In the case of the wing structure the main fitness criteria is chosen to be the weight. If the structure fails, it has no fitness at all. A chromosome with a lower structural weight will have a higher fitness. To produce a new generation two parental chromosomes will be chosen based on their fitness. Chromosomes with a higher fitness will have a higher chance on becoming a parent. The offspring will be a new chro-

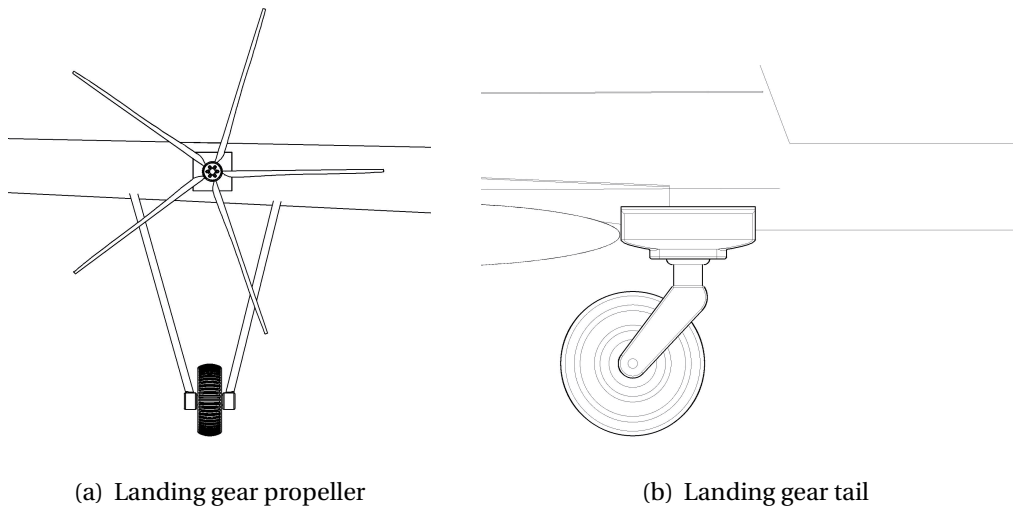


Figure 8.3: Landing gear layout

mosome of which the variables are chosen randomly between the two parents with a small chance of a mutation. The new generation will be tested for fitness and this loop will be continued until the best chromosome converges to a certain optimum. This resulted in an optimization process that converged faster than conventional optimization methods.

### Propeller Attachment

The propellers will be attached to two ribs. These ribs are strengthened using a box-like structure to carry the extra loads (including torque) and vibrations the propeller induces. The ribs with box structure transfer these loads to the main spar. This structure can be seen in figure 8.4.

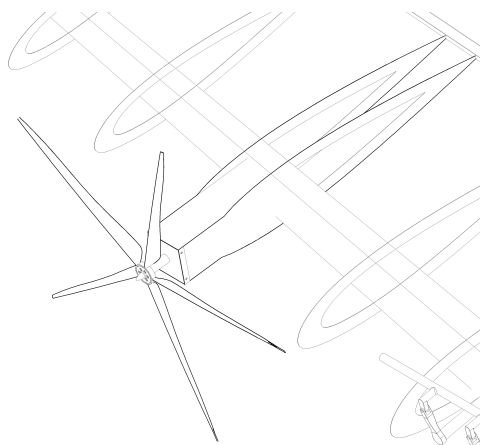


Figure 8.4: Propeller attachment

## 8.2. Assumptions

To do the stress analysis assumptions were made. These assumptions are listed below. Also, further assumptions that were used in some cases are listed below.

### General Assumptions

1. Direct and shear stresses on planes normal to the beam surface are constant across the thickness [68].
2. The material deforms in a linear, elastic manner [68].
3. The material of the beam is assumed to be homogeneous even though a carbon fiber fabric (twill 2x2) is used in the design [68].
4. For carbon fiber reinforced polymer (CFRP), the properties of HexPly M79 200T2 have been used <sup>5</sup>.

### Bending

1. Plane cross-sections of the beam remain plane and normal to the longitudinal fibers of the beam after bending [68].
2. The effective skin in bending is 60% of the chord at a distance of half of the wing thickness at the spar.

### Shear

1. Axial constraint effects are negligible [68].
2. The shear stresses normal to the beam surface may be neglected [68].
3. The beam is of uniform section so that the thickness may vary with distance around each section but is constant along the beam [68].

### Other

1. The load distribution at the ultimate load factor is equal to the load distribution in cruise.
2. The dihedral is set to zero.

## 8.3. Material Selection

### 8.3.1. Frame

For the frame two materials have been analyzed. These were aluminum and CFRP. It was noted that an aluminum frame would result in the aircraft mass to exceed the requirement of 70 kg. Therefore a CFRP frame was chosen. The estimated aircraft weight, when using an aluminum frame and when using a CFRP frame, can be found in table 8.1.

### 8.3.2. Sail

To select a sail material research was done into the sails that hang gliders use. Two main types of sails are used here: Dacron sails and Mylar sails. Dacron has a lot of advantages. These advantages include: the price, mass, flexibility, colour options and durability. The advantage of Mylar is that it hardly stretches and therefore ensures a high performance. This

---

<sup>5</sup>[http://www.hexcel.com/user\\_area/content\\_media/raw/HexPly\\_M79\\_eu\\_DataSheet.pdf](http://www.hexcel.com/user_area/content_media/raw/HexPly_M79_eu_DataSheet.pdf)

	Dimension	Unit
Aluminium	79.4	kg
CFRP	65.1	kg

Table 8.1: Mass comparison

makes the hang glider feel like new all the time. A big difference can be found in durability: the Dacron sail can be exposed to UV for about 1000 hours while a Mylar sail can only be exposed to UV for about 200-400 hours. Since the mass and durability and therefore also maintainability and ease of use are found more important than its performance, it was decided to use a Dacron sail <sup>6</sup>.

## 8.4. Results

### 8.4.1. Wing Analysis

The result from the wing structure analysis can be seen in the Final Design Overview. These properties are obtained from the genetic algorithm used to optimize the wing structure.

The type of spar that was found to be optimal is a rectangular spar. Also, a circular spar and a D shaped spar were analyzed. The rectangular spar was found optimal because the lifting forces are more significant compared to the forces in the drag direction. This allows the rectangular beam to be slender in the drag direction. The circle would have a uniform radius and thus will be over designed in the drag direction. A combination of the two is a D shaped spar. This type has the advantage of integrating the rigid leading edge as part of the spar. To use this advantage the spar need to be located at the leading edge which is not optimal for the torsional stresses through the beam. The inertia distribution of this cross section is better than the circular but worse than the square beam. The extra leading edge reinforcement required with the rectangular spar adds less structural mass than the D shaped spar resulting in the most optimal spar being the rectangular shaped spar.

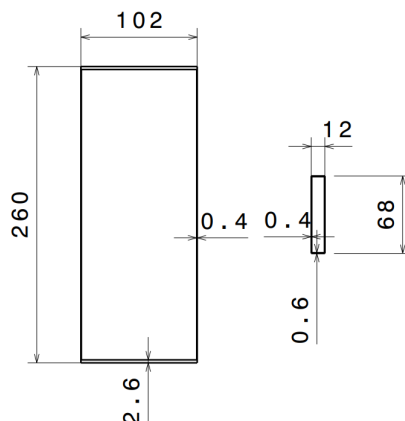


Figure 8.5: Cross section of the spar at the root (left) and at the tip (right)

<sup>6</sup><http://freeflightadvice.com/sail-cloth-options/>

The dimensions of the optimized spar can be seen in table 8.2 and in figure 8.5. The thick airfoil that is used allows the spar to get relatively thick compared to other hang gliders at the root. This decreases the weight of the spar as less material is required to create a larger moment of inertia. The spar is tapered as the required inertia decreases over the span. The result is a spar that is estimated to weigh 9.4 kg. This weight includes the foam that is required for the production of the spar.

	Dimension	Unit
Height at the root	260.0	mm
Width at the root	102.0	mm
Height at the tip	68.0	mm
Width at the tip	12.0	mm
Vertical thickness	0.4	mm
Horizontal thickness at the root	2.6	mm
Horizontal thickness at the tip	0.6	mm

Table 8.2: Spar dimensions

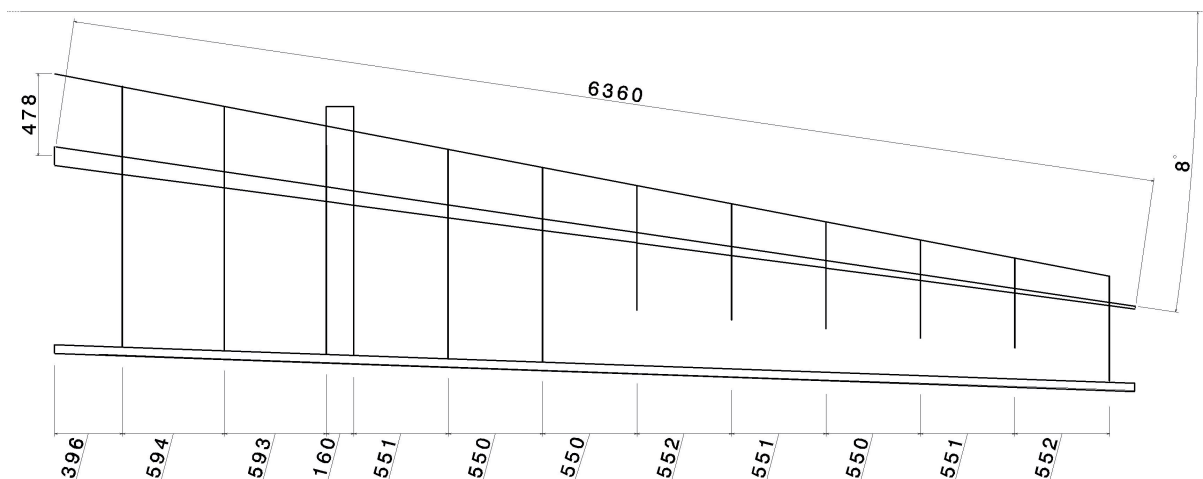


Figure 8.6: Main wing structure layout

The rib locations have been decided to be located at important locations which are the propeller attachment locations, the aileron and the start of the pilot cutout. Furthermore the ribs have been distributed evenly across the remainder section of the wing. As a non-rigid skin is used, the aerodynamic forces acting on it will deform the shape of the airfoil. This unwanted effect can be reduced by lowering the spacing between the ribs. The maximum airfoil deformation limits the maximum rib spacing. The computed maximum rib spacing is 0.62 meters. Since the ribs are evenly distributed between the important points this spacing is slightly lower and can be seen in figure 8.6. The estimated weight of the ribs equals 6.8 kg.

The skin used is a non-rigid Dacron sail. The reasoning behind this choice is that the material is light weight, cheap, and flight proven for hang gliders <sup>7</sup>. For the optimization the skin thickness was chosen variable which resulted in a skin thickness of 0.2 mm. This has been compared to the thicknesses used on existing hang gliders. The thickness of the skin of hang gliders was 30% thinner than that of the Velo-E-Raptor and therefore the thickness was verified. The total weight of the skin is estimated to be 6.8 kg.

### 8.4.2. Tail Analysis

The tail has been analyzed in two separate sections. These are the lifting surfaces and the tail structure that hold these lifting surfaces in place. The lifting surfaces consist of the horizontal stabilizer, the vertical stabilizer and their corresponding control surfaces. The tail structure is shaped like a fork that wraps around the pilot and connects to the main spar in the wing. The beams that define this structure are designed separately and optimized for a minimum weight.

The tail surfaces have been chosen to have a similar structure compared to the wing structure. The parameters defining the spar of the wing can be seen in table 8.3 and in the Final Design Overview. Due to the relative low span and low forces, the spar is allowed to be relatively small compared to the main wing. For the vertical tail surface no estimated forces were obtained. For this reason the weight of the vertical surface is estimated as a fraction of the horizontal tail weight with respect to their equivalent surface areas. The tail surface structures are estimated to weigh 3.2 kg.

	Dimension	Unit
Spar Height	52.0	mm
Spar Width	35.0	mm
Spar horizontal thickness	0.8	mm
Spar vertical thickness	0.4	mm
Spar sweep	0.0	°
Spar root location	22.0	mm

Table 8.3: Spar dimensions of the horizontal tail surface

The tail structure is analyzed as four separate circular beams. The optimization concluded that the tail structure will have a radius of 45 mm and a thickness of 1 mm. The structure diameter has been kept constant along the beams to decrease the difficulty of production. The estimated weight of this structure is 2.2 kg.

### 8.4.3. Landing Gear Analysis

The landing gear is analyzed separately in two sections; the front landing gear and the rear landing gear. The front landing gear is located at the propellers to protect them from ground contact. The rear landing gear is located at the aft of the tail.

---

<sup>7</sup><http://freeflightadvice.com/sail-cloth-options/>

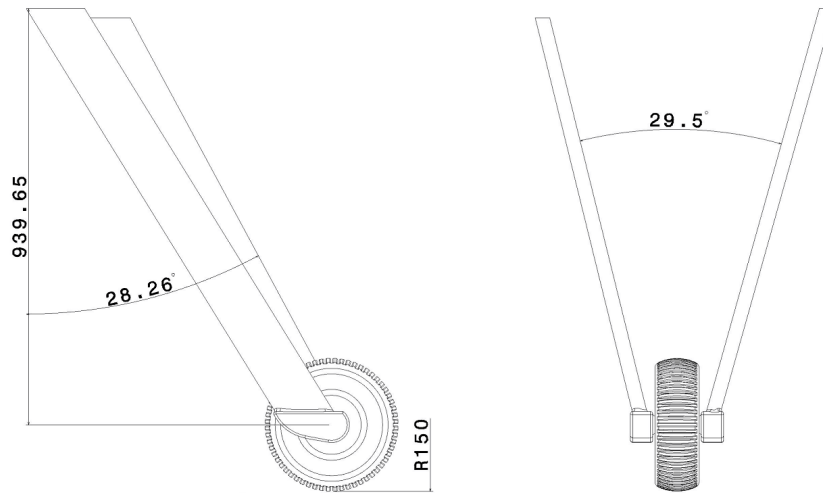


Figure 8.7: Front landing gear

The front landing gear consist of two struts that are angled in a V-shape with the wheel located at the bottom between the two struts. The struts are designed to catch a vertical speed of 3.0 m/s and an equivalent horizontal force. Typical vertical design speeds for landing gears are between 1.83 and 3.05 m/s [1] [60]. The shape of the struts are oval with a height four times as large as the width of the strut. This shape adds the least amount of aerodynamic drag as is explained in section 4.3.4. Furthermore, the front landing gears are angled forwards to protect the propellers in a frontal tip over and reduce the moment induced by the horizontal forces on the landing gear. The results of the optimization can be seen in table 8.4 and a technical drawing of the landing gear can be seen in figure 8.7. The estimated weight of the front landing gear including wheels equals 5.2 kg. The rear landing gear is estimated to weigh 1 kg.

	Dimension	Unit
Strut width	33.0	mm
Strut height	132.0	mm
Strut thickness	1.0	mm
Strut length	1030	mm
Angle between struts	32.8	°
Inclination angle	27.2	°

Table 8.4: Front landing gear properties

The rear landing gear is mounted on the tail as can be seen in figure 9.1(b)

#### 8.4.4. Mass Estimation

After the iteration process was complete, a final mass estimation was done. This mass estimation can be found in table 8.5. In this table the control surfaces weight estimates the required actuators in the aircraft. Furthermore the pilot attachment includes: cycling mechanism, harness, system to change pilot position. Its weight is estimated from equivalent bike

frames and hang glider harnesses. Others includes all other mass that has not been properly estimated. An example for this is the bolts required for construction or the electric wiring throughout the aircraft.

	Mass		Mass	Unit
Wing	25.5	Battery	8.8	kg
Control surfaces	3.0	Propulsion	7.2	kg
Tail surface	3.2	Pilot attachment	5.0	kg
Tail structure	2.2	Others	4.0	kg
Landing gear	6.2			kg
Total	65.1			kg

Table 8.5: Mass estimation of the Velo-E-Raptor

## 8.5. Verification and Validation

### 8.5.1. Verification

For verification of the program unit tests were done. These included testing whether the forces induced were transformed into shear forces, axial forces and moments the correct way by matching them to hand written calculations. Also, the moments of inertia were doubly checked so that they matched with the intended moment of inertia. Furthermore the bending stress calculations were verified using examples in [68]. Also the shear flow calculations were checked using examples from this book.

To do a system test, the programs that were written for the stress analyses were compared to results produced by the generative structural analysis function in CATIA. Simple models were entered in both the Python program and in CATIA. Multiple forces were applied to these models to see whether similar results were produced. A example of such CATIA generated deflection test can be seen in figure 8.8(a) and the matching stress test can be seen in figure 8.8(b).

	Test	CATIA model	Python model	Unit	Difference
Full spar test	Max. stress	514	470	[Mpa]	9.4%
	Max. deflection	1370	1270	[mm]	7.8%
Square beam	Max. stress	321	298	[Mpa]	13.1%
	Max. deflection	420	405	[mm]	6.3%
Circular beam	Max. stress	459	406	[Mpa]	7.7%
	Max. deflection	670	630	[mm]	3.7%
Max. difference					13.1%

Table 8.6: CATIA verification of three different beams focused on the von Mises stress and the maximum deflection

Here, both the stresses and deflections were compared to the computed numbers. A list of these test can be seen in table 8.6. All these tested load cases differed no more than 13.1% in both stress and deflection, where the CATIA analysis always showed the highest stresses

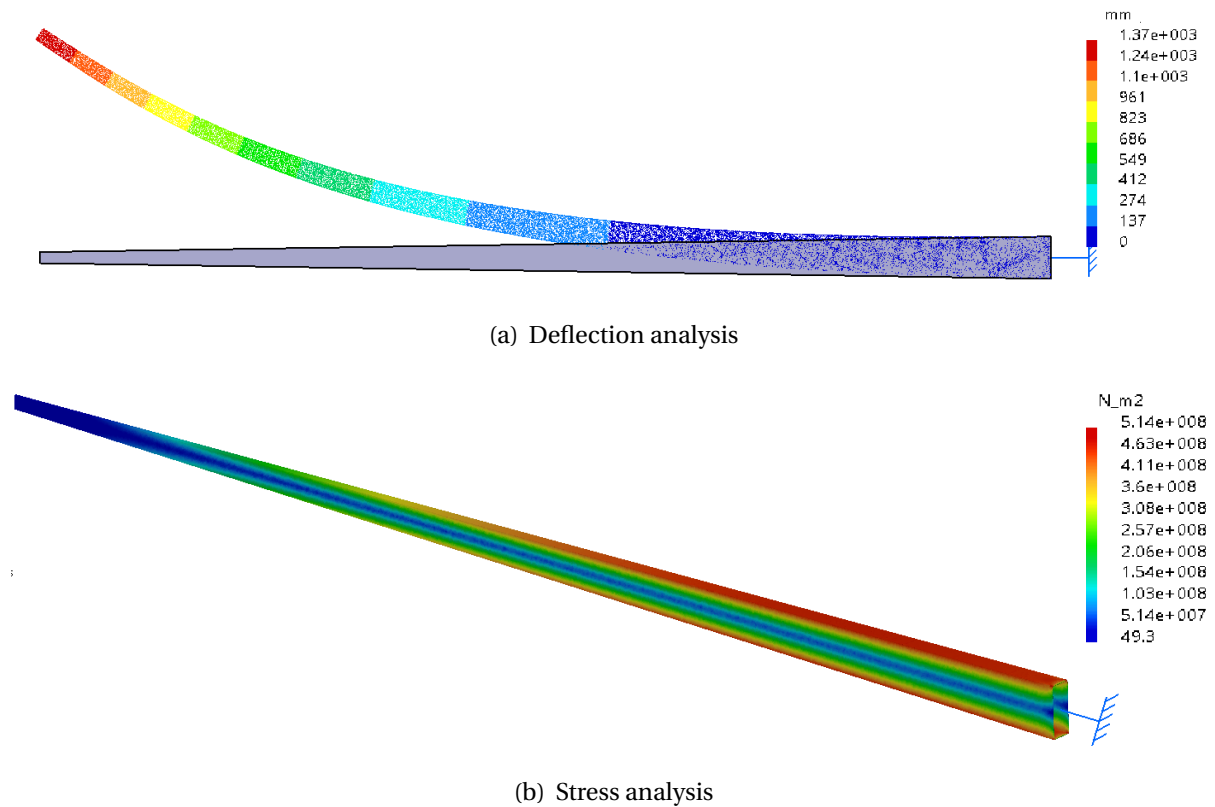


Figure 8.8: CATIA analysis of the main spar under the ultimate load

and biggest deflections. This is caused by stress concentrations at the corners and the root of the spar. These stress concentrations are not taken into account in the calculations and for this reason a extra safety margin of 1.15 is used in the calculation of the structure.

### 8.5.2. Validation

In order to validate the results produced, the final design was compared to other existing hang gliders and ultralight aircraft. Comparing them was difficult since no similar aircraft were found. The hang gliders had a different wing layout and structure and the ultra light aircraft were made of aluminum and had full landing gears. It was decided to compare the mass of the Velo-E-Raptor to that of a topless hang glider with a CFRP frame and a similar MTOW (the Willswing T2C 154). A topless hang glider is a hang glider without a kingpost which is a vertical beam on top of the hang glider with struts to strengthen the wing. Such a structure has not been found advantageous in the Velo-E-Raptor.

The mass of the topless hang glider with a CFRP frame was 29.8% more than that of the wing of the Velo-E-Raptor <sup>8</sup>. This difference was accounted to the thickness of both wings. The wing of the Velo-E-Raptor is thicker than the wing of the hang glider and therefore the wing can be more lightweight due to the higher moment of inertia per mass of the spar. Another reason that the wing of the Velo-E-Raptor is more lightweight is that it has a tapered spar

<sup>8</sup><https://www.willswing.com/hang-glidert2c/>

which is not used in the current hang gliders. A final reason why the hang glider has a bigger mass is that it has to be disassembled into a transportable size. This need for disassembly will result in extra weight in the hang gliders.

Further validation of the design has to be performed after the DSE and a short description can be found in section 8.8.

## 8.6. Production

In this section the part manufacturing will be explained first, followed by an explanation of the assembly of those parts resulting in the Velo-E-Raptor.

### 8.6.1. Part Manufacturing

#### Carbon Fiber Reinforced Polymer

The frame of the Velo-E-Raptor will be made of a CFRP. Two kinds of carbon fibers are widely used: PAN-based fibers and Pitch-based fibers. The production of PAN-based fibers involves polymerization of acrylonitrile and Pitch-based fibers involve destructive distillation of petroleum or coal tar [47]. For the Velo-E-Raptor the PAN-based fibers have been selected due to their availability and higher tensile strength than that of the Pitch-based fibers [47]. Several types of resin are available: unsaturated polyester, vinyl ester, epoxy, phenolic and cyanate resins [46]. For aerospace applications epoxy resin is widely used and also offers the best properties for the Velo-E-Raptor due to its high flexural strength.

The production of the spar requires a structural foam. Since most of the low mass foams are vulnerable to high temperatures, low processing temperatures of the CFRP are required. After some research, it was found that HexPly® M79 200T2 has excellent properties for the Velo-E-Raptor. It can be cured at a temperature of only 70°C, it has excellent mechanical properties and it has a good processability<sup>9</sup>. For convenience, the same CFRP will be used in the whole structure.

#### Spar

Now that the frame material has been specified, the fabrication process of the spar will be explained. The spar is tapered and has a rectangular cross section. To manufacture this in one piece, structural foam will be used. For this foam to be as lightweight as possible, foam is needed with a minimal density that can be used under the processing temperature of 70°C. The perfect foam was found: it is the Divinycell® H35 from Diab. With a density of only 38 kg/m<sup>3</sup>, low water absorption and a maximum processing temperature of 90°C, this foam is excellent for inside the spar of the Velo-E-Raptor<sup>10</sup>. On this foam, the pre-impregnated fibers can be placed and with only a vacuum bag the CFRP can be cured<sup>11</sup>. There is no need for an autoclave that fits the whole spar.

---

<sup>9</sup>[http://www.hexcel.com/user\\_area/content\\_media/raw/HexPly\\_M79\\_eu\\_DataSheet.pdf](http://www.hexcel.com/user_area/content_media/raw/HexPly_M79_eu_DataSheet.pdf)

<sup>10</sup><http://www.diabgroup.com/en-GB/Products-and-services/Core-Material/Divinycell-H>

<sup>11</sup><http://www.easycomposites.co.uk/#!/fabric-and-reinforcement/carbon-fibre-reinforcement/pre-preg-carbon-fibre>

### **Ribs and Stringers**

The ribs will be formed using a mould. On this mould the prepreg can be positioned and with a vacuum bag the ribs can be cured.

The stringers at the leading- and trailing edge will either be made using a mould and a prepreg or using pultrusion.

### **Tail**

To produce the tail, an Aquacore mandrel will be used. This is a mandrel that is soluble in cold tap water<sup>12</sup>. This material can be used with curing temperatures up to 190 °C<sup>13</sup>. When the mandrel is produced and it is wrapped with Teflon tape, it then can be transported in an airtight bag. When ready to use, the bag is removed and prepreg carbon can be applied. With a vacuum bag the CFRP is cured. When the material is cured, the Aquacore is washed away with tap water and the Teflon tape is removed.

### **Skin**

The skin that will form the airfoil will be made of Dacron, more specifically a 4.0 ounce woven polyester fabric (per sailmaker's yard, or 170 grams per square meter<sup>14</sup>). This fabric can be bought of the shelf. Once the fabric is bought, it has to be cut and stitched in the correct dimensions.

### **Control Surfaces**

The frame that is required for the control surfaces will be manufactured in the same manner as the ribs.

### **Landing Gears**

The landing gears require oval tubing. To guarantee the strength of the landing gears, they will be manufactured instead of bought. They will also be produced using an Aquacore mandrel. This way, the landing gears can be as light as possible as the fiber directions will be optimized. The wheels will be bought.

To connect the landing gears to the spar a special flange will have to be produced which can be seen in figure 8.9(a). This flange will fit over the spar to connect the oval beams of the landing gear to the spar. This flange will be made of aluminum as producing this from carbon fiber may prove to be very difficult. Since the aluminum will start a galvanic reaction with carbon fiber, a layer of glass fiber will be used between the two surfaces<sup>15</sup>. With this glass fiber the two surfaces can be bonded together after surface treatments<sup>16</sup>.

## **8.6.2. Assembly**

### **Tail to Spar Connection**

Now that the wing, tail and landing gear are produced, the Velo-E-Raptor can be assembled. The two tail tubes will be connected to the spar using flanges which can be seen in

<sup>12</sup><http://www.acmtucson.com/products/water-soluble-molds-and-tooling/raw-materials/aquacore.html>

<sup>13</sup><http://www.eng-tips.com/viewthread.cfm?qid=200552>

<sup>14</sup><https://www.willswing.com/hang-gliders/hang-glider-sailcloth-information/>

<sup>15</sup><http://www.eng-tips.com/viewthread.cfm?qid=339948>

<sup>16</sup><http://forums.mtbr.com/frame-building/glue-carbon-fiber-aluminum-982094.html>

figure 8.9(b). Those flanges will be attached to the spar with both adhesive and blind fasteners. For the blind fasteners holes are needed in the spar. The amount of holes will be limited as they affect the spar structure. It is of paramount importance that, when making these holes, no delamination will occur. The tail tubes will be mechanically fastened to the flanges such that the tail can be disassembled for transport in a container.

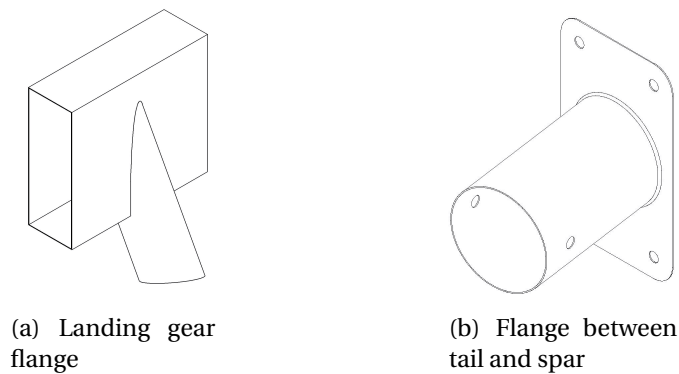


Figure 8.9: Flange layout

There are two dominant methods of machining carbon fiber structures. These are: rotary machining (drilling holes) and abrasive waterjet machining<sup>17</sup>. For making holes rotary machining is necessary. For abrasive waterjet machining first a starting hole has to be made using rotary machining. Since the spar is filled with a structural foam, waterjet cutting will not be an option. Therefore use will be made of the rotary machining method. When using this method it is extremely important to keep the temperature below critical values of both the resin and the structural foam. Therefore, tools with integrated cooling channels to minimize the tool temperature will be used.

### Motor Attachment

As can be seen in figure 8.4 the motor will be located in a box that is formed by two ribs. Two ribs are located at a distance of 6 cm more than the diameter of the the motor which is 10 cm. This box with a 16x16 cm cross section provides enough torsional rigidity, as each engine produces a torque of only 16.8 Nm. As can be seen in the figure, the ribs extend in front of the leading edge to form a box together with two horizontal plates. First, ribs are bonded to the spar. Then, a vertical plate between the ribs is bonded to which later the motor will be attached. Then, the horizontal plates will be bonded between the ribs. This forms a box with an open section at the end where the motor and gearbox are placed. This motor has a minimum of 3 cm on each side such that it can be replaced when needed. Finally a plate will be bolted on this box with the nut glued on the inside such that it can be opened and closed from one single side.

### Landing Gear Connection

Since the spar is tapered, it is relatively easy to bond the flanges of the landing gears to the

<sup>17</sup><http://www.compositesworld.com/articles/machining-carbon-composites-risky-business>

spar. This connection will distribute the loads over the spar, without weakening the spar by using mechanical fasteners. To protect both the aluminum and CFRP, a layer of glass fiber is used to avoid contact between the two surfaces.

### **Skin Attachment**

The skin exist of one single sail that is bonded to the ribs and the trailing and leading edge stringers. This will be done starting at the trailing edge stringer. This stringer will be inserted in one end of the sail like a tent pole after which the stringer is attached to the ribs. From this stringer, the sail will be bonded moving over the top side of the wing to the leading edge and then over the bottom side back to the trailing edge. This will ensure a perfect fit on the top side of the wing, where a perfect fit is most important aerodynamically. The skin has to be bonded under tension to prevent preliminary buckling. A reworkable glue will be used such that the sail can be replaced <sup>18</sup>. The tail surface will be produced in a same manner as the wing is produced.

## **8.7. Conclusion**

The conclusion of the structures department is that it is possible to design the Velo-E-Raptor for an ultimate load factor of 9 with a mass lower than 70 kg if the structure is produced of CFRP. It was also found that the design can be manufactured without any major problems and that a structural foam inside the spar has to be used for production.

## **8.8. Project Design and Development Logic**

During the DSE there were not enough resources for the full detailed design of the aircraft. Therefore things that were not addressed yet during the project are described in this section.

### **Detailed Wing Design**

In the post DSE phase a detailed wing design has to be performed. The ribs are now assumed to be plates which have to be further designed. It needs to be investigated whether more stringers are necessary. Also, the stress concentrations need to be determined and designed for. Finally, a vibration analysis has to be done to prevent phenomena like resonance.

### **Structural Attachments**

The structural attachment of the motors and control surfaces have to be further designed. Now, an approximation was made of the imposed forces and required structure. But, these were simple estimations and more accuracy is required to guarantee structural integrity.

### **Material Properties**

Multiple material properties have to be further analyzed. These include the fiber direction, the effects of temperature, the effect of initial material imperfections and the fatigue characteristics. Since only weight can be saved when designing the fiber directions in a proper way, this will have to be done in more detail. Also fatigue has to be further analyzed such that proper maximum life spans can be set.

---

<sup>18</sup><https://www.masterbond.com/properties/reworkable-polymer-systems>



# 9

## Operations

### 9.1. Lay-out

User experience is an important objective for the design of the Velo-E-Raptor. Not only in the sense that flying has to be cool and exhilarating, but also in the sense that the aircraft can be used easily, flies comfortably, and is safe at all times. This section explains how these design objectives were incorporated in the design of the Velo-E-Raptor.

#### 9.1.1. Pilot Attachment to Aircraft

The pilot attachment to the aircraft is directly linked to the operations needed for takeoff and landing. For safety reasons it was decided to use landing gears both in front and behind the pilot, which fully support the weight of the aircraft. However, if the landing gears fail, it is important that the pilot is able to carry the weight of the aircraft ergonomically.

When carrying heavy loads, the center of gravity of the load should be as close to the center of gravity of the human as possible. Also it should be prevented that all loads are carried on the shoulders. Different kinds of safety harnesses that are used in mountain sports and for industrial use were investigated. The Exofit Strata harness was used as a starting point for the harness design of the Velo-E-Raptor. This harness distinguishes itself from other safety harnesses by the use of a load distribution system that takes the weight off the shoulders and redistributes it down to the hips, reducing forces on the shoulders up to 85%<sup>1</sup>. Also a back protector will be incorporated in the harness.

To connect the harness to the aircraft four karabiners are used in combination with energy absorbing lanyards. A safety belt is used to fasten the pilot onto the chest support, ensuring that the pilot stays in place during flight. In figure figure 9.1(a) a top view of the pilot is shown that indicates the main features of the harness and pilot attachment.

#### 9.1.2. Body Support

To allow the pilot to lie comfortably in the prone position, the body of the pilot will be supported by a hip, breast and chin support made of foam, coated with leather.

---

<sup>1</sup><http://www.capitalsafety.com/caadmin/Pages/DBI-SALA-ExoFit-STRATA-Harness-Helps-Workers-Lighten-Up.aspx>

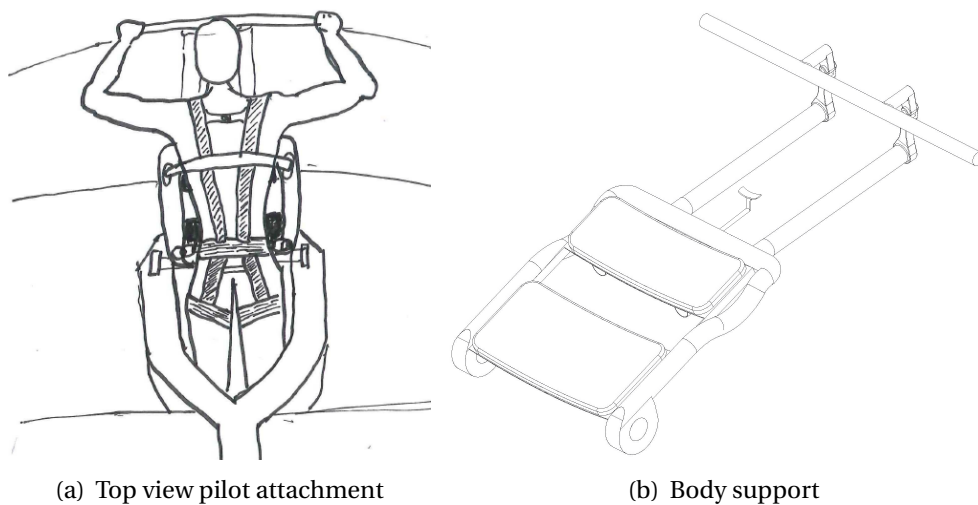


Figure 9.1: Pilot support

Firstly, research was done into the ergonomics of the prone position. As a starting point a literature study concerning the ability of men to perform basic operations in aircraft while relegated to prone or supine position [44] was used, containing many articles on prone flying published between 1951 and 1961. It was found that a 'perfect' prone positions does not exist; different configurations can be made comfortable under the conditions that the different part of the body (legs, upper part of the body and neck) are correctly placed with respect to each other. To validate if the supports are designed ergonomically they need to be tested in real life.

Choosing the inclination of the upper body it has to be taken into account that the pilot influences the view of the pilot; the higher the inclination, the better the view. On the other hand, to minimize drag the inclination shall be as small as possible. For the Velo-E-Raptor an inclination of 20 degrees of the upper back was chosen. As a reference there was looked at tests performed with some specific aircraft using the prone position, namely the Meteor 8 [32] and the Horton-IV [36].

To ensure a comfortable body position, the neck of the pilot is supported with a chin support. The chin should be positioned slightly lower than the upper back<sup>2</sup>. In figure figure 9.1(b) the lay-out of the different supports are shown. The body support can be adjusted for different pilot heights. The hip support is at a fixed position; the chest and chin support can be moved (and then fastened) along the support bar. The control bar will then slide along.

<sup>2</sup><http://www.nestofdragons.net/weird-airplanes/proned-pilots/letter-from-geoff-steele/>

### 9.1.3. Helmet

The pilot will need to wear a helmet when flying the Velo-E-Raptor, mainly for safety considerations, but also to enhance the aerodynamic performance of the aircraft. The helmet also allows for a more comfortable flight at higher speeds. It contains a Head-Up-Display (HUD) for aircraft control, which is further elaborated on in section 9.1.5. The helmet also contains an in-ear plug for control feedback and cancels the, already low, noise of the propellers.

### 9.1.4. Control

The control input system will be a control bar that can be controlled with both hands. It is attached to the pilot's chest support. To pitch up, the pilot will move the bar towards himself and to pitch down away from himself. Rolling to the right means moving the control bar to the right, and vice versa to roll to the left. This way of controlling enhances the free as a bird experience. The control input is shown in figure 9.2(a) and figure 9.2(b). One of the reasons to choose a wind shield is that the control bar can be influenced at high speed. It will create more drag and the chance of the pilot not being able to control the Velo-E-Raptor properly is not desirable.

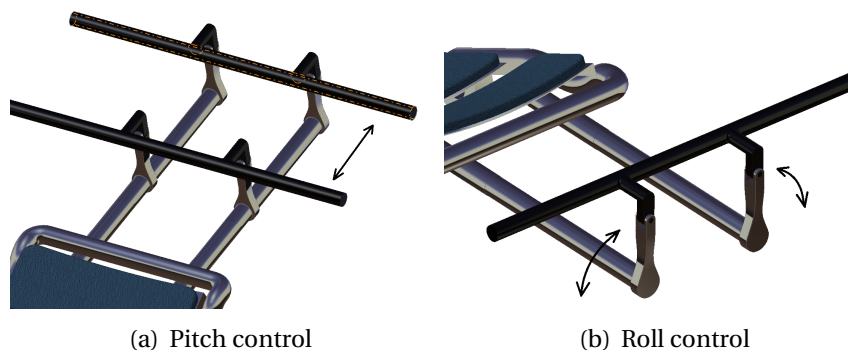


Figure 9.2: Control input

### 9.1.5. Flight Instrumentation

One of the main difficulties of flying aircraft is that speed and height cannot be controlled independently. That is why flight instrumentation and control help are key for the ease of control of an aircraft. For the Velo-E-Raptor, it is important to provide the pilot with enough clear information to fly safely, without presenting too much information, which can result in the pilot losing oversight and understanding [3]. For this reason the information is divided over three resources: visual, auditory and kinesthetic.

#### Visual

The pilot will use a Head-Up-Display. The use of a HUD is not common in general aviation yet, but it can help improve the pilot's safety to a high extend in the future. Low-cost HUD's are already used in sports like skiing or motorbiking<sup>3</sup> and expensive HUD's in fighter aircraft<sup>4</sup>. However, a low-cost HUD should be developed for the Velo-E-Raptor, like the Aero

<sup>3</sup><https://www.reconinstruments.com/products/snow2/>

<sup>4</sup><https://theaviationist.com/tag/helmet-mounted-display/>

Glass<sup>5</sup>. This HUD will be implemented in the pilot's helmet and will provide the pilot with the following information through angles and lines on the HUD:

- The current flight direction and climb angle
- The maximum climb angle
- The horizon line
- The optimal glide angle

The following information is displayed in two bars on both sides of the HUD:

- The current airspeed
- The current height

Besides, in a corner of the Head-Up-Display the following will be provided to the pilot:

- The battery energy level
- Master alarm indicator, which shows a red bulb in case of emergency
- The current time

In figure 9.3 an example picture of this interface is shown. The Head-Up-Display will be connected to the flight computer via a cable. The pilot can plug in the cable to the helmet while attaching to the aircraft. This cable goes through the wing opening in front of the pilot to the flight computer and can be stored there as well.

There will be a phone standard attached to the control panel. This holder can be moved along the control bar. The pilot's phone can show the navigation panel for the pilot. Navigation could be provided to the user through a phone application such as Xavion<sup>6</sup>. Also, applications like Pilot Aware<sup>7</sup> could help the pilot in locating other vehicles during flight. Besides, the phone could be used for communication with ground stations.



Figure 9.3: Head-Up-Display interface<sup>8</sup>

## Auditory

The most important warnings are presented both visual and auditory for redundancy. Firstly,

---

<sup>5</sup><https://glass.aero/shop/>

<sup>6</sup><http://xavion.com/>

<sup>7</sup><http://www.pilotaware.com/features/>

the pilot will be alarmed when the fly-by-wire system intercepts during flight envelope protection. This is done by using earplugs inside the helmet. This plug will tell the pilot what the pilot was exceeding. A further explanation of the flight envelope protection can be found in section 7.3

Secondly, the pilot will get a notification of the battery level at 80%, 60% and 40%. At 25% an alarm notification is given. The pilot can then decide where to land or to head back to its takeoff point. Finally, there is a master alarm that rings when the flight computer detects an error or dysfunction. When the master alarm rings, the pilot will be expected to land as soon as possible. During all auditory warnings, a warning message will appear on the top of the pilot's interface.

### **Kinesthetic**

The last way to provide flight feedback to the pilot is using his ability to feel. This is mainly caused by the feedback produced by the control bar, which is discussed in section 7.3. The control bar will start to vibrate just before the flight computer will intervene.

### **Buttons**

There will be a couple of buttons on the control bar. The following buttons can be found:

- The right hand side of the bar will have a button to add extra power to the Velo-E-Raptor.
- Brake control on the left hand side of the bar
- In the middle of the control bar there is button to activate opening of the parachute.
- A button to send an emergency signal using the EPRIB , see section 9.1.7.
- Stay conscious button, see section 9.1.7.
- Possibly, some buttons for different flight modes, see section 7.3.

### **9.1.6. Pedal System**

The pedal system is already described in section 5.2.2. From an operations point of view it is most important to mention that the pedal system can be adjusted for different leg lengths. To find the pedals easily the pilot can first place one foot on the structure that connects the pedal system to the aircraft. The pedals will include toe clips to ensure the pilot does not lose the pedals during flight.

### **9.1.7. Safety Equipment**

In the exceptional case that the aircraft might crash, precautions are taken to minimize the injuries of the pilot. These are elaborated on below.

The first precaution is a parachute that will be attached to the aircraft. The parachute uses an automatic activation device, which measures the aircraft's height and vertical velocity vector. This measurement system deploys the parachute at a height of approximately 70 meter when it notices that the aircraft is falling down. This will also be implemented in the control system of the Velo-E-Raptor.

To minimize the impact on the pilot during crash an energy absorption zone is essential. For the velo-E-Raptor the landing gear and pedal system provides this energy absorption zone. Also a back protector is added at the rear part of the harness and for the attachment of the pilot to the wing energy absorbing lanyards are used.<sup>9</sup>

A transponder SSR 1030 MHz Mode S will be implemented in the wing near the battery and flight computer. This enables air traffic control to detect the Velo-E-Raptor. The flight computer will recognize from GPS when to turn the transponder on or off, so the pilot does not have to worry about it during flight. The pilot will also be obligated to carry an Emergency Position Indicating Radio Beacon (EPRIB) on its harness. In case of emergency the pilot should be able to send an emergency signal that asks for help. The EPRIB will be triggered automatically when the parachute is deployed.

In case of unconsciousness of the pilot the following measurements are taken. The flight computer will ask for voice recognition if the pilot has not given control input for 15 seconds. If the pilot does not answer or pushes the 'stay conscious' button, after a repetition, the parachute will be launched to guarantee a safe landing.

## **9.2. Flight Procedures**

The flight procedures stated in the functional flow block diagram in the baseline report [40] were investigated. The most critical ones are elaborated on in this section.

### **9.2.1. Pilot Training**

In the beginning the pilot training will be focused on current glider pilots, as they will be the first ones to try out the Velo-E-Raptor. They are already used to glider airplanes. The training will therefore focus on the use of the instruments, the specific maintenance checks (see section 13.3.2) and emergency procedures. This training will give feedback about the critical training aspects and the best way to set-up the pilot training in the future.

### **9.2.2. Takeoff**

The pilot first attaches himself to the aircraft using the karabiners and safety belt. The take-off position is shown in figure 9.4(a). With the motors switched on, the pilot can start running. Once the aircraft is airborne the pilot places his feet onto the pedals. The flight control system notices when the pilot releases the control bar with the help of capacitive touch sensors. When the pilot releases the control bar, the system is triggered to keep flying in the same flight path. The pilot can thus make a safe transition to the in-flight position without having to control the aircraft. Finally, the pilot will be flying in the cruise position, shown in figure 9.4(b).

## **9.3. Conclusion**

The main goals of the operations department were that the detailed design would be cool and exhilarating, could be used easily, would fly comfortably and above all, would be very

---

<sup>9</sup><http://www.campheightsafety.com/ppe/camp-energy-absorbing-lanyards/air-absorber/>

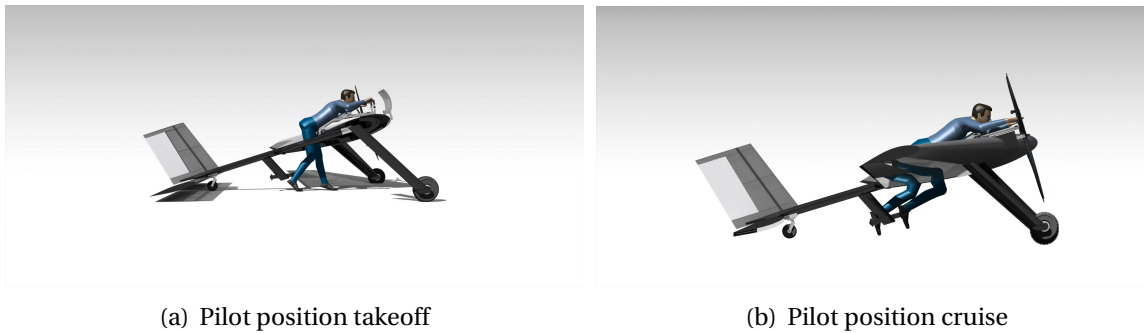


Figure 9.4: Pilot transition during flight

safe.

The "cool" user experience is achieved by the prone pilot position and intuitive control bar. Several studies show that the prone flying position can be made comfortable, but the supports should be further designed and tested. The Head-Up-Display allows for better monitoring of the flight conditions and is the main contribution to the ease of use of the Velo-E-Raptor. Finally, the flight envelope protection, emergency parachute and landing gears with crash zones are the most important contributions to the safety of the aircraft. However, the aircraft's safety depends also on the functioning of the aircraft, which is further elaborated on in chapter 13.

In conclusion, from an operational perspective, the Velo-E-Raptor distinguishes itself from current (hang) gliders in attractiveness, ease of use, comfort and most of all safety.

## 9.4. Project Design and Development Logic

For Post-DSE, several important followup activities of the operations department are established. These activities can be observed in appendix A, where an indication of time and resource allocation is given.

The first important future activity will be refining the body support and control mechanism. The body supports should be designed in more detail to increase the ergonomics of the support system. A prototype should be produced to test comfort during an hour of flight. Besides, the Head Up Display should be developed for application in the Velo-E-Raptor. The use of a HUD is not common in general aviation, as it is mostly used for other sports applications or expensive fighter aircraft. Its interface should be designed by professional interface designers, which will help increasing the ease of flying for pilots. The control bar and system should also be designed in more detail for user-friendliness.

Finally, with respect to safety, an elaborate emergency plan should be produced. This should include all emergency procedures in case of hazardous situations or functional failures.



# 10

## Sustainability

During the detailed design process, sustainability was implemented at all levels. Five different sustainability aspects are distinguished: the design phase, production, lifetime, end-of-life and the social impact of the Velo-E-Raptor.

### 10.1. Design

To enhance sustainability in the design process, it is key to implement multiple functions in one element. The following design elements are a result of this philosophy.

Firstly, the Velo-E-Raptor uses electric power for takeoff. Contrary to internal combustion engines, electric motors are generally more power efficient, easier to maintain and have the opportunity to be charged with "clean" energy.

The modularity of the Velo-E-Raptor contributes positively to sustainability. It enables the replacement of damaged parts without having to replace an entire structure. For example, the skin is often the first item to wear out, but easily replaceable. Only having to replace the skin instead of replacing the entire wing enhances the Velo-E-Raptor's sustainability.

### 10.2. Production

About 40% of the aircraft's structural weight is made out of carbon fiber. As described in section 8.6.1, HexPly® M79 200T2 will be used in the Velo-E-Raptor's main structure, which is mostly the spar, ribs, struts and the tail. Producing carbon fiber is fourteen times as energy intensive as producing steel <sup>1</sup>.

Dacron, which is a PET material, is used as skin material and contributes about 10% to the total structural weight. PET plastic requires a tiny fraction of world's oil in production, but most of that is made from waste refinery byproducts.

The battery weight is also around 10% of the total structural weight. As described in section 5.2.2, the GSYUASA LSE series lithium cobalt oxide batteries are chosen for the Velo-E-Raptor. In general, lithium-ion batteries are considered more sustainable than nickel cadmium and nickel metal hybrid batteries, because they have a much smaller demand for rare

---

<sup>1</sup><https://recyclenation.com/2015/10/is-carbon-fiber-better-for-environment-than-steel/>

earth metals for production. However, application of these lithium-ion batteries increases the consumption of lithium and cobalt that have also limited reserves [51].

The two electrical Hacker A150-8 motors are around 8% of the total weight. The motor is made of copper and aluminum. Due to the high value of pure copper, a large portion of copper production now comes from recycled sources. In the US, recycled copper accounts for about 32% of annual supply <sup>2</sup>. Aluminum will also be used in the Velo-E-Raptor for the pedals and the attachment of the landing gear. As the amount of aluminum in the Velo-E-Raptor is small, the aluminum part production will not have a large effect on the environment.

The pilot's harness and attachment will be mostly made of nylon. The production of nylon is not eco-friendly. It creates nitrous oxide: a greenhouse gas that is about 300 times more potent than carbon dioxide. The production process also requires a lot of water for cooling the fibers. Manufacturing nylon is a very energy-intensive process <sup>3</sup>. However, nylon is the most commonly used material for harnesses and has proven rigidity and safety. That is why nylon will be used for the pilot's harness.

The wing is filled with Divinycell-H35 foam, which is about 8% of the aircraft's weight. This is an expanded polystyrene (EPS) foam <sup>4</sup>. EPS is made up of 98% air, leaving 2% as oil derived plastic. Almost no waste is created during the production of EPS <sup>5</sup>.

### 10.3. Lifetime

Carbon fiber does not corrode, degrade or rust contrary to metals. It can have a much longer lifespan than metals, and is therefore expected to last longer than a comparable metal structure <sup>6</sup>. However, carbon fiber composites are subject to failure modes that are hard to predict, such as delamination. This is a downside, since it is often not visible by inspection. That is why care should be taken when using carbon fiber composites. How this should be done is further explained in section 13.3.1.

The CFRPs have a lower density than metals like steel or aluminum. Therefore less energy is needed for takeoff, because of the aircraft's lower weight. A smaller battery, smaller control surfaces and therefore less material is needed.

Dacron has a lifespan of about one thousand hours, but its performance decays over its lifetime <sup>7</sup>. The skin degrades due to UV radiation, but factors like sand and water can also influence the lifespan.

---

<sup>2</sup><https://www.thebalance.com/copper-production-2340114>

<sup>3</sup><http://goodonyou.eco/material-guide-nylon/>

<sup>4</sup>[https://en.wikipedia.org/wiki/Polystyrene#Expanded\\_polystyrene\\_.28EPS.29](https://en.wikipedia.org/wiki/Polystyrene#Expanded_polystyrene_.28EPS.29)

<sup>5</sup><https://www.kore-system.com/blog/bid/75102/Expanded-Polystyrene-EPS-and-its-Impact-on-the-Environment>

<sup>6</sup><https://recyclenation.com/2015/10/is-carbon-fiber-better-for-environment-than-steel/>

<sup>7</sup><http://freeflightadvice.com/sail-cloth-options/>

Lithium-ion batteries suffer from a small form of self-discharge. The lifespan of a battery is typically specified in number of full charge-discharge cycles. As explained in section 5.1.2, the lithium-ion-cobalt battery has an expected life of 1000 cycles. The capacity of the battery gets less when the number of cycles gets larger. Capacity loss is expressed in percentage after a number of cycles and is about 40% for a thousand cycles for lithium-ion batteries <sup>8</sup>.

## 10.4. End-of-Life

As explained above, carbon fiber is energy intensive to produce. However, it can be recycled <sup>9</sup>. Though, carbon fiber recycling is a fairly new process. In this process, the polymer matrix of the CFRP waste decomposes in an oxygen-less environment at temperatures of about 500 °C <sup>10</sup>. At the end, the carbon fiber residue remains and can be reused.

Another less expensive way of recycling carbon fiber is done by milling. This results in shorter fibers, which are weaker and less valuable. This is also called "downcycling". This has been done on a large scale for CFRPs, resulting in CFRP roads and electronics cases.

Currently, carbon fiber is not recycled on a big scale. However, regulations in the automotive industry force cars to consist of at least 85 mass percent <sup>11</sup> of recyclable materials. Therefore, it is expected that research will be done in possibilities to recycle CFRP. This will likely result in an increase in recycled carbon fiber in the next decade. Hence, it is expected that in the future, when the end-of-life of the first generation of Velo-E-Raptor is reached, the recyclability of CFRPs will have improved immensely.

Recycling of PET, or Dacron, is well-developed, since these materials have applications in other fields <sup>12</sup>, with a 92% availability of PET recycling within the US [45]. PET can be recovered by simple washing processes or chemical treatment to break down the PET into raw materials or intermediates, which are then converted into new PET resins. A final option for PET that is unsuitable for material recycling is to use it as an energy source <sup>13</sup>.

Recycling lithium-ion batteries is more complicated than lead-acid or nickel-metal hybrid batteries. This is mainly because lithium-ion batteries have more different materials in each cell. This makes it even harder as these materials are in powder form during separation. Lithium-ion batteries have mostly one hundred or more individual cells, contrary to a small number of large lead plates in a lead-acid battery. The result is that the extraction of lithium from old batteries is five times more expensive as mined lithium [51].

The metals used in the lithium-ion batteries are recyclable. It is only a matter of time until lithium-ion batteries will be recycled on a large scale. Automotive lithium-ion batteries have

---

<sup>8</sup>[http://batteryuniversity.com/learn/article/how\\_to\\_prolong\\_lithium\\_based\\_batteries](http://batteryuniversity.com/learn/article/how_to_prolong_lithium_based_batteries)

<sup>9</sup><http://www.compositesworld.com/columns/recycled-carbon-fiber-its-time-has-come->

<sup>10</sup>[https://www.ict.fraunhofer.de/content/dam/ict/en/documents/I-PDF%20Fraunhofer%20ICT%20KUint\\_2014\\_6\\_S62\\_en.pdf](https://www.ict.fraunhofer.de/content/dam/ict/en/documents/I-PDF%20Fraunhofer%20ICT%20KUint_2014_6_S62_en.pdf)

<sup>11</sup><http://www.compositesworld.com/articles/recycled-carbon-fiber-update-closing-the-cfrp-lifecycle-loop>

<sup>12</sup><https://www.interempresas.net/Plastico/Articulos/20985-Mayor-rendimiento-para-aplicaciones-de-reciclaje-de-film-BOPP-y-BOPET.html>

<sup>13</sup>[http://www.petresin.org/pdf/PET\\_whatisitandwheredoesitcomefrom.pdf](http://www.petresin.org/pdf/PET_whatisitandwheredoesitcomefrom.pdf)

only been in commercial use for about five years, and it will take some time until they are used in large volumes. Simply not enough batteries have reached the end of their lives to support large-scale recycling plants. Several recycling methods have been proposed, each with its advantages and disadvantages [51]. It must be noted that due to the presence of metals like lithium, copper and cobalt the battery waste can create risk for soil and water pollution.

Copper can be recycled with almost no loss of performance <sup>14</sup>. It is one of the most recyclable metals and that is why it is very sustainable at end-of-life. Recycled aluminum takes only 5% of the energy newly produced aluminum uses <sup>15</sup>. That is why 75% of the aluminum ever produced is still in use today, according to the International Aluminium Institute <sup>16</sup>. Unfortunately, nylon is not biodegradable. At the moment there are several companies reusing and recycling nylon into new products. Though this is not common practice yet. EPS is water-resistant and does not degrade over time. Fortunately, it can be reused efficiently in the production of new EPS <sup>17</sup>.

## 10.5. Conclusion

In the end, the Velo-E-Raptor should have a positive influence on society. The Velo-E-Raptor's circular economy model, described in section 13.2, contributes to the sustainability of the product. A Velo-E-Raptor will be used more often when shared, resulting in less Velo-E-Raptor production in the end. Besides, the operator can extend the Velo-E-Raptor's life as maintenance can be better monitored. This prevents customers neglecting maintenance checks. The materials stay in possession of the operator and that allows for a more straightforward end-of-life recycling.

Currently, using the weight estimations from section 8.4.4, it is estimated that about 78% weight of the material can be reused. Dacron, rubber, copper, and EPS are already recycled on a large scale. Carbon fiber and lithium-ion batteries are expected to be recycled on a large scale at the end-of-life of the first produced Velo-E-Raptors. The calculations include a margin of 10% for every material for losses and damaged parts. In any case it could be said that the requirement of at least 70% of recyclable materials has been met. However, the production of most materials is not as sustainable as needed for future purposes, as most materials still make use of oil. Anyhow, when eventually almost all materials can be recycled, the circular economy loop of the Velo-E-Raptor can be closed.

---

<sup>14</sup><http://copperalliance.org/wordpress/wp-content/uploads/2017/03/ica-copper-recycling-1405-A4-low-res.pdf>

<sup>15</sup><http://recycling.world-aluminium.org/review/sustainability/>

<sup>16</sup><http://recycling.world-aluminium.org/review/sustainability/>

<sup>17</sup><https://www.kore-system.com/blog/bid/75102/Expanded-Polystyrene-EPS-and-its-Impact-on-the-Environment>

## Sensitivity Analysis

As explained in section 2.2, for every method used, the inputs and outputs were tested by performing a sensitivity analysis. The numerical results will not all be presented in this report. Instead, in this section, the important results and conclusions will be explained.

### 11.1. Weight

Any improvement in performance will lead to an increase in weight. If for example the aircraft is not stable, the wing, tail or control systems can be altered, resulting in an increase of weight. Another example: if the performance requirements are not met, planform or propulsion parameters can be changed, but weight will increase as well. The challenge is to make sure all requirements are met while still keeping a safe margin below the 70 kg weight requirement.

Another effect that arises when increasing weight is the "snowball effect". When weight is increased by 10%, an additional 4.1% of wing surface is necessary to match the original performance. A larger wing surface results in a larger wing structure, resulting in an additional weight increase of 2.7%. When running this iteration, the weight increase converges to a total of 13.7%. This also works in the opposite direction: if the weight would be reduced somewhere in the design, the wing surface can become smaller again.

After detailed design a configuration was found with a weight of 65.1 kg, with all stability requirements and almost all performance requirements being satisfied, as can be seen in chapter 16. The Velo-E-Raptor is however still in the conceptual design phase, so errors are bound to be made in the various models used for calculations. Because weight is an output of every subsystem and because of the snowball effect, the weight is very sensitive to change during future development. This poses a big risk to the Velo-E-Raptor project, and changes in weight should always be monitored closely during future design stages.

### 11.2. Stability

A similar method as used for the weight sensitivity analysis can be applied to stability. To determine whether the aircraft is still stable when certain parameters change, the following tests were done. First a check was done to see what happens to the trim angle when the pilot is either 65 kg or 85 kg. The design was optimized for static stability for someone weighing 75 kg, and due to the large impact the pilot mass has on the overall weight, any change will

be noticeable. Table 11.1 shows some important parameters for different pilot masses. As can be seen all pilot weights provide a stable aircraft for very minimal elevator deflection at trim and have an acceptable stability margin.

One of the dangers however for stability is in the pilot position. Again, because of the large contribution of the pilot mass to aircraft weight, a shift in center of gravity of the pilot means a large shift in center of gravity for the aircraft. To see the impact of this the center of gravity of the pilot was shifted 10 cm backwards and the stability margin (S.M.) was recalculated for each pilot weight. As can be seen in the final row of table 11.1 the S.M. becomes critical for all pilot weights.

There is a probability that the pilot center of gravity position will shift during flight or because of manufacturing. This would result in a risk for the rest of the project. An unstable aircraft would mean that new iterations would have to be done in collaboration with the other departments, possibly starting a negative snowball effect. This is something that has to be monitored closely in future development.

Table 11.1: Sensitivity of stability to pilot mass and position

	$m_{\text{pilot}} = 65 \text{ kg}$	$m_{\text{pilot}} = 75 \text{ kg}$	$m_{\text{pilot}} = 85 \text{ kg}$	Unit
$C_{L_{\text{trim}}}$	0.351	0.375	0.405	–
$\alpha_{\text{trim}}$	2.88	3.3	3.5	°
$\delta_{e_{\text{trim}}}$	0.56	0.29	-0.12	°
S.M. ( $x_{c.g.pilot}=0.8$ )	0.06	0.07	0.08	–
S.M. ( $x_{c.g.pilot}=0.9$ )	0.001	0.006	0.011	–

## Market Analysis

For the baseline report a market analysis was performed that assessed the various customer segments, their needs and buying patterns, the current competition and the size and volume of the market [40]. Since the Velo-E-Raptor is aimed to be introduced as an aircraft for a new type of exciting, but safe airsport the market analysis was mainly used to identify customer requirements and design goals. In this chapter the market analysis performed for the baseline report was updated with a stakeholder analysis, new insights and numbers on the Dutch recreational aircraft market, coming from an analysis on the economical value of the Dutch General Aviation market. This analysis eventually allows for the establishment of a target cost of the Velo-E-Raptor.

### 12.1. Stakeholder Analysis

#### **Pon Holdings B.V.**

Pon Holdings B.V. is an international trading and service organization for A-brands such as Cervélo, Volkswagen, Caterpillar, MAN and Continental <sup>1</sup>. With a powerful brand portfolio Pon is an important player in the global bicycle market. With a worldwide growing interest in electrically powered bikes (e-bikes) the project of the Velo-E-Raptor, making use of a similar human powered, electrically assisted power system is of special interest to Pon. Showing that their technology can be used not only on bikes, but also on a new type of aircraft that is not only safe but also cool and exciting to fly with (and such can be used for a new type of airsports), can improve the image of the e-bike, and Pon in general to a younger audience. In this way the Velo-E-Raptor could be used for PR related activities for Pon.

#### **Future Users**

The future users of the Velo-E-Raptor are important in two ways: firstly they represent the target audience of possible PR activities of Pon, and secondly, when introduced into the market, these are the first people expected to be interested in using the Velo-E-Raptor. The specification of future customers and analysis on customer needs is performed in the following sections.

#### **Regulatory Bodies**

The biggest constraint of the Velo-E-Raptor and small aviation in general is the regulations it has to comply with. In order to fly the Velo-E-Raptor in the Netherlands, it has to comply

---

<sup>1</sup><http://www.pon.com/en>

with both Dutch (set by the Ministry of Infrastructure and the Environment) and European regulations. When looking into the different categories of aircraft the Dutch regulations distinguishes, there is one type of aircraft that fits the Velo-E-Raptor mission in particular: "zeilvliegtuig". A detailed analysis on the design constraints set by regulations and following requirements can be found in the baseline report [40].

### **Future Operator**

For the second life phase of the Velo-E-Raptor (i.e. when the Velo-E-Raptor will be produced on a bigger scale and people start practicing this new type of aircraft) the role of the operator will become increasingly important. In this life phase product requirements on maintainability and availability will play a crucial role in the success of the Velo-E-Raptor. This will be further elaborated on in chapter 13.

## **12.2. Customer Segment**

For the specification of future costumers, in the market analysis of the baseline report [40] research was done into the most popular air sports at this moment. Future users of the Velo-E-Raptor can be assumed to be found in this market segment. Also the market for a new type of aircraft bridging the gap between sailplanes and hang gliders were taken into account. The two most significant of these products are the Ruppert Archaeopteryx and the Aériane Swift.

### **Gliding**

Sailplanes or gliders are fixed wing aircraft that come in both powered and unpowered configurations. Most glider pilots are connected to gliding clubs that have a fleet and provide the required assistance and facilities to enable flight. Members pay yearly membership fees that cover all costs (i.e. aircraft and flight cost, maintenance, storage and remaining facilities). Membership fees differ per gliding club, starting from €500 and increase to €1,000. On average members fly between fifty and seventy times a year.

The gliding clubs are also responsible for the training of new pilots. Normally a new pilot is able to fly solo after fifty to seventy-five flights. After that the pilot will continue training for their glider pilot licence for which several exams must be taken.

### **Hang Gliding**

A hang glider consists of an aluminum alloy or composite frame covered by a synthetic sailcloth to form a wing. The pilot hangs in prone position under the wing inside a harness. The hang glider is controlled by shifting the body with respect to the control frame. If thermals are being used properly, thousands of feet of altitude can be gained and pilots can soar for hours. Most people in the Netherlands learn to fly hang gliders via hang gliding schools. A regular course for beginners will take you a couple of days. After that different training programs can be taken depending on your level and ambition.

### **Paragliding**

A paraglider is a glider with a wing made out of a flexible fabric. This canopy comprises a

large number of interconnected cells. The pilot is supported under the wing in a sitting position by a network of suspension lines. Learning to fly a paraglider is generally considered to be easier than hang gliding. One can expect to fly solo, under supervision, after a couple of days of training.

### **Archaeopteryx**

The Archaeopteryx is a foot-launched hang glider with a configuration closer to conventional airplanes. The aircraft is essentially a small, minimalist sailplane which can be carried on one's shoulders and launched as such<sup>2</sup>. The performance is between that of regular hang gliders and sailplanes. Piloting the aircraft is very similar to piloting a sailplane. Because of this, most potential customers choose to fly sailplanes instead, because they are generally more available at local clubs and have a better performance. The main interest is from people who want to fly in an aircraft close to a sailplane, while only requiring a hang gliding license. Different configurations are available of which the powered version is not foot-launched.

### **Aeriane Swift**

The Swift is a direct competitor of the Archaeopteryx<sup>3</sup>. The Swift is also foot-launched and controlled like a normal aircraft. Therefore, like the Archaeopteryx, the Swift is in between hang gliders and sailplanes. Multiple versions of this aircraft are produced. These versions are equipped with a fairing and windshield, a combustion engine or an electric engine<sup>4</sup>. For this vehicle, the powered version is not able to perform foot-launched takeoff.

## **12.3. Market Size and Product Cost**

The market size per type of aircraft differs per country. For now, the focus is on the Dutch market for that is where the product is aimed to be launched. However, the possibilities of selling the Velo-E-Raptor internationally will be an opportunity since the Dutch market only comprises a small part of the world wide market.

### **Gliding**

In the Netherlands there are over 2,200 active glider pilots making approximately 100.000 flights a year at forty gliding clubs<sup>5</sup>. Various types of gliders are being used, varying from training to competition gliders. There are three leading manufacturers in Europe which cover almost the entire market: Alexander Schleicher, DG Flugzeugbau and Schempp-Hirth Flugzeugbau.

An average glider costs \$90,000 to which \$40,000 can be added for a duo or motorized configuration. Private ownership of gliders is not uncommon but it is expensive since the fixed cost per flight hour are high if the glider is not used daily. Fixed costs as storage, insurance and maintenance can easily increase up to \$5,000 a year.

---

<sup>2</sup><https://www.ruppertcomposite.ch/#wk-304e>

<sup>3</sup><http://www.aeriane.com/products/aircrafts/swift/swiftlight/>

<sup>4</sup><http://www.icaro2000.com/Products/Trike/Trike.htm>

<sup>5</sup><http://www.knvvl.nl/>

## Hang Gliding and Paragliding

In the Netherlands there are approximately 2,500 hang glider and paraglider pilots. Together they make 20,000 flights a year. In order to determine the size of the hang gliding market in the Netherlands various hang gliding importers and dealers were contacted. People from Flying Dutchman and Aespiro, both hang gliding importers in the Netherlands, told that on average twenty hang gliders are sold in the Netherlands per year.

For the product price of hang gliders five leading companies were analyzed: Wills Wings, North Wing, Moyes Malibu, Bautek and Finsterwalder. An analysis on these manufacturers and the prices of their hang gliders are illustrated in Table 12.1.

Table 12.1: Retail prices of new hang gliders

Manufacturer	Price	
	Low end model	High end model
Wills Wings	€4,500	€8,150
North Wing	€4,100	€6,780
Moyes Malibu	€5,000	€6,000
Bautek	€5,500	€6,650
Fonsterwalder	€4,500	€5,500

For powered hang gliding a powered harness is used with a conventional hang glider wing. The most reliable and commonly used harness is the Mosquito NRG manufactured by Swedish Aerosport. This harness has a price ranging between \$7,000 and \$8,000<sup>6</sup>. A couple of other manufacturers exist worldwide that sell powered harnesses in the same price range, all of them using combustion engines. A promising entry into this market is the electrically powered E-Lift by the German company of Toni Roth. In the Netherlands only a handful of pilots practice powered hang gliding.

A similar price analysis was performed on paragliders and paramotors and can be found in the baseline report [40]. Since the Velo-E-Raport uses a rigid primary structure, for the price estimation the paraglider and paramotor are not taken into account.

## The Archeopteryx

Despite good performance and a mature design, the Archeopteryx never saw large success. Only eighteen models have been built since the product was made available in 2010. The lack of success is likely due to a lack of demand and a steep price. The Archeopteryx costs between €77,000 and €100,000 depending on the version. There are three versions available. The standard version includes the minimum for the functioning of the product. The race version adds a cockpit fairing and windshield. The electric version further adds electric propulsion, which can only be used with wheeled takeoff<sup>7</sup>.

## Aeriane Swift

Despite having lower glide performance, the Swift is a lot more successful than the Ar-

<sup>6</sup><http://www.swedishaerosport.se/products/product/mosquito-nrg/>

<sup>7</sup>[https://en.wikipedia.org/wiki/Ruppert\\_Archeopteryx](https://en.wikipedia.org/wiki/Ruppert_Archeopteryx)

chaeopteryx, with at least 138 models sold<sup>8</sup>. This is due to its significantly lower costs, ranging from €25,750 to €42,000, depending on the version. It is because of the significantly lower price that the Swift manages to fill most of the market for foot-launched sailplanes.

## 12.4. Costumer Needs

The market analysis performed in the baseline report [40] gave a good inside in what future costumers will find particularly important. These costumer needs are based mainly on market trends and user requirements for the considered air sports. The following design goals were identified:

- **Availability:** this is the need of the aircraft to be accessible for everyone. For the Velo-E-Raptor it was decided that availability will be ensured by the use of a circular business model. In section 13.2 this is further elaborated on.
- **Attractiveness:** the Velo-E-Raptor should be cool and attractive in order to attract to a young target audience. This soft requirement has been a criteria in many design choices during the design of the Velo-E-Raptor.
- **Safety:** safety has been a paramount objective for the design of the Velo-E-Raptor. A comprehensive analysis on how safety has been incorporated in the Velo-E-Raptor can be found in chapter 13.
- **Ease of handling :** It is found to be important that flying the Velo-E-Raptor is easy. For this reason there was looked at different methods to assist the pilot in flight. In section 9.1.5 the incorporation of flight instruments in the form of a HUD will be further elaborated on.

## 12.5. Target Consumer Cost

Establishing a target cost based on reference aircraft is found to be very difficult since there is such a big variety of aircraft within the general aviation segment. On the other hand, aircraft with characteristics similar to that of the Velo-E-Raptor are rare on the market right now. The electrically powered versions of the Archaeopteryx and Aeriane Swift come closest. However, the cost of these two aircraft is very different; the Swiss made Archaeopteryx is more than double the price of the Aeriane Swift.

However, the business model chosen for the Velo-E-Raptor will be very different from that of the aircraft mentioned above. A circular business model is chosen in which the Velo-E-Raptor will be shared by members that pay a monthly fee. This business model will be further explained in section 13.2 This business model allows for a first estimation on the target cost of the Velo-E-Raptor. This costumer based pricing approach is based on placing a product in the market that matches customer needs, at a price level that optimizes both profit and customer satisfaction. The purpose if this cost estimation is to establish a target cost for aircraft such that an investment in a badge of aircraft is returned within five years.

---

<sup>8</sup><http://www.ultralight-glider.fr/fr/>

The assumptions made for this estimation are based on the analysis on the different customer segments and needs. Since users have to share the aircraft, the number of aircraft needed must be established first. The following assumptions are made:

- 100 members fly 45 hours per year (4500 hours in total)
- One aircraft can be flown 4.5 hours a day (1602 hours per year in total)
- Members pay a membership fee of €500 per year for a period of five years

Using these assumptions it was calculated that a total of three aircraft is needed to let every member fly 45 hours a year. Given that the members together pay €250,000 in five years, and that an investment in three aircraft must be returned in five years, the cost per aircraft should be no higher than €83,300.

A target cost of €83,300 per aircraft would in this case not only include the acquisition cost, but also the cost to operate and maintain, facilitate and support the aircraft. Though this might be an ambitious target for the first life phase of the Velo-E-Raptor in which R&D and production cost will probably drive the cost per aircraft way beyond this target cost, on the long term it would allow for a profitable business case.

## 12.6. SWOT analysis

For the SWOT analysis that is shown in figure 12.1 the final design of the Velo-E-Raptor is analyzed with respect to other aircraft in its segment. It gives a brief overview of the most important remarks from the market analysis.

<p><b>S</b>trength</p> <ol style="list-style-type: none"> <li>1. Safest aircraft in its segment.</li> <li>2. 'Free as a bird' experience available for everyone.</li> <li>3. Available through collaborative consumption model.</li> <li>4. Aircraft is recyclable for about 78%.</li> </ol>	<p><b>W</b>eakness</p> <ol style="list-style-type: none"> <li>1. Aircraft must prove itself first.</li> <li>2. Aircraft does not comply with Dutch regulations yet.</li> <li>3. High investment and production costs.</li> <li>4. The design is sensitive to weight increase.</li> </ol>
<p><b>O</b>ppportunity</p> <ol style="list-style-type: none"> <li>1. Application of circular economy in a lot of other industries, but not in aviation.</li> <li>2. The high threshold of other aviation sports asks for a sport with a lower threshold.</li> <li>3. The use of state of the art technologies.</li> <li>4. A lot of growing opportunities.</li> </ol>	<p><b>T</b>hreat</p> <ol style="list-style-type: none"> <li>1. Constantly changing and strict regulations.</li> <li>2. The general fear of flying will make it hard to get the general public to fly.</li> <li>3. If a pilot will get injured in flight, the design will probably be unsuccessful.</li> <li>4. Hobby/sport flight is not popular among young people.</li> </ol>

Figure 12.1: SWOT analysis Velo-E-Raptor

## 13.1. Reliability

As a first step in the reliability study of the Velo-E-Raptor a Failure Modes, Effects and criticality Analysis (FMECA) was performed. This method serves to highlight possible failure modes, identify the effects and causes and to see what compensating provisions are taken, or yet have to be taken to prevent functional failure. The most critical functions will be further discussed. Also the FMECA serves as input for the safety and risk analysis.

### 13.1.1. FMECA

For this FMECA the most critical functions of the Velo-E-Raptor were identified. Per subsystem it was assessed what causes a certain functional failure and what the possible effects might be. For some failures compensating provisions have already been taken to either decrease severity or probability of occurrence of a certain failure (cause). Since no specific failure rates are known, the following probability of occurrence levels are used to rank the probability:

**Level A** - Frequent: the event is likely to occur often

**Level B** - Probable: the event will occur several times

**Level C** - Occasional: the event likely to occur

**Level D** - Remote: the event is unlikely but possible to occur

**Level E** - Improbable: So unlikely, it can be assumed occurrence may not occur

For the severity the following severity classes and criteria are used:

**Category 1** - Catastrophic: death/severe injury, system loss

**Category 2** - Critical (injury, major system damage)

**Category 3** - Marginal (minor injury, minor system damage, delay or loss of availability or system degradation)

**Category 4** - Minor (no injury or system damage, unscheduled maintenance or repair necessary)

The FMECA is shown in Appendix B.

## 13.1.2. Compensating Provisions

### Structural Failure

From the structural functions, failure cause 2.1 and 3.3 were identified to be critical. Both are caused by structural damage of the aircraft and should be prevented at all times. Two preventive measures have been taken to ensure structural integrity of the Velo-E-Raptor during operations, by decreasing the probability of occurrence of structural failure. Firstly, it was assessed which safety margins should be applied. This can be found in chapter 8. However, since structural damage cannot always be prevented, maintenance of the aircraft is of the utmost importance. In section 13.3 will be explained how structural integrity will be guaranteed by means of maintenance.

### Battery Failure

If the batteries of the Velo-E-Raptor set fire or explode during a flight or crash, the effects will be severe for both pilot and aircraft. Even though the probability of occurrence of such an event is considered to be very low, it is highly recommended to further research the use of the chosen batteries and perform a comprehensive test program on the safety aspects of the used batteries. Another remark should be made on the battery location that, because of the significant weight of the batteries with respect to the total aircraft weight, was now chosen such that it contributes to the stability of the Velo-E-Raptor. It should be further investigated what the effect of this location is on the crash behaviour of the aircraft.

As indicated in the FMECA the loss of battery power is not rated as a critical failure. In principle the Velo-E-Raptor is perfectly able to fly and land without engine power. However, it should be noted that if the aircraft has no battery power left to return to the intended landing site, another landing spot needs to be chosen as soon as possible. If no suitable spot is found, this can lead to a critical situation. It is therefore important that the pilot is always aware of the battery status and that a warning system is present. This is further elaborated on in chapter section 9.1.5.

### Uncontrollable Aircraft

Failure of the control functions (function 10 to 12 from FMECA) have in most cases critical or catastrophic effects. Assuring that the control systems has enough redundancy was therefore found to be especially important. However, a problem that was faced during the design of the control system was that determining the actual reliability of the (functions of) the control system was not yet possible at this stage.

When further developing the electronic control system of the Velo-E-Raptor it is recommended to first set requirements on the reliability needed, for that will have a big influence on its configuration. Since auxiliary and additional functions such as the flight envelope protection systems (function 10) are less critical (if the failure is recognized the function can be taken over by the pilot) the reliability of these functions may be lower (between  $10^{-3}$  and  $10^{-4}$  than that of the system that converts the pilot input to control surface deflection (function 10). The probability of such a failure must be extremely improbable i.e. a probability of failure per flight hour in the order of  $10^{-9}$  [24].

## Bird Strike

Collision between aircraft and bird, also known as bird strike, is something that at this moment can only be prevented by the pilot himself. Especially the propellers, placed at the leading edge of the wings are prone to bird strike. Bird strike tests should therefore be performed to see to what extent the propellers are affected. For the future a possible solution to this problem could be the use of bird radars, such as a LIDAR system <sup>1</sup>. Nowadays bird radars are mainly used on the ground to track exact position, altitude, speed and direction of birds, or flocks of birds <sup>2</sup>. With this information it can be identified what the risk of bird strike at a particular moment and place might be. In the future bird radars may also be able to support real-time decision-making and automated deterrence.

## 13.2. Availability

The product support takes into account all considerations needed to assure the effective support of the product through its programmed life cycle [21]. A current trend is the implementation of circular economy in the design, support and end-of-life of products. The circular economy approach aims to create a system that allows for the long life, optimal reuse, refurbishment, remanufacturing and recycling of products and materials <sup>3</sup>.

The Velo-E-Raptor will be part of a collaborative consumption plan, which is achieved by the sale of the Velo-E-Raptor as a service. This way the sharing can be regulated and controlled by the manufacturer. The Velo-E-Raptor will be provided to the user through a subscription to the Velo-E-Raptor community, which requires a monthly fee. This membership will give the customer limitless access to usage of the Velo-E-Raptor. In order to sign up for the community, one would need some certification provided by the operator. Also, a deposit is required to account for theft and wrecking. The minimum age is 14 years old, which is the usual minimum age for hang gliding and gliding clubs. It is provided that the customer has at a minimum the smallest required person length of 1.65 m and a mass of 65 kg.

In the beginning, the Velo-E-Raptor stations will probably be at existing gliding clubs. This makes it cheaper to start and more accessible than building stations. The aim is to have own stations in a further development stage. It is important that there are more Velo-E-Raptors at the same time at a station to allow for groups flying all at once. After all, flying the Velo-E-Raptor should be a social activity.

The Velo-E-Raptor can be transported on a trailer in a 45 feet long cube shipping container, like the Pacton txd342t <sup>4</sup>. If a Velo-E-Raptor has landed far from its station, it might be necessary to use the trailer to bring it back. It is possible to demount the aircraft in six separate parts: the main wing, the horizontal tail wing, the vertical tail wing, the structure in between, including the pedals and support wheel, and the two propellers plus support wheel. The trailer will have two floors. The bottom floor is reserved for the main wing. The propellers, horizontal tail wing, vertical tail wing and the part in between will be placed on the upper

---

<sup>1</sup><http://www.faunaphotonics.com/technology/>

<sup>2</sup><http://www.robinradar.com/bird-strike-prevention/>

<sup>3</sup><https://kenniskaarten.hetgroenebrein.nl/en/knowledge-map-circular-economy/definition-circular-economy/>

<sup>4</sup><http://www.pacton.nl/uploads/files/products/21/pacton-tdx342t-bep1-1469178219.pdf>

floor. These have a length of about 9 meters all together. Foam can be used to separate the different components and prevent damage during transportation.

Generally, the aim is to fly the Velo-E-Raptor from station to station. In the Post-DSE phase it could be an option to consider making the main spar of two separate components. This would allow for transportation in a trailer with half the length, such as the archaeopteryx trailer<sup>5</sup>.

The first step in offering the Velo-E-Raptor to the public is through PON. Probably four or five Velo-E-Raptors will be produced. These prototypes will be used for exhibitions and marketing stunts. This way, the Velo-E-Raptor can be further developed with respect to safety, cost, performance and user friendliness. It is the first step in making the Velo-E-Raptor available: show it to a big and diverse group of people. Then, when the people (and the Velo-E-Raptor) are ready, the Velo-E-Raptor will be launched on the market.

### 13.3. Maintainability

The Velo-E-Raptor should be airworthy at all times. That is why its maintenance is a very important aspect with respect to safety. The Velo-E-Raptor is not subjected to any regulations regarding maintenance. However, the manufacturer is expected to have a plan for optimal maintenance and safety assurance. The requirement stated that the user should be able to maintain the Velo-E-Raptor himself has been dropped. This is because the main design requirement is safety and everyone maintaining their own aircraft will increase safety risks. A global overview of maintenance checks and the most likely replacement and repair procedures are outlined.

#### 13.3.1. Maintainability of the Design

In the current design phase, it is important to keep in mind that the Velo-E-Raptor should be easily maintainable. Every part should be accessible for maintenance checks, repair and replacement. In figure 13.1 the main constructive components can be seen. It consist mainly of: the wing skin, the spars and ribs, the landing gear, the propellers, the propulsion system, pilot attachment and control system and cables.

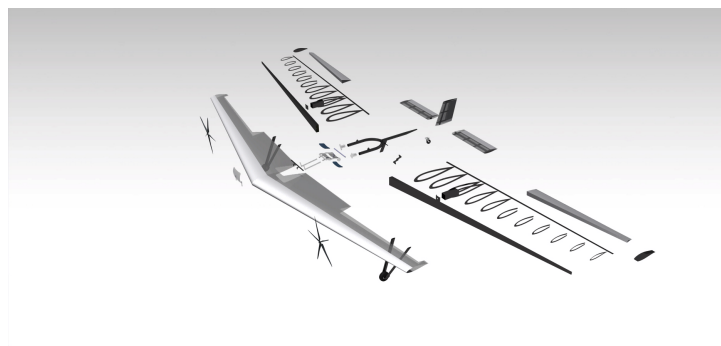


Figure 13.1: Exploded view of the Velo-E-Raptor

---

<sup>5</sup><https://www.ruppert-composite.ch/>

The wing skin is attached to the frame by re-workable glue, which is explained in section 8.6.2. The main hazards to the wing skin are tears and UV damage. Therefore it is recommended to check for this frequently. As mentioned before, the skin lifetime is 1000 hours of UV exposure<sup>6</sup>. A simple option for wing skin testing is the use of light coming through the cloth that will look different at places where the cloth is thinned from UV damage, wear and fatigue<sup>7</sup>. After detachment from the wing structure, the wing skin cannot be used again due to possibly created tears in the sail. To avoid UV damage, a cover will be developed to avoid UV light during storage of the Velo-E-Raptor.

During wing skin replacement, the inspection of the spars and ribs should be done. The carbon fiber structure will need to be inspected for structural failure modes and should be tested for fatigue, cracks and delamination. This is best tested with ultrasonic and thermographic methods<sup>8</sup>. However, this is very expensive and complicated. That is why the regular checks will consist mainly of visual inspection for cracks and so-called 'tap test' for delamination. This test is done by tapping with a coin and carefully listening for variations in sound can be an indicator for delamination. A hollow sound or "dead" tone, are indicators that delamination has occurred<sup>9</sup>. In the exceptional case that unscheduled maintenance should be performed on the internal wing components like spars, ribs, but also cables, the wing skin needs to be disconnected and replaced. The flight sensors are placed on the wing ribs and can be approached in the same manner as the rib replacement. It must be noted that if a rib, with sensor on it, needs replacement, the sensors needs to be unscrewed and attached on the new rib. The HUD is a completely separate component and will be checked and maintained separately.

The landing gear is one of the critical components with respect to failure. Inexperienced pilots will be flying the Velo-E-Raptor and not always land in the most desirable way. The landing gear is most likely to fail at the intersection of the flange and the spar, when the moment created on this point will become too large. Attention should be paid to this intersection during maintenance. Also, as the landing gears are also mostly made of carbon fibre, they should be inspected and tested as explained above for the spars and ribs.

The propellers can be detached from the wing structure. Their blades are most likely to fail and can be replaced individually. The motors are placed just behind the propellers in the wing. The propeller needs to be disconnected in order to reach the motors for maintenance.

The pedal system can be maintained easily, just like a bicycle. The lubrication of the pedal system is important in order for the system to work properly. When the pedals are worn out, new pedals can be installed. The dynamo, crank set and serpentine belt should be checked regularly. The battery can be dismounted for charging, replacement and repair. Both the battery and the flight computer are placed in the wing, just before the pilot. The wing is not covered with Dacron over its thickness in front of the pilot. This allows for extraction of the battery and other equipment. The battery should be the easiest to reach, as it needs

---

<sup>6</sup><http://freeflightadvice.com/sail-cloth-options/>

<sup>7</sup><http://www.sailfeed.com/2014/11/inspect-your-sails-identifying-uv-damaged-cloth/>

<sup>8</sup>[https://en.wikipedia.org/wiki/Carbon\\_fiber\\_testing](https://en.wikipedia.org/wiki/Carbon_fiber_testing)

<sup>9</sup>[http://bike-manual.com/brands/fisher/om/road/carbon\\_fiber.html](http://bike-manual.com/brands/fisher/om/road/carbon_fiber.html)

charging and it should be checked for performance. As a consequence, the battery and flight computer need to be covered to avoid water damage.

The pilot attachment can be maintained quite straightforwardly. The harness will need to be checked regularly and can be replaced in case of malfunctioning, as well as the attachment rings and belts. The body support can be inspected for wear and all supports can be replaced separately.

The control surfaces can be detached from the wing structure. Locally, in front of the actuators, a small zipper should be implemented in the wing skin to allow for the repair or replacement of the actuators. The control bar can be disassembled from the pilot support system to repair or replace. As said before, the flight control computer is placed in front of the wing and its maintenance will follow the same procedure. Cables are placed in tubes attached to the ribs. These can be reached at the control surface locations using the same opening as for the actuators and at the wing opening in front of the pilot, where the battery and flight computer are placed.

### **13.3.2. Maintenance Plan**

It should be clear to the user that the Velo-E-Raptor is delivered ready to fly. Therefore the user is not allowed to make any adjustments that are not mentioned in the manual provided by the manufacturer. Maintenance is the operator's responsibility. However, the user needs to perform a final safety check just before flight. This check will be an important aspect of the pilot training. The maintenance plan is mostly based on current hang glider regulations<sup>10</sup>.

#### **Pre-flight Procedure**

The most important aspects in pre-flight maintenance check procedure are discussed below. A checklist will be provided and must be signed by both the operator and the user before flight.

- All connectors should be checked before every flight.
- The skin needs to be examined for damage.
- The battery charger has a Battery Management System that alarms when cells are incapable of charging or something is wrong in the charger itself. This should be checked before flight.

#### **Regular Check**

The operator will do a regular check to monitor the overall condition of the Velo-E-Raptor. The maintenance plan will make use of a predictive maintenance method. Predictive maintenance aims for the most efficient moment in time to perform maintenance actions, but before performance is lost. The difference with respect to preventive maintenance is the monitoring of the actual condition of equipment, rather than an average or expected life estimation<sup>11</sup>. An advantage is that maintenance can be performed while the equipment is still in service. That is why an inspection of all reachable parts shall be performed on a regular basis. This will mainly consist of the following:

<sup>10</sup>[http://www.aeros.com.ua/manuals/DiscusC\\_manual\\_en.pdf](http://www.aeros.com.ua/manuals/DiscusC_manual_en.pdf)

<sup>11</sup>[https://en.wikipedia.org/wiki/Predictive\\_maintenance](https://en.wikipedia.org/wiki/Predictive_maintenance)

- Every mechanical component should be checked for unacceptable wear and cables for kinks, wear, damage and corrosion
- Bolts should be inspected for tightness. Holes, mountings, tubes and plates need to be inspected for damage.
- The skin needs to be inspected for tears, UV damage wear, loose stitching, etc.
- Pulleys, battens, propellers, motors, the pilot turning system and the pedal system should be checked for lubrication.
- The pilot attachment and harness should be checked thoroughly.
- The control system needs to be checked for calibration.
- The motor, battery and propeller should be inspected for their performance.

### Special Circumstances

Under special circumstances, additional checks should be performed. In most cases the user interface can suggest certain checks. The user cannot take off, until the check is performed and marked by the operator.

- After a hard landing, exposure to salt water and a crash an elaborate inspection is done to ensure that all damaged parts are found.
- A wet glider must be dried before storing.
- There should be a special check for ice forming (mostly on the leading edge) in winter conditions.
- The sail needs to be kept clean to extend its lifespan.

Using the predictive maintenance approach, more detailed guidelines will be produced on how to act when damage will be encountered in the above mentioned subsystems. These guidelines are generally based on statistics and will be established after thoroughly testing the Velo-E-Raptor for its performance.

## 13.4. Safety

To analyze the Velo-E-Raptor's safety, a hazard analysis with respect to the pilot's safety has been done. In the FMECA, section 13.1.1, the most critical functional failures are discussed. These are further elaborated upon below and afterwards additional hazards are discussed. The severity index used in the hazard analysis is the same as in the FMECA.

### 13.4.1. Functional Hazards

<b>Hazard:</b>	Structural failure of the wing
<b>Initiator events:</b>	a) Wing skin wear   b) spar or ribs fail
<b>Undesirable events:</b>	Loss of lift
<b>Phase:</b>	All phases
<b>Consequences:</b>	a) Loss of altitude   b) uncontrollable aircraft
<b>Severity:</b>	Critical
<b>Risk reduction</b>	a) Safety factors for structural wing design   b) wing skin needs to be checked just before take off   c) parachute for high altitudes

**Hazard:** Uncontrollable aircraft  
**Initiator events:** Aircraft in: a) stall b) spin c) spiral d) control system failure  
**Undesirable events:** The aircraft makes uncontrollable, undesirable manoeuvres  
**Phase:** All flight phases  
**Consequences:** Sudden crash of the aircraft  
**Severity:** Catastrophic  
**Risk reduction** a) The flight envelope protection system does not allow for stall, spin or spiral b) the HUD provides the pilot with clear feedback on which angle not to exceed to prevent stall c) the control system has three of everything for redundancy d) the pilot can deploy its parachute at a minimum height of 70 m.

**Hazard:** Structural failure of the landing gear  
**Initiator events:** a) Hard landing b) flanges not fastened properly  
**Undesirable events:** High loads on the pilot during landing  
**Phase:** Landing  
**Consequences:** a) Severe pilot injury b) structural damage to aircraft c) or to propeller  
**Severity:** Critical  
**Risk reduction** a) Safety factors for structural landing gear design b) if one landing gear fails, the other can still carry loads  
c) ergonomically supported pilot harness to minimize point loads on the pilot

**Hazard:** Structural failure of the pilot attachment  
**Initiator events:** High loads on the attachment during flight  
**Undesirable events:** Pilot gets dismounted from the aircraft and can fall out of the aircraft  
**Phase:** All phases  
**Consequences:** Severe pilot injury  
**Severity:** Catastrophic  
**Risk reduction** a) The pilot attachment consists of four individual fasteners  
b) the pilot is also attached to the body support c) the parachute is attached to the pilot as well and can be deployed above 70 m.

**Hazard:** Propeller blades detach  
**Initiator events:** a) Blades break due to structural failure  
b) Loose bolts and nuts due to vibrations and temperature changes  
**Undesirable events:** a) Propeller blade hits pilot b) or aircraft  
**Phase:** All phases  
**Consequences:** a) Severe pilot injury b) structural damage to aircraft  
**Severity:** Catastrophic  
**Risk reduction** a) Pilot helmet protection b) blade attachment inspection

### 13.4.2. Additional Hazards

<b>Hazard:</b>	Pilot unconscious
<b>Initiator events:</b>	a) Medical b) environmental c) accidental causes
<b>Undesirable events:</b>	Pilot loses control
<b>Phase:</b>	All phases
<b>Consequences:</b>	Severe pilot injury
<b>Severity:</b>	Catastrophic
<b>Risk reduction</b>	a) The flight computer monitors the pilot's consciousness b) and deploys parachute in case of emergency
<b>Hazard:</b>	Emergency landing
<b>Initiator events:</b>	a) Sudden loss of lift b) uncontrollable aircraft
<b>Undesirable events:</b>	a) Landing on water b) landing somewhere else
<b>Phase:</b>	Landing
<b>Consequences:</b>	a) Pilot can drown b) collision during landing
<b>Severity:</b>	Catastrophic
<b>Risk reduction</b>	The aircraft is designed to be floating for a limited amount of time, but enough for the pilot to get out of the aircraft
<b>Hazard:</b>	Fire
<b>Initiator events:</b>	a) Battery inflames b) impact during a collision
<b>Undesirable events:</b>	Both the aircraft and the pilot can burn
<b>Phase:</b>	All phases
<b>Consequences:</b>	Severe injury to the pilot
<b>Severity:</b>	Catastrophic
<b>Risk reduction</b>	a) Careful battery choice b) further research should be done, as explained in section 13.1.1
<b>Hazard:</b>	Pilot has misleading or lack of information
<b>Initiator events:</b>	a) HUD shows wrong or no feedback to pilot b) flight conditions can not be determined correctly
<b>Undesirable events:</b>	a) Pilot is unaware of dangerous flight conditions b) flight computer is unaware of dangerous flight conditions
<b>Phase:</b>	All phases
<b>Consequences:</b>	Sudden crash of the aircraft
<b>Severity:</b>	Critical
<b>Risk reduction</b>	a) The control system has a threefold redundancy for every part b) the pilot can still fly using gps help on his phone c) in the end the pilot can deploy its parachute at a minimum height of 70 m

**Hazard:** Aircraft nose-over  
**Initiator events:** a) Sudden application of brakes b) Unexpected wheel block  
**Undesirable events:** Nose-over of the aircraft  
**Phase:** Takeoff and Landing  
**Consequences:** a) Propeller damage b) Aircraft nose damage c) pilot injury  
**Severity:** Critical  
**Risk reduction** a) extra large tires  
b) more to the front nose wheels

**Hazard:** Bird strike  
**Initiator events:** A bird hitting the propeller or other part of the aircraft  
**Undesirable events:** a) The propeller getting seriously damaged b) the aircraft losing control due to the bird's impact c) bird hitting the pilot  
**Phase:** All phases  
**Consequences:** a) Loss of propulsion b) loss of control  
**Severity:** a) Marginal b) catastrophic  
**Risk reduction** a) Future endeavor: bird radars b) flight computer makes sure the aircraft stays in its flight envelope during a bird strike  
c) the windshield will protect the pilot in case of a bird strike

**Hazard:** Pilot fails to transition  
**Initiator events:** a) The body support spring system does not work properly  
b) the pilot's feet cannot find the pedals c) the harness gets stuck  
**Undesirable events:** a) Unintended control input during transition  
b) the pilot stays hanging vertically in the wing after takeoff  
c) the pilot cannot transition back for landing  
**Phase:** a) Takeoff b) landing  
**Consequences:** a) Loss of control during flight b) the pilot needs to land as soon as possible when transitioning for cruise is not possible  
**Severity:** Marginal  
**Risk reduction** a) The flight computer takes over control during transition  
b) the pilot can land on the landing gears in case of emergency

In conclusion, the Velo-E-Raptor is able to reduce the most critical hazards to the pilot's safety. The flight computer prevents loss of control in case of stall or spin, but also during unconsciousness of the pilot. The landing gear provides more structural safety in case of emergency than only foot launch and landing. Still, there are things that need to be further investigated such as a careful battery choice and the aircraft tendency to tip nose-over. These follow-up activities can be found in appendix A.

## Cost estimation

Before the Velo-E-Raptor can be produced on large scale, the Research and Development (R&D) phase will first be continued following the product design and development logic. A major portion of these developments is related to the design and production of a number of prototypes. A first cost estimation for this phase serves as an indication for the investment costs needed to kick-start this project.

For the cost estimation the cost breakdown structure that can be found appendix A was used as a starting point. Because of a high degree of uncertainty that is inherent to the production of prototypes, this cost estimation is based only on some of these cost components. The costs are divided into two parts: the material and component cost, which is based on cost estimations per subsystem, and the labor cost.

Firstly, an estimation on material and component cost was performed per subsystem. Table 14.1 gives an overview of the cost estimation per subsystem. Prices found in dollars have been converted to euros using an exchange rate of 0.8796 EUR/USD

Table 14.1: Material and component cost estimation per subsystem

	Cost estimation
Structural components	€3,790
Power and propulsion	€11,230
Control system	€7,400
Flight instruments	€4,500
Pilot configuration	€1,600
Safety equipment	€930
Total	€29,450

### 14.1. Material and Component Cost

#### Structural Components

The cost estimation for the aircraft structure only includes the material cost and not the cost of labor needed to process the materials and manufacture the different components. The labor cost will be estimated separately.

To determine the material cost of the structure of the design research was done into the prices of the used materials. A wide big price ranges (28-85 \$/kg) exist for CFRP.<sup>1</sup> To be on the safe side, it was decided that CFRP of the best quality is used and therefore the highest cost of \$85 was assumed. The process from manufacturing carbon fiber to production of finished components is wasteful; it is estimated that more than 30% of produced carbon fiber ends up as waste at some point in the process<sup>2</sup>. With a total CFRP mass of 27.1 kg the total material cost, using the 30% margin is \$4,225. The structural foam costs \$240<sup>3</sup>.

For the skin Dacron is used. Also for this material a wide range of price ranges can be found. These prices range from \$8 to \$24 per square meter<sup>4</sup>. Using the most expensive material, a sail surface area of 28.5 m<sup>2</sup> gives a total of \$684.

The cost of the wheels will be around \$100 a piece<sup>5</sup>. The tires will cost an additional \$30 per tire<sup>6</sup>. This will make a total of \$390. Adding this all together and converting to euros this gives a total cost of €3,790.

### **Power and Propulsion**

To determine the cost of the power and propulsion system research was done into the retail prices of the main components. For the batteries an estimate was made because the actual price of the battery used in the Velo-E-Raptor is not available. To get an estimate one battery from the NASA aerospace flight program was used<sup>7</sup>. This battery is also a lithium cobalt oxide battery of high quality and therefore is representative for the battery used in the Velo-E-Raptor. Calculating the price for the amount of energy needed for the Velo-E-Raptor, an estimate of €5,500 was made.

The motors of the Velo-E-Raptor are existing motors with a price of €905 each. Each motor needs a planetary gearbox of €105 and a water cooling system which cost €40<sup>8,9</sup>. The power from the batteries to each of the motors is regulated by two electrical speed controllers (ESC) which cost €495 each. The total cost for the electrical motors with a gearbox, ESC and cooling system is €3,090.

The propellers of the Velo-E-Raptor need to be custom made which makes it difficult to predict the actual cost. For a first estimation a similar five bladed propeller is used as a reference which has a cost of €1,070, giving a total of €2140 for two propellers<sup>10</sup>.

---

<sup>1</sup><https://www.infosys.com/engineering-services/white-papers/Documents/carbon-composites-cost-effective.pdf>

<sup>2</sup><http://www.compositesworld.com/columns/recycled-carbon-fiber-its-time-has-come->

<sup>3</sup><http://www.aircraftspruce.com/catalog/cmpages/divinycellfoam.php>

<sup>4</sup><https://www.sailmakersupply.com/category/sailcloth>

<sup>5</sup>[https://www.air-techinc.com/topic\\_std\\_prods.php?catid=221&pmid=20](https://www.air-techinc.com/topic_std_prods.php?catid=221&pmid=20)

<sup>6</sup>[https://www.air-techinc.com/topic\\_no\\_cats.php?ptid=90&pmid=20](https://www.air-techinc.com/topic_no_cats.php?ptid=90&pmid=20)

<sup>7</sup>NASA Engineering and Safety Center Technical Report - NASA Aerospace Flight Battery Program - Part 1 - Volume II

<sup>8</sup><https://hackermotorusa.com/shop/>

<sup>9</sup><https://hobbyking.com/>

<sup>10</sup><http://www.warpdriveprops.com/>

The pedal system consists of pedals, a serpentine belt system, dynamo and a control computer. The pedals with toeclips and bearings together cost €180, the serpentine belt system €70, the dynamo €100 and the control computer with the sensors and throttle €150. All together the pedal system costs €500.

### **Control System**

To estimate the cost of the control subsystem, research was done into retail prices of the main components, namely the flight computers, sensors, actuators and cables. In section 7.5 it is explained which components and what specific types are chosen for the control system of the Velo-E-Raptor.

In total 4 pressure sensors of \$20 each are used, in combination with two pitot tubes of \$167 and two gyros of \$250. This gives a total cost of \$914 for the sensors. To move the control surfaces eleven actuators of \$500 per piece are used. For force feedback 4 actuators of \$160 per piece are chosen. For the cables a cost of (0.95 \$/feet) was found, giving \$190 for 200 ft. Lastly two flight computers of €512 each are needed. Converting all prices to euros and adding all components together, total the control system is estimated to cost €7,396

### **Flight Instruments**

As elaborated on in section 9.1.5 the flight instruments used for the Velo-E-Raptor will be incorporated in the HUD. The cost of this HUD is estimated to be €2,000, accounting for the fact that the HUD can not be bought 'off the shelf' but needs to be developed first. The required transponder mode S costs €2,000 and the EPRIB €500. In total this comes down to €4500 on flight instruments. It should be noted that the transponder is mandatory in the Netherlands, but not in other countries.

### **Pilot Configuration**

For the pilot configuration the following components are taken into account: the pilot supports, the harness and the windshield. The different elements of the pilot supports will be made off foam, coated with leather. These components are assumed to cost €500 in total. As explained before, the design of the harness is based on the ExoFit Strata that has price of €470<sup>11</sup>. The back protector and safety parachute need to be incorporated in this harness as well. The total price of the harness is therefore assumed to be €800. Lastly a windshield is estimated to cost €300,-<sup>12</sup>. For the cost of the safety parachute research was done into the safety parachute used by the Aeriane Swift. This is the Apco Mayday 20 SLT which costs €932.<sup>13</sup>

## **14.2. Labor Cost**

To estimate the development cost of the aircraft the amount of man-hours needed for engineering, tooling and manufacturing should be estimated first. After this the labor cost can easily be determined. Especially during the research, development, testing, and evaluation (RDT&E) phase of the prototypes, the main portion of the total cost will be labor cost. Once

---

<sup>11</sup><http://fallprotectionusa.com/exofit-strata.html>.

<sup>12</sup><http://www.northwing.com/tall-windshield-retrofit.htm>

<sup>13</sup><http://shop.airways-airports.com/apco-mayday-light.html>

the aircraft starts to be produced on a larger scale, the labor cost per aircraft will decrease.

For military aircraft a method used to estimate the development cost is the "development and procurement cost of aircraft" (DAPCA) method. It is developed by the RAND Corporation<sup>14</sup> and is generally known as the DAPCA-IV method. This method establishes special cost estimating relationships (CERs), which are a set of statistical equations that predict aircraft acquisition costs using only basic information like empty weight and maximum airspeed. This method can be used to estimate the RDT&E costs. However, the method is not applicable for General Aviation (GA) aircraft, which grossly overestimates the development cost for GA aircraft. Therefore the original DAPCA-IV method was adapted to GA aircraft, which is known as the Eastlake model. The model is used to estimate the development cost of light GA aircraft based on the weight of the aircraft structure and maximum level of airspeed. Correction factors can be used to account for more complicated manufacturing methods. The methods estimates the man-hours needed for three areas, engineering, tooling and manufacturing using the following expressions respectively:

$$H_{eng} = 0.0396 \cdot W_{af}^{0.791} \cdot V_H^{1.526} \cdot N^{0.183} \cdot F_{CERT} \cdot F_{CF} \cdot F_{COMP} \cdot F_{PRESS} \quad (14.1)$$

$$H_{tool} = 1.0032 \cdot W_{af}^{0.764} \cdot V_H^{0.899} \cdot N^{0.178} \cdot Q_m^{0.066} \cdot F_{CERT} \cdot F_{CF} \cdot F_{COMP} \cdot F_{PRESS} \quad (14.2)$$

$$H_{MFG} = 9.6613 \cdot W_{af}^{0.74} \cdot V_H^{0.543} \cdot N^{0.542} \cdot F_{CERT} \cdot F_{CF} \cdot F_{COMP} \quad (14.3)$$

$W_{af}$  = weight of the structural skeleton

$V_H$  = maximum level airspeed in KTAS

$N$  = number of planned aircraft to be produced over a 5-year period

$F_{CERT}$  = 0.67 in equation equation (14.1) and 0.75 in equation (14.3)  $F_{CF}$  = 1.03 for a complex flap system, = 1 if a simple flap system

$F_{COMP}$  =  $1 + F_{COMP}$  in equation equation (14.1) and equation (14.2) and  $1 + 0.25 \cdot F_{COMP}$  in equation (14.3), a factor to account for the use of composites in the airframe, which is one for a complete composite aircraft

$F_{PRESS}$  = 1.03 for a pressurized aircraft, = 1 if unpressurized.

$Q_m$  = estimated production rate in number of aircraft per month (= 1/12 if one prototype is assumed to be build in one year.

Filling in these equations with an aircraft frame weight (including CFRP structure, structural foam and Dacron sail) of 39 kg converted to pound force, and a maximum airspeed of 32.59 m/s converted to knots, the total amount labor man-hours (mh) is estimated to be 1471.

To validate these numbers different references were used. A first reference was found in a research of the AGATE / SATS programme of NASA. Since these programs were stopped after 9/11 no original reports are available. However, the sheets that are available give an estimation of the total amount of labor needed for the manufacturing of GA aircraft frames of different materials. A total of 2,500 mh is used for the total labor needed for manufacturing a composite airframe<sup>15</sup>. Another reference used is an article on the amount of man-hour

<sup>14</sup><https://www.rand.org/content/dam/rand/pubs/reports/2007/R761.1.pdf>

<sup>15</sup>Sheet with numbers obtained from R. van Gent at 20-06-2016

work needed for the manufacturing of Cirrus aircraft, namely 2,800 mh <sup>16</sup>. Since the total amount of labor strongly depends on the complexity of the aircraft, and the Velo-E-Raptor is a very lightweight and relatively simple aircraft the higher total for the Cirrus aircraft is understandable.

A last validation was performed by comparing the numbers found with an article on the production of the first Aeriane Swift <sup>17</sup>. This article states that the first prototype was built by three engineers in three months, resulting in a total of 1440 mh. This is quite close to the 1471 mh found with the Eastlake methods. However, this aircraft did not use a complex Fly-By-Wire (FBW) system. For it is difficult at this stage to estimate the labor needed to further develop this system, and the references found indicate significantly higher amount of mh needed, for now a safety margin of 1.5 will be used to compensate for the fact that at this stage an accurate cost estimation is still very difficult to perform. This gives a total of  $1540 \cdot 1.5 = 2310$  mh. Assuming that an engineer costs €60 per hour, the total labor cost for one Velo-E-Raptor will be €138,600.

The cost estimation performed does not take into account that this is a completely new type of aircraft and that the research and development phase of the Velo-E-Raptor has not yet been finished. This is reflected in the post-DSE activities needed to complete the design, which can be found in appendix A. Using the Gantt chart it was estimated that the post DSE-activities can be completed in 52 weeks by one engineer. Given that one engineer works 40 hours a week, the total man hours needed for further research and development is 2080 man hours. Assuming that an engineer costs €60 per hour this gives an additional one-off cost for R&D of €124,800

### 14.3. Total Cost

Adding the product cost of €29,450 and the labor cost per aircraft of €138,600, the total cost for one aircraft is estimated to be €168,050. To perform all post-DSE activities another €124,800 one-off investment cost is needed. If five aircraft would be produced for the first badge, the aircraft would cost €193,010 each. If the Velo-E-Raptor would be further developed and manufactured by the project group the labor cost and post-DSE could be decreased a lot. Note that the calculated labor costs are calculated with the labor costs of an engineer. When producing more Velo-E-Raptors, normal craftsmen can be hired. This reduces the labor costs significantly. It should therefore be further investigated if and how the total cost of the Velo-E-Raptor will decrease when produced on a bigger scale. At that stage further cost estimations should also be performed that give insight in cost for operations and maintenance.

Comparing this first cost estimation to the target cost of €83,300 established in the market analyses it is clear that the labor cost are too high to make the Velo-E-Raptor profitable for the given business case. Even though the total cost is assumed to decrease when produced on a bigger scale, it should be further investigated how the total cost of the Velo-E-Raptor can be decreased.

---

<sup>16</sup><https://www.flightglobal.com/news/articles/cirrus-streamlines-manufacturing-130885/>

<sup>17</sup><http://aero.stanford.edu/Reports/SWIFTArticle1991.html>



## Technical Risk Assessment

### 15.1. General Analysis Procedure

Now that the post-DSE activities have been defined a technical risk assessment can be made for the future development of the Velo-E-Raptor. The risk assessment concerns events that can have an impact on the final project phase by affecting either cost, schedule or performance. To get a complete overview of what these events might be they were categorized by general project risks and separate departments. The three impact factors as well as probability were scaled from 1 to 5, each with it's own criteria. For an overview of how the scales were defined see figure 15.1. This risk map shows the separate events and how critical they are for the post-DSE design process. The top right corner contains the most critical risks, however the risk map shown is a map after risk management and therefore does not include any highly critical risks. For a complete list of risks and how they were assessed before and after management see figure 15.1. For the severity the average was taken of the three impact factors and round to the nearest upward integer; e.g. average = 2.1, severity = 3.0.

### 15.2. Risk Management Methods

To manage risks effectively several different techniques were used, depending on the nature of the event. The first is having a proper contingency plan for any process that requires resources. By taking a buffer into account the impact an underestimation of the actual value has is lowered significantly. Another way risks can be managed is by mitigation. This means that the risk is closely monitored and if it becomes a threat a mitigation strategy is in place to deal with it. This method focuses more on reducing the impact than the probability. A method that may seem similar is risk avoidance, however in avoidance the focus lies on reducing probability. By re-evaluating the underlying reason a risk poses a threat to the project, one can find the source of the problem and think of other ways to achieve the same goal, therefore avoiding the initial risk. Finally the fourth and last method used is risk acceptance. Some risks with a low criticality can be accepted as long as the team is aware of it's consequences. Figure 15.1 states the mitigation strategy used per risk and it's effect on it's probability and impact.

SeverityCategory	Cost	Schedule	Performance	Probability					Qualitative Probability	Quantitative Probability
				1 Very low Highly unlikely	2 Low Unlikely	3 Moderate Possible	4 High Probable	5 Very High Certain		
<b>5 Extreme</b>	> 2x cost multiplier	Two months additional delay or more	Multiple driving requirements shall not be met	<0.05	0.05 - 0.15	0.15 - 0.35	0.35 - 0.75	>0.75		
<b>4 Serious</b>	1.5x - 2x cost multiplier	Two months additional delay	A driving requirement is not met	SM3,OP1	SC2					
<b>3 Moderate</b>	1.25x - 1.5x cost multiplier	A month additional delay	Multiple driving requirements are negatively affected	AE1,GP1,GP2	AE2,SC1,OP3,GP3	OP2	SM1, SM2			
<b>2 Minor</b>	1.05x - 1.25x cost multiplier	A week additional delay	A driving requirement is negatively affected	PP2,	AE3,PP1,SC3					
<b>1 Trivial</b>	≤ 1.05x cost multiplier	A few days additional delay	Some low-level requirements negatively affected							

Figure 15.1: Risk map for the post-DSE project phase containing all risks after mitigation of the most critical ones.

ID	Risk	Probability (P)	Severity			Criticality (P x S)	Management strategy	Probability (P)	Severity			Criticality (P x S)
			Performance	Schedule	Cost				Performance	Schedule	Cost	
<b>Aerodynamics</b>												
AE1	The aerodynamic effect of vibrations and wing deformation is unexpectedly large	2	3	3	1	6	Aversion	1	3	3	1	3
AE2	CFD calculations take unexpectedly long due to the unconventional design	3	1	4	3	9	Aversion	2	1	4	3	6
AE3	Wind tunnel tests show significantly more interference drag than anticipated	2	4	1	1	4	Acceptance	2	4	1	1	4
<b>Performance &amp; Power</b>												
PP1	The propeller design cannot be manufactured	2	2	3	1	6	Mitigation	2	2	2	1	4
PP2	The chosen off-the-shelf batteries are taken out of production	1	1	2	2	2	Contingency	1	1	2	1	2
<b>Stability &amp; Control</b>												
SB1	The pilot position in the wing has an unexpectedly large effect on stability	3	4	3	1	9	Aversion	2	4	3	1	6
SB2	Personal development of the flight envelope system proves to be unfeasible, enforcing the need for an off the shelf system	4	1	1	4	8	Acceptance	4	1	1	4	8
SB3	Wind tunnel tests give significantly different results than expected	2	3	3	1	6	Contingency	2	3	2	1	4
<b>Structures &amp; Materials</b>												
SM1	The structural mass of the aircraft goes up due to unforeseen effects such as material imperfections, fatigue or unexpected stress concentrations.	4	4	2	3	16	Mitigation	4	2	2	3	12
SM2	The structural mass of the aircraft goes up due to new design characteristics such as retractable landing gear and serrated trailing edge.	4	4	2	3	16	Mitigation	4	2	2	3	12
SM3	Deformation of the skin during flight has a bigger impact on aircraft performance than expected, resulting in the need for more structural mass or rigid skin.	2	5	2	2	8	Aversion	1	5	2	2	4
<b>Operations</b>												
OP1	A large amount of prototypes is needed before a feasible design is reached	2	1	5	5	8	Aversion	1	1	5	5	4
OP2	Individual components such as batteries, materials and flight instruments prove significantly more expensive than expected	3	1	1	5	9	Contingency	3	1	1	4	6
OP3	The ergonomic configuration proves to be uncomfortable and unfeasible and has to be reassessed	2	3	3	1	6	Mitigation	2	3	2	1	4
OP4	The HUD proves to be too distracting and not useful in flight	2	5	1	1	6	Acceptance	2	5	1	1	6
<b>General Project Risks</b>												
GP1	The requirement list gives an unsatisfactory representation of what the client and market expects	2	5	4	1	6	Aversion	1	5	4	1	3
GP2	The client is not satisfied with the final aircraft performance	2	5	2	1	6	Aversion	1	5	2	1	3
GP3	The final design is not approved for recreational flight by aviation authorities	3	5	1	1	9	Aversion	2	5	1	1	6

Figure 15.2: Complete list of risks including probability, severity and management strategies.



## Compliance Matrix

In table 16.1, the compliance matrix can be found. In this matrix, all requirements from the baseline report are shown [40], and whether the final Velo-E-Raptor configuration satisfies the requirements or not. For every requirement, a brief explanation is given. Every requirement that was not met, or that was decided to be dropped, has been communicated with the customer.

The requirements are marked to indicate the different types of requirements:

<sup>X</sup> Killer requirement

<sup>D</sup> Driving requirement

<sup>K</sup> Key requirement

Table 16.1: Compliance matrix

<b>VER-REG-01</b>	The Velo-E-Raptor shall comply with European regulations. <sup>D</sup>	Not Satisfied
See subrequirements.		
<b>VER-REG-01.1</b>	The Velo-E-Raptor shall only be able to take off and land using the operator's legs. <sup>D</sup>	Not Satisfied
As explained in the midterm report [41, ch.10], the decision was made to drop this requirement. This is further explained in section 3.5.		
<b>VER-REG-01.2</b>	Any battery component on the Velo-E-Raptor shall agree with "Directive 2006/66/EC" of the European Union legislation. <sup>D</sup>	Satisfied
The battery type used is a commonly used chemistry, widely used in Europe and space applications. This is further explained in section 5.2.2.		
<b>VER-REG-02</b>	The Velo-E-Raptor shall comply with Dutch regulations. <sup>D</sup>	Not Satisfied
Even though all subrequirements are satisfied, the requirements set by Dutch regulations will not be met. This is further explained in the midterm report [41, ch.10] and section 3.5.		
<b>VER-REG-02.1</b>	The Velo-E-Raptor shall be able to stay airborne using only aerodynamic forces. <sup>D</sup>	Satisfied
No hard limit is specified for this requirement by law, only that the aircraft does not stay airborne by forces applied from the ground. With a glide ratio comparable to current hang gliders, this requirement is considered to be satisfied.		
<b>VER-REG-02.2</b>	The Velo-E-Raptor shall have a mass of not more than 70 kg excluding pilot. <sup>D</sup>	Satisfied
The mass of the final configuration is 65.1 kg. An explanation and breakdown of the final mass is given in section 8.4.4		
<b>VER-REG-02.3</b>	The Velo-E-Raptor shall have a mode-S SSR transponder and radio communication on board at any time during flight. <sup>D</sup>	Satisfied
Both instruments will be on board of the Velo-E-Raptor. This is further explained in section 9.1.7.		

Table 16.1: Compliance matrix, continued

<b>VER-REG-02.4</b>	Any battery component on the Velo-E-Raptor shall agree with "Regeling beheer batterijen en accu's 2008" from Dutch legislation. <sup>D</sup>	Satisfied
The battery type used is a commonly used chemistry, widely used in Europe and space applications. This is further explained in section 5.2.2.		
<b>VER-SAF-01</b>	The Velo-E-Raptor shall cause no fatalities. <sup>X</sup>	Not Satisfied
While great emphasis is put on safety, this is a killer requirement that will never be satisfied, as explained in the baseline report [40, ch.4].		
<b>VER-SAF-02</b>	The Velo-E-Raptor shall have a fail-safe system for emergency landings. <sup>D</sup>	Satisfied
Both the landing gear and an emergency parachute can be used to guarantee a safe landing for the pilot. This is further explained in section 9.1.7		
<b>VER-SAF-02.1</b>	The fail-safe system shall not require any pilot input. <sup>D</sup>	Satisfied
The parachute will be able to deploy without pilot input. This is further explained in section 9.1.7.		
<b>VER-SAF-02.2</b>	In case of an emergency landing on water the Velo-E-Raptor including pilot shall stay afloat. <sup>D</sup>	Satisfied
When the takeoff weight is put on the main wing planform, the density of the planform is 90 kg/m <sup>3</sup> . Water has a density of 997 kg/m <sup>3</sup> . In case water is flowing into the wing, the aircraft will stay afloat until 91% of the volume of the wing is filled with water.		
<b>VER-SAF-02.3</b>	In case of an emergency landing on water the pilot shall be able to detach himself from the aircraft. <sup>D</sup>	Satisfied
For an emergency exit, the pilot is able to release himself from the aircraft. This is further explained in section 9.1.1.		
<b>VER-SAF-02.4</b>	In case of an emergency landing, the Velo-E-Raptor shall be able to send an emergency signal without input from the pilot. <sup>D</sup>	Satisfied
When the flight computer senses a critical failure or ejection from the pilot during flight, an emergency signal will be sent out. This is further explained in section 9.1.7.		
<b>VER-SAF-02.5</b>	In case the pilot loses control of the Velo-E-Raptor, the Velo-E-Raptor shall deploy a safety system. <sup>D</sup>	Satisfied
Because of the fly by wire system, the Velo-E-Raptor is in control of the aircraft and able to overwrite the pilot input. This is further explained in section 7.3. Besides, the parachute can be used, as explained in section 9.1.7		
<b>VER-SAF-03</b>	The pilot shall be able to fly and land safely when the motor fails. <sup>K</sup>	Satisfied
When one motor fails, the other switches off as well to prevent lateral stability problems. With a glide ratio of 13.5, the pilot should still be able to find a suitable landing spot without the engines. In emergency conditions, the parachute can always be used.		
<b>VER-SAF-04</b>	The Velo-E-Raptor shall be a stable aircraft during all operations. <sup>K</sup>	Satisfied
The Velo-E-Raptor is designed to be a stable aircraft both statically and dynamically, both in longitudinal and lateral directions. This is further explained in section 6.2. All subrequirements are satisfied for this reason.		
<b>VER-SAF-04.1</b>	The Velo-E-Raptor shall be statically stable in longitudinal direction. <sup>K</sup>	Satisfied
<b>VER-SAF-04.2</b>	The Velo-E-Raptor shall be dynamically stable in longitudinal direction. <sup>K</sup>	Satisfied
<b>VER-SAF-04.3</b>	The Velo-E-Raptor shall be dynamically stable in lateral direction. <sup>K</sup>	Satisfied
<b>VER-SAF-05</b>	It shall be possible to do a safety check on all components of the Velo-E-Raptor.	Satisfied
It is possible to do a safety check on all components on the ground. This is further explained in section 13.3.2.		
<b>VER-SAF-06</b>	The Velo-E-Raptor shall be a controllable aircraft during all operations. <sup>K</sup>	Satisfied
The control surfaces are designed with this requirement in mind. Even during stall, the Velo-E-Raptor is controllable due to the wing region with the control surfaces stalling the latest. This is further explained in section 4.3.		

Table 16.1: Compliance matrix, continued

<b>VER-SAF-07</b>	The Velo-E-Raptor shall have a stall warning system.	Satisfied
The Velo-E-Raptor will have a stall vane, to tell the flight computer when the aircraft is about to stall. This is further explained in section 7.2. The computer will warn the pilot when close to stall conditions		
<b>VER-SAF-08</b>	The Velo-E-Raptor shall have at most 20 critical failures per 100.000 flight hours. <sup>D</sup>	Unknown
While great emphasis is put on safety as well as redundancy for the critical systems, this requirement can only realistically be validated by operating the Velo-E-Raptor after production.		
<b>VER-SAF-09</b>	The Velo-E-Raptor shall not harm the pilot during normal operations. <sup>K</sup>	Satisfied
The Velo-E-Raptor is designed to ensure safety for the pilot in any conditions. Under regular operations and prescribed maintenance checks, the Velo-E-Raptor will not harm the pilot. This is further explained in section 13.3.2.		
<b>VER-SUS-01</b>	The Velo-E-Raptor shall have a noise emission no higher than 60 dB(A) at 1 meter distance. <sup>D</sup>	Satisfied
For the propeller, a method was found to estimate the noise. It was found that for the propeller only the noise would not reach over 51 dB(A). This is further explained in section 5.1.1.		
<b>VER-SUS-02</b>	The Velo-E-Raptor design shall be adjustable for different pilot characteristics with respect to the original design. <sup>D</sup>	Not Satisfied
See subrequirements.		
<b>VER-SUS-02.1</b>	The Velo-E-Raptor design shall be adjustable for different pilot height ranges with respect to the original design. <sup>D</sup>	Satisfied
Both the cycling system and body support are adjustable to pilot height. This is further explained in section 9.1.2.		
<b>VER-SUS-02.2</b>	The Velo-E-Raptor design shall be adjustable for different pilot weight ranges with respect to the original design <sup>D</sup>	Not Satisfied
The current design of the Velo-E-Raptor is a prototype, and no research has been put into the scalability of the aircraft. For persons heavier than 85 kg, the weight of the aircraft will very likely increase above the 70 kg limit, which would make the design unfeasible.		
<b>VER-SUS-03</b>	The Velo-E-Raptor shall consist of at least 70 mass percentage recyclable materials.	Satisfied
The Velo-E-Raptor consists of 78 mass percentage recyclable materials. This is further explained in section 10.4		
<b>VER-SUS-04</b>	The Velo-E-Raptor shall be storable without inflicting damage upon itself or the environment.	Satisfied
Under prescribed operations and careful handling, the Velo-E-Raptor will not damage itself or the environment. This is further explained in section 13.3.		
<b>VER-SUS-05</b>	The materials used for the Velo-E-Raptor shall not be hazardous to the environment <sup>K</sup>	Satisfied
All materials chosen are not hazardous to the environment. This is further elaborated in section 10.2		
<b>VER-SUS-06</b>	The production of the Velo-E-Raptor shall be eco-friendly.	Satisfied
The production methods are chosen to be eco-friendly. This is further explained in section 10.2		
<b>VER-SUS-07</b>	Operating the Velo-E-Raptor shall not damage the ground area used for landing or takeoff.	Satisfied
With the addition of a landing gear with rubber wheels, this requirement is considered to be satisfied.		
<b>VER-SUS-08</b>	The Velo-E-Raptor shall not lose mass during operations.	Satisfied
See subrequirements.		
<b>VER-SUS-08.1</b>	The Velo-E-Raptor shall not lose liquid components during operations.	Satisfied
During regular operations and when regular maintenance checks are done, the Velo-E-Raptor engine will not lose any engine liquids such as oil.		

Table 16.1: Compliance matrix, continued

<b>VER-SUS-08.2</b>	The Velo-E-Raptor shall not lose parts during operations. During regular operations and when regular maintenance checks are done, the Velo-E-Raptor will not lose any parts	Satisfied
<b>VER-SUS-08.3</b>	The Velo-E-Raptor shall not emit greenhouse gases during operations. An electrical engine is used, which produces no greenhouse gases.	Satisfied
<b>VER-SUS-09</b>	For storage of the Velo-E-Raptor the loss of components shall be prevented. As long as the customer is handling the aircraft with care, this requirement is considered to be satisfied.	Satisfied
<b>VER-PER-01</b>	The Velo-E-Raptor shall be able to reach a maximum airspeed of at least 75 knots. <sup>D</sup> 75 knots is unachievable for the Velo-E-Raptor design. Current hang gliders have a never-exceed speed of around 54.0 knots, which is defined by flutter reasons. The theoretical maximum speed of the final Velo-E-Raptor configuration is 63.3 knots, without considering flutter. This is further explained in section 4.6.3 and section 5.2.3.	Not Satisfied
<b>VER-PER-02</b>	The Velo-E-Raptor shall have a stall speed of at most 25 knots. <sup>D</sup> The stall speed of the final Velo-E-Raptor configuration is 24.4 knots. This is further explained in section 5.2.3.	Satisfied
<b>VER-PER-03</b>	The Velo-E-Raptor shall have a takeoff length of at most 50 meters. <sup>K</sup> The performance calculations uses this requirement as input. Therefore, the Velo-E-Raptor is designed for exactly this landing distance. This is further explained in section 5.1.3.	Satisfied
<b>VER-PER-04</b>	The Velo-E-Raptor shall have a service ceiling of at least 10,000 feet. The performance calculations uses this requirement as input. Therefore, the Velo-E-Raptor is designed for exactly this service ceiling. This is further explained in section 5.1.3.	Satisfied
<b>VER-PER-05</b>	The Velo-E-Raptor shall have sufficient electrical energy to sustain flight for 30 minutes without the use of human power. <sup>D</sup> The battery capacity is determined using this requirement as input. Therefore, the Velo-E-Raptor is designed for exactly this endurance. This is further explained in section 5.1.3.	Satisfied
<b>VER-PER-06</b>	The propulsion system of the Velo-E-Raptor shall deliver enough power to reach cruise altitude without the use of human power. <sup>K</sup> The battery capacity and power are determined using this requirement as input. Therefore, the Velo-E-Raptor is designed for exactly this climb characteristic. This is further explained in section 5.1.3.	Satisfied
<b>VER-PER-07</b>	The Velo-E-Raptor shall be able to perform a rate-of-climb of at least 1.3 meters per second without the use of human power. The climb rate of the final Velo-E-Raptor configuration is 5.87 m/s. This is further explained in section 5.2.3.	Satisfied
<b>VER-PER-08</b>	The Velo-E-Raptor shall be able to take off from a terrain with a slope between -10 and +5 degrees. The power available of the Velo-E-Raptor is not limited by the takeoff condition. With the additional power available, the Velo-E-Raptor is able to take off at a slope of +6.1 degrees. Taking off at a negative slope is never a problem, as gravity works in the pilot's favor.	Satisfied
<b>VER-PER-09</b>	The Velo-E-Raptor shall have a gliding ratio of at least 15. The maximum gliding ratio of the final Velo-E-Raptor configuration is 13.5. This is further explained in section 5.2.3. While the requirement is not satisfied it is close, and comparable with current flexible hang gliders. Perhaps after aerodynamic optimization as explained in section 4.6.2, the gliding ratio can be increased upon slightly in a further design stage.	Not Satisfied

Table 16.1: Compliance matrix, continued

<b>VER-PER-10</b>	The maximum load factor of the Velo-E-Raptor shall be at least 6.	Satisfied
The structural strength of the Velo-E-Raptor is designed with this requirement as input, with a safety factor of 1.5 added on top of it for an ultimate load factor of 9. This is further explained in section 8.1.		
<b>VER-OPS-01</b>	The Velo-E-Raptor shall be easily transportable. <sup>K</sup>	Not Satisfied
As already explained in the midterm report [41, ch.7], the decision was made to drop this requirement. This also applies to the subrequirements, except VER-OPS-01.1.		
<b>VER-OPS-01.1</b>	The Velo-E-Raptor shall be transportable by the use of public road. <sup>K</sup>	Satisfied
This subrequirement was reintroduced to ensure the Velo-E-Raptor is transportable from production to customer. The Velo-E-Raptor tail can be demounted at which point it fits in a 45 feet high cube shipping container. This is further explained in section 13.2.		
<b>VER-OPS-01.2</b>	The Velo-E-Raptor shall be transportable by car. <sup>K</sup>	Not Satisfied
<b>VER-OPS-01.3</b>	The Velo-E-Raptor shall be transportable by foot. <sup>K</sup>	Not Satisfied
<b>VER-OPS-02</b>	The Velo-E-Raptor shall be easily maintainable. <sup>K</sup>	Not Satisfied
Due to safety reasons, the decision was made to drop this requirement. This also applies to the subrequirements. This is further explained in section 13.3.		
<b>VER-OPS-02.1</b>	All parts shall be replaceable by the customer. <sup>K</sup>	Not Satisfied
<b>VER-OPS-02.2</b>	The costumer shall be able to maintain the Velo-E-Raptor without any training. <sup>K</sup>	Not Satisfied
<b>VER-OPS-03</b>	A short, safe training shall be available.	Satisfied
In the operation plan, a short safe training is included. This is further elaborated in section 9.2.1.		
<b>VER-OPS-04</b>	The Velo-E-Raptor shall be designed for the physically average, healthy Dutch person. <sup>K</sup>	Satisfied
See subrequirements		
<b>VER-OPS-04.1</b>	A pilot with a weight between 65 and 85 kg shall be able to operate the Velo-E-Raptor. <sup>K</sup>	Satisfied
The stability and controllability of Velo-E-Raptor were determined with this requirement as input. Therefore, the Velo-E-Raptor is designed for exactly this weight range. This is further explained in section 6.1.2		
<b>VER-OPS-04.2</b>	A pilot with a height between 1.65 and 1.85 meters shall be able to operate the Velo-E-Raptor. <sup>K</sup>	Satisfied
Both the cycling system and body support are adjustable to pilot height. This is further explained in section 9.1.2.		
<b>VER-OPS-04.3</b>	The Velo-E-Raptor shall be flyable with zero, or more, flight hours experience excluding training. <sup>K</sup>	Satisfied
The training provided will be sufficient to fly the Velo-E-Raptor for the first time. The fly-by-wire control system will help the pilot control the aircraft and will take over in any unsafe situations. This is further explained in section 7.3.6.		
<b>VER-OPS-04.4</b>	The Velo-E-Raptor shall be flyable without a pilot license. <sup>K</sup>	Satisfied
Due to Dutch regulations, a pilot license is not necessary. This is further explained in the baseline report [40, ch.10].		
<b>VER-OPS-05</b>	The Velo-E-Raptor shall be flyable with 10 mm/hr rain.	Satisfied
Precautions have been made to satisfy this requirement. The wing is water tight, the electrical subsystems are located inside the wing structure and the instrumentation is water tight as well.		
<b>VER-OPS-06</b>	The Velo-E-Raptor shall be flyable with maximum gusts of 20 meters per second.	Satisfied
In the requirement list of the baseline, the maximum gust speed was to be determined. In section 5.2.3 the maximum gust speed allowable was determined to be 20 meters per second.		
<b>VER-OPS-07</b>	It shall be possible to assemble the Velo-E-Raptor by an average person within 45 minutes. <sup>K</sup>	Satisfied
This requirement was set with the idea of a highly transportable aircraft which required assembly and disassembly. Because transportability requirements are dropped as explained in the midterm report [41, ch.7], assembly is no longer necessary.		

Table 16.1: Compliance matrix, continued

<b>VER-OPS-07</b>	It shall be possible to disassemble the Velo-E-Raptor by an average person within 45 minutes. <sup>K</sup>	Satisfied
This requirement was set with the idea of a highly transportable aircraft which required assembly and disassembly. Because transportability requirements are dropped as explained in the midterm report [41, ch.7], disassembly is no longer necessary.		
<b>VER-OPS-09</b>	The main structure of the Velo-E-Raptor shall have a lifetime of 15 calendar years under normal operating circumstances.	Satisfied
The materials used in the Velo-E-Raptor are chosen to satisfy this requirement. Only the flexible wing material will need to be renewed every 3 years. This is further explained in section 13.3.2.		
<b>VER-OPS-10</b>	The Velo-E-Raptor shall not be uncomfortable during flight.	Satisfied
This requirement is subjective to the pilot's experience. The ergonomics of the pilot have been considered during the design, as explained in section 9.1.2, and therefore this requirement is considered satisfied.		
<b>VER-OPS-11</b>	The pilot shall be able to change positions for takeoff and landing. <sup>D</sup>	Satisfied
In the final Velo-E-Raptor configuration, the pilot is able to change positions between flying and landing or takeoff. This is further explained in section 9.2.2.		
<b>VER-OPS-12</b>	The Velo-E-Raptor power output shall be controllable during flight. <sup>K</sup>	Satisfied
The power output is controllable during flight, as explained in section 5.2.2.		
<b>VER-OPS-13</b>	During cruise the velocity shall be maintainable.	Satisfied
Using the control system to pitch, velocity is maintainable during flight. This is further explained in section 7.3.		
<b>VER-OPS-14</b>	During cruise the altitude shall be maintainable.	Satisfied
Using the control system to pitch, altitude is maintainable during flight. This is further explained in section 7.3.		
<b>VER-CUS-01</b>	The Velo-E-Raptor shall look attractive.	Satisfied
Attractiveness is subjective. The attractiveness of the Velo-E-Raptor has been considered every step of the way, especially for pilot position and control systems. It is the foundation of the Velo-E-Raptor project, and therefore this requirement and its subrequirements are considered satisfied.		
<b>VER-CUS-01.1</b>	The Velo-E-Raptor shall look next-gen.	Satisfied
<b>VER-CUS-01.2</b>	The Velo-E-Raptor shall look cool.	Satisfied
<b>VER-CUS-01.3</b>	The Velo-E-Raptor shall look fast.	Satisfied
<b>VER-CUS-02</b>	The Velo-E-Raptor shall be available for sports usage. <sup>K</sup>	Satisfied
The usage of the Velo-E-Raptor is not restricted by the final configuration. Therefore it can be used for sports usage. The final configuration was chosen with sports usage in mind.		
<b>VER-CUS-03</b>	The Velo-E-Raptor shall be available for recreational usage. <sup>K</sup>	Satisfied
The usage of the Velo-E-Raptor is not restricted by the final configuration. Therefore it can be used for recreational usage. The final configuration was chosen with recreational usage in mind.		
<b>VER-CUS-04</b>	The Velo-E-Raptor shall be partially powered by human power. <sup>D</sup>	Satisfied
The Velo-E-Raptor uses the power generated by the cycling system in two ways: as a throttle input, to determine the output of the propulsion system, and to charge the batteries using a generator. This is further explained in section 5.2.2.		
<b>VER-CUS-05</b>	The Velo-E-Raptor shall have a field of view of 180 degrees on the horizontal plane.	Satisfied
The view of the pilot is not obstructed by anything in the horizontal plane in the final Velo-E-Raptor configuration. The field of view is 360 degrees on the horizontal plane.		

Table 16.1: Compliance matrix, continued

<b>VER-CUS-06</b>	The Velo-E-Raptor shall have a field of view of 110 degrees on the vertical plane.	Satisfied
The view of the pilot is only obstructed by the wing planform in the vertical plane. Therefore, the pilot has at least a view of 180 degrees on the vertical plane.		
<b>VER-CUS-07</b>	The Velo-E-Raptor shall have an intuitive control system. <sup>K</sup>	Satisfied
The ease of use and intuitivity of the control system is considered at every step of the design, and fundamental to the Velo-E-Raptor design. The control system is further explained in section 9.1.4 and section 9.1.5. Even though intuitivity is subjective, this requirement is considered satisfied.		
<b>VER-CUS-08</b>	The Velo-E-Raptor shall be maneuverable enough to perform sharp and quick turns.	Satisfied
The minimum turn radius is 15 meters. For a 360 degree turn, the minimum turn rate is 6.0 seconds. This is further explained in section 5.2.3. These values are comparable to current hang gliders on the market. Even though this requirement is open to interpretation, it is considered satisfied.		
<b>VER-CUS-09</b>	The purchase cost of the Velo-E-Raptor shall not be more than €25,000. <sup>K</sup>	Not Satisfied
The cost of the Velo-E-Raptor is estimated to be €160,266. This is further explained in section 14.3.		
<b>VER-CUS-10</b>	Renting a Velo-E-Raptor shall not be more expensive than €50 per flight excluding club contribution.	Unknown
The cost per flight of the final Velo-E-Raptor could not be estimated at this stage. This is further explained in section 14.3.		
<b>VER-SYS-01</b>	The Velo-E-Raptor shall have some form of navigation system.	Satisfied
Navigation instrumentation will be on board of the Velo-E-Raptor. This is further explained in section 9.1.5.		
<b>VER-SYS-02</b>	The pilot of the Velo-E-Raptor shall be able to communicate with external entities.	Satisfied
A smartphone will be on board of the Velo-E-Raptor for communication. This is further elaborated in section 9.1.5. This means anyone with a smartphone can communicate with the pilot. Therefore the subrequirements are satisfied as well.		
<b>VER-SYS-02.1</b>	Communication with people on the ground shall be possible.	Satisfied
<b>VER-SYS-02.2</b>	Communication with surrounding aircraft shall be possible.	Satisfied
<b>VER-SYS-03</b>	The Velo-E-Raptor shall be able to monitor the energy level of the power subsystem. <sup>K</sup>	Satisfied
A sensor will be present on all batteries, and the flight computer can show the pilot the energy levels. This is further explained in section 9.1.5.		
<b>VER-SYS-03.1</b>	The Velo-E-Raptor shall warn the pilot when the energy level of the power subsystem is low. <sup>K</sup>	Satisfied
A sensor will be present on all batteries, and the flight computer can warn the pilot at a certain power level. This is further explained in section 9.1.5.		
<b>VER-SYS-04</b>	The operator of the Velo-E-Raptor shall be able to see flight data during flight. <sup>K</sup>	Satisfied
A display with flight data will be available, including the parameters given in these subrequirements. This is further explained in section 9.1.5.		
<b>VER-SYS-04.1</b>	The flight data shall contain altitude. <sup>K</sup>	Satisfied
<b>VER-SYS-04.2</b>	The flight data shall contain angle of attack. <sup>K</sup>	Satisfied
<b>VER-SYS-04.3</b>	The flight data shall contain vertical velocity. <sup>K</sup>	Satisfied
<b>VER-SYS-04.4</b>	The flight data shall contain horizontal velocity. <sup>K</sup>	Satisfied



## Conclusion and Recommendations

As described in chapter 1, the Velo-E-Raptor was designed to meet a stringent set of requirements. Following on the technical analysis performed, it became clear that choices had to be made on which requirements were going to be met. The priority was set to the requirements on safety and experience, as these play a crucial role in the overall success of the Velo-E-Raptor. The mission of this Design Synthesis Exercise project: "Design an electrically assisted, human powered and sustainable method of flight that is accessible and safe for entertainment and sports usage" is satisfied.

One main achievement of the design process was the pilot positioning through the wing, which allows for a unique flight experience and attractive design. However, to achieve this in combination with the electrical power amplification, this had consequences for weight and center of gravity location. Furthermore, flaps could not be added due to weight restrictions, which resulted in a higher landing speed. To ensure safety during takeoff and landing, a landing gear was added. Except for the two safety requirements on statistical failures per flight hour, which cannot yet be determined at this stage, all safety requirements have been met. This however resulted in not meeting the regulatory requirements of being a foot-launched aircraft.

Another achievement that was made is the implementation of electrical power amplification, as has not been done before. A custom propeller design combined with a power system that combines human power and stored electric energy, driven by a control system that ensures a safe operation, was successful. Furthermore, inherent static and dynamic stability was reached. The requirements on controllability, stability and ease of operation were met. The addition of elements such as the propellers and landing gear, as well as the pilot positioning, resulted in high drag and therefore not meeting the gliding ratio requirement. Additionally, the noise production of the design was not yet quantified.

Lastly, the design has been made with focus on sustainability and accessibility. Compared to other aircraft, the Velo-E-Raptor performs well on sustainability. With its zero emission, detailed sustainability analysis of materials used, it meets all of the sustainability requirements. The accessibility has been ensured by developing the Velo-E-Raptor for use in sport clubs, where due to centralized acquisition and maintenance the lowest cost and highest reliability can be ensured, while making the sports social and training easily accessible.

The requirements set on the cost of the Velo-E-Raptor have not been met. This is mainly due to high labor cost that are inherent to the RDT&E phase. While the initial cost is still higher than the target cost, a profitable business model can be established in the long run when the Velo-E-Raptor is produced on a bigger scale and total costs are reduced significantly.

A number of recommendations can be made with respect to the design. Difficulties that arose in the design process were for a large part due to the pilot integration in the wing, which complicated the analysis process for aerodynamics as well as stability and control. Access to a wind tunnel to perform tests on interference and stability is therefore advisable, which can also be used to determine deformation, noise and flutter characteristics that were not yet quantified. Furthermore, additional design optimization to reduce weight, increase the gliding ratio and decrease noise is advised. Moreover, an autopilot should be designed to increase safety even further. A detailed overview of the advised post DSE activities can be found in appendix A.

# Bibliography

- [1] AGARD. Landing gear design loads. *North Atlantic Treaty Organization*, 1991.
- [2] Stoll A.M. Design of quiet uav propellers. Technical report, Stanford University, 2012.
- [3] Borst C. Display design principles. TU Delft AE4316 Aerospace Human-Machine Systems.
- [4] Brown D. and Ollerhead J.B. Propeller noise at low tip speeds. Technical report, Wyle Labaraties, 1971.
- [5] Johnson D. A flight test evaluation of the as-w22, April 1983.
- [6] Van der Velden W.C.P. and Oerlemans S. Numerical analysis of noise reduction mechanisms improved trailing edge serrations using the Lattice Boltzmann method. *AIAA 2017-1379*, 2017.
- [7] Wilson D.G. *Bicycling science*, 2004.
- [8] Wood D.H. Full-scale tests of metal propellers at high tip speeds. Technical report, National Advisory Committee for Aeronautics, 1931.
- [9] Raymer D.P. *Aircraft Design: A Conceptual Approach*. American Institute of Aeronautics and Astronautics, 1992.
- [10] Carrera E. and Cosatto C. Flight mechanics analysis of a motorized trike with composite wing. *Journal of Aerospace Engineering*, October 2010.
- [11] Gonzalez Garcia E. and Becker J. Uav stability derivatives estimation for hardware-in-the-loop simulation of piccolo autopilot by qualitative flight testing. *AeroDreams*, page 8. <http://www.aerodreams-uav.com/docs/aeroduav-conf.pdf>.
- [12] Torenbeek E. *Synthesis of Subsonic Airplane Design*. Delft University Press, Delft, 1982.
- [13] Van Kampen E. *AE4301 - Automatic Flight Control System Design*. TU Delft, October 2016.
- [14] Kilkenny E.A. Full scale wind tunnel tests on hang glider pilots. Technical report, Cranfield Institute of Technology, UK, 1984.
- [15] Hartman E.P. and Biermann D. The aerodynamic characteristics of full-scale propellers having 2, 3 and 4 blades of clark y and r. a. f. 6 airfoil sections. Technical report, NACA, 1938.
- [16] Chami M. et al. Safe li-ion technology for micro and mild hybrid application based on cea bipolar lfp/lto technology. *World Electric Vehicle Journal*, Vol. 3, .

- [17] Coiro D.P. et al. Improving hang-glider maneuverability using multiple winglets. *AIAA*, Vol. 45, No. 3, .
- [18] De Marqui C. et al. Identification of flutter parameters for a wing model. Technical report, Brazilian Society of Mechanical Sciences and Engineering, 2006.
- [19] Drela M. et al. Athena vortex lattice 3.36 user primer, 2017.
- [20] Griffith E.D. et al. Low noise propeller technology demonstration. Technical report, Lockheed-California Company, 1974.
- [21] Hamann R.J. et al. Systems engineering and technical management techniques, 2006.
- [22] Jackson P. et al. *Jane's All the World's Aircraft*. Jane's Information Group., 2016.
- [23] James G. et al. Numerical validation of the squire–young formula for profile-drag prediction. *Journal of Aircraft*, 52, 2015, p. 948-955, .
- [24] Kenneth J. et al. Digital fly-by-wire flight control validation experience. Technical Memorandum 72860, NASA, National Aeronautics and Space Administration, 1978.
- [25] Lyon C.A. et al. Summary of low speed airfoil data. Technical report, University of Illinois, 1997.
- [26] Manzo M.A. et al. Nasa aerospace flight battery program. Technical report, NASA, 2010.
- [27] Mariens J. et al. Quasi-three-dimensional aerodynamic solver for multidisciplinary design optimization of lifting surfaces. *Journal of Aircraft*, March 2014, .
- [28] Melkert J.A. et al. Propulsion & power - ae2230-ii, 2016.
- [29] Mialon B. et al. Validation of numerical prediction of dynamic derivatives: two test cases, 2011. [http://www.cerfacs.fr/cfdbib/repository/TR\\_CFD\\_11\\_87.pdf](http://www.cerfacs.fr/cfdbib/repository/TR_CFD_11_87.pdf).
- [30] Mulder J.A. et al. *Flight Dynamics*. TU Delft, March 2013.
- [31] Reichert M. et al. Lithium-ion cell nail penetration safety experiments under adiabatic conditions. Technical report, MEET Battery Research Center, Muenster, Germany, 2014.
- [32] Smith R.H.P. et al. Flight trials of the prone position meteor. Final report of Flying personnel research committee of the Royal Air Force Institute of Aviation Medicine, november 1955.
- [33] Sriramulu S. et al. The relationship of the nail penetration test to safety of li-ion cells. Technical report, TIAX LLC, Lexington, MA, 2012.
- [34] Stoll A.M. et al. Drag reduction through distributed electric propulsion. Technical report, American Institute of Aeronautics and Astronautics, 2014.
- [35] Vos R. et al. Aerospace design and systems engineering elements i – ae1222-ii, 2017.

- [36] Von Hermann F. Prone flying. *Sailplane and glider*, 20(6):5–7, 1952.
- [37] McCullough G.B. and Gault D.E. Examples of three representative types of airfoil-section stall at low speed. Technical report, National Advisory Committee for Aeronautics, 1951.
- [38] Ruijgrok G.J.J. *Elements of airplane performance*. 2013.
- [39] Massaro G.M. Multi-disciplinary design of a high aspect ratio, gravity control hang glider with aero elastically enhanced manoeuvrability. *International Congress of the Aeronautical Sciences (ICAS)*, 2000.
- [40] TU Delft Group 08 DSE Spring 2017. Baseline report velo-e-raptor, 2017.
- [41] TU Delft Group 08 DSE Spring 2017. Midterm report velo-e-raptor, 2017.
- [42] Hubbart H.H. Aeroacoustics of flight vehicles theory and practice. Technical report, NASA, 1991.
- [43] Abbott I.H. and Von Doenhoff A.E. *Theory of wing sections*. Dover Publications, Inc., 1959.
- [44] Goldmann J. Human capabilities in the prone and supine positions: an annotated bibliography. Special bibliography performed by Lockheed Missiles and Aerospace company, may 1962.
- [45] McIver J. 2015-16 centralized study on availability of recycling for beverage containers. Technical report, RRS, Moore Recycling Associates Inc., 2016.
- [46] Sloan J. Composites 101: Fibers and resins. *CompositesWorld*, 2016.
- [47] Zhang J. *Different surface treatments of carbon fibers and their influence on the interfacial properties of carbon fiber/epoxy composites*. PhD thesis, ÉCOLE CENTRALE PARIS, September 2015.
- [48] Anderson J.D. *Fundamentals of Aerodynamics, second edition*. McGraw-Hill, Inc., 1991.
- [49] Marte J.E. A review of aerodynamic noise from propellers, rotors, and lift fans. Technical report, California Institute of Technology, 1970.
- [50] Van Ingen J.L. The  $e^N$  method for transition prediction. Historical review of work at TU Delft. AIAA, 2008-3830.
- [51] Gaines L. The future of automotive lithium-ion battery recycling: Charting a sustainable course. *Elsevier*, 1-2:2–7, 2014.
- [52] Veldhuis L.L.M. Review of propeller-wing aerodynamic interference. *International Congress of the Aeronautical Sciences (ICAS)*, 2004.
- [53] Drela M. Xfoil: An analysis and design system for low Reynolds number airfoils. Technical report, University of Notre Dame, 1989.

- [54] Drela M. Xfoil 6.9 user primer, 2001.
- [55] Drela M. and Gilles M.B. Viscous-inviscid analysis of transonic and low reynolds number airfoils. *AIAA*, 25.
- [56] Sadraey M. *Aircraft Performance: Analysis*. VDM Verlag Dr. Müller, Nashua, New Hampshire, USA, 2009.
- [57] Maughmer M.D. The design of winglets for low-speed aircraft. Technical report, Pennsylvania State University, 2001.
- [58] Hansen M.O.L. *Aerodynamics of Wind Turbines*. Earthscan, 2008.
- [59] Howe M.S. Aerodynamic noise of a serrated trailing edge. *Journal of Fluids and Structures* 5, 1991.
- [60] Heerens N.C. Landing gear design in an automated design environment. Master of science thesis, TU Delft, March 2014.
- [61] NOAA. *U.S. Standard Atmosphere, 1976*. U.S. Government Printing Office, Washington D.C., 1976.
- [62] Dees P. Hang glider design and performance. *AIAA*, September 2010.
- [63] Dorman P. Study of the aerodynamics of a small uav using avl software, April 2006. <https://www.scribd.com/document/102823675/AVL-Report>.
- [64] Fink R. *USAF Stability and Control DATCOM*. McDonnell Douglas Corporation, October 1960.
- [65] Nelson R.C. *Flight Stability And Automatic Control*. WCB McGraw-Hill, second edition edition, 1998.
- [66] Hoerner S.F. *Fluid-Dynamic Drag*. Vancouver, Washington, USA, 1965.
- [67] Hoerner S.F. *Fluid-Dynamic Lift*. New York City, USA, 1975.
- [68] Megson T.H.G. *Aircraft Structures for Engineering Students*. Elsevier Aerospace Engineering Series, 2007.
- [69] Kim T.Y. Reduction of tonal propeller noise by means of uneven blade spacing. Technical report, University of California, 2016.
- [70] Cook M. V. and Spottiswoode M. Modelling the flight dynamics of the hang glider. *The Aeronautical Journal*, page 20, January 2006.
- [71] van Gelder J. et al. Simulation of the dynamic behaviour of cessna citation ii, March 2017.
- [72] Štorch V. et al. Measurement of noise and its correlation to performance and geometry of small aircraft propellers. Technical report, Faculty of Mechanical Engineering, CTU, Prague, Czech Republic, 2016.

# A: Project Design and Development Logic

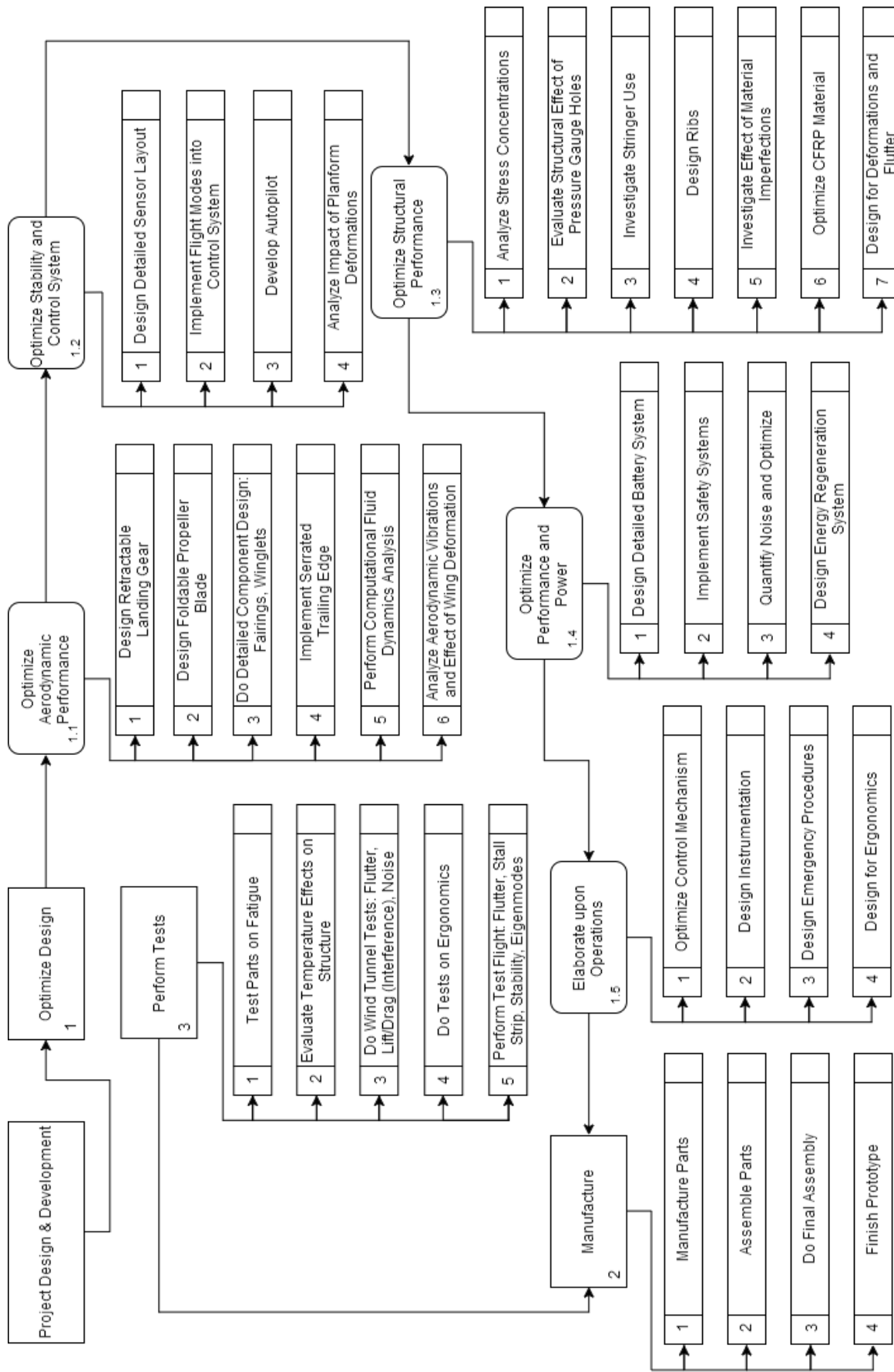


Figure A.1: The Project Schematic Project Design & Development

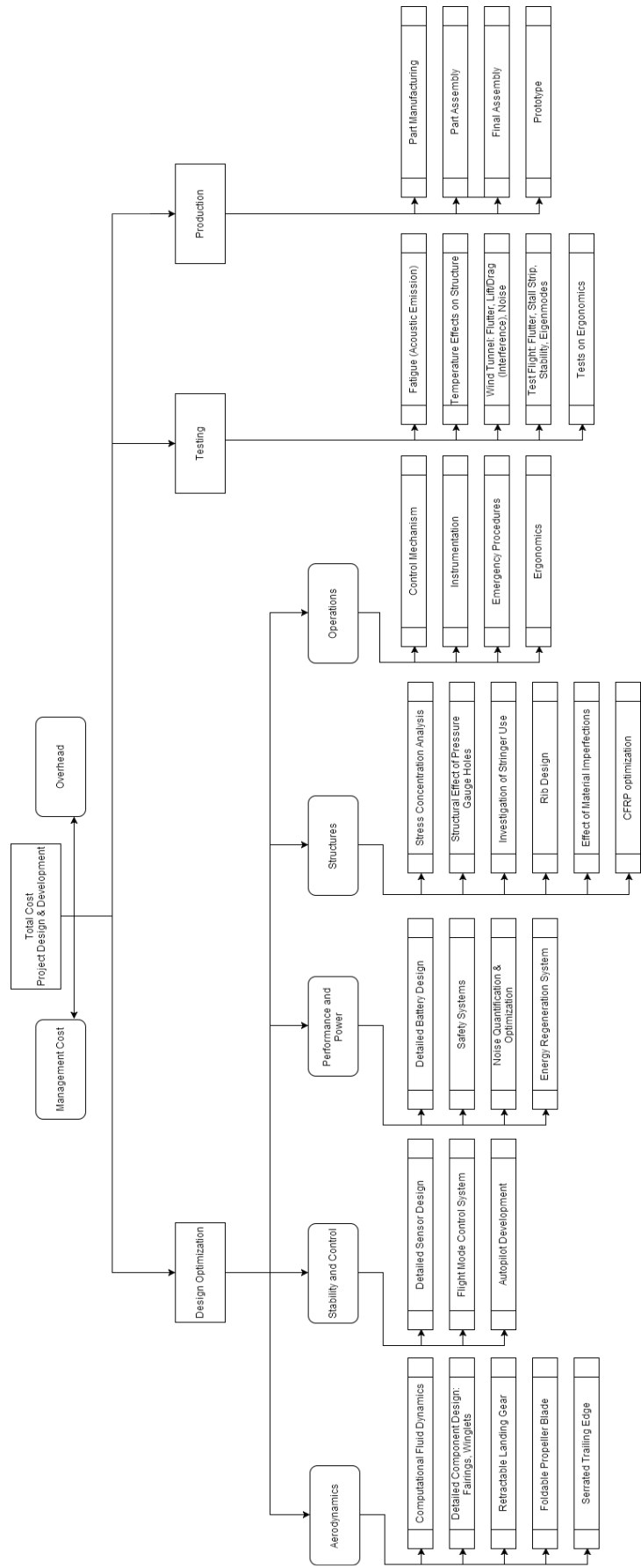


Figure A.2: The Project Design & Development Cost Breakdown Structure

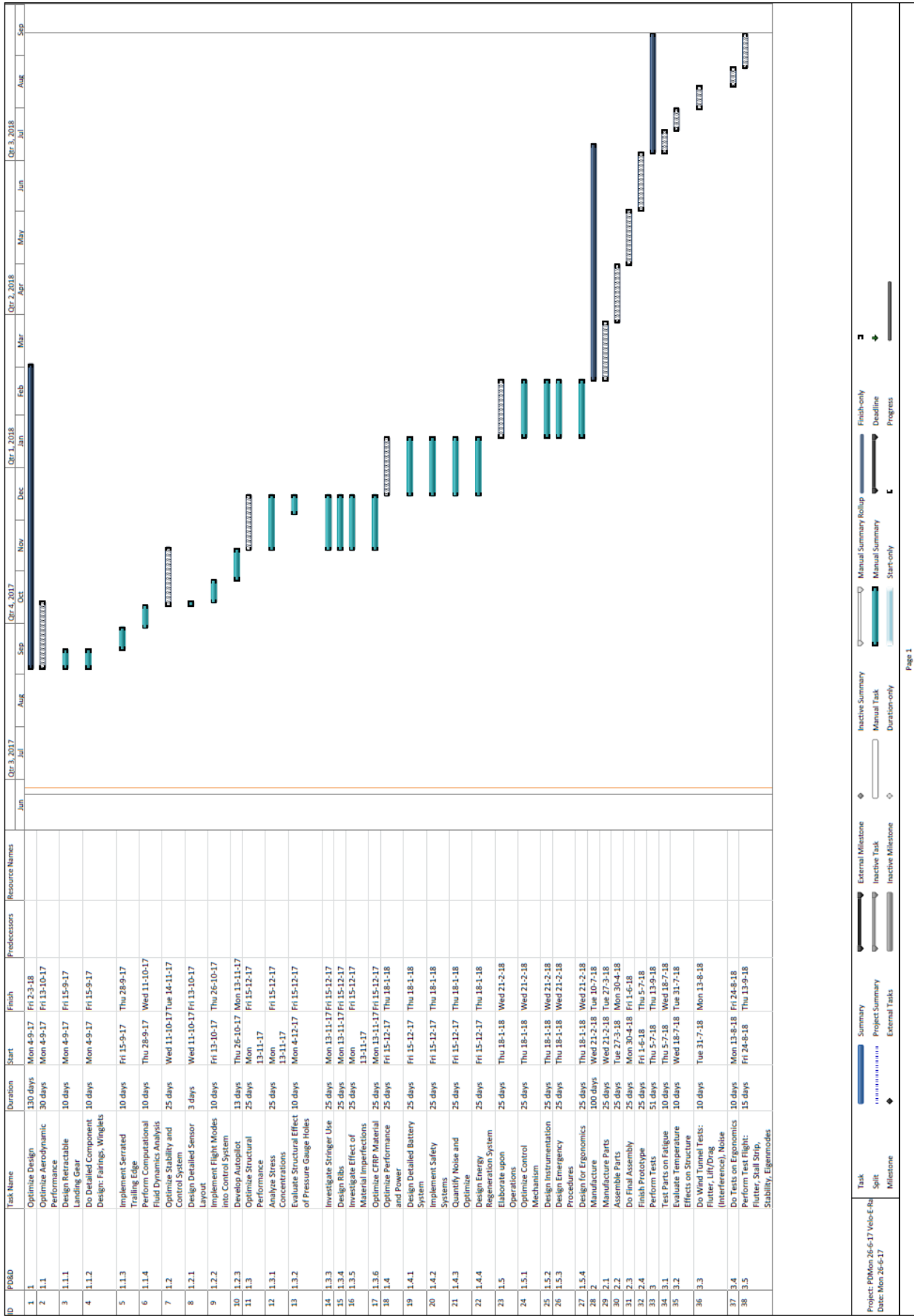


Figure A.3: The Project Development Gantt chart

# B: Failure Mode Effect & Criticality Analysis

function ID	Function	failure ID	Functional failure	Failure effect	failure cause ID	Failure Cause	Mitigation	Probability	Severity
	The normal characteristic action of the function		How the item failed to perform its function	What is the result of the functional failure		Why the functional failure occurs	Compensating provisions		
<b>Structural functions</b>									
1	Attachment of pilot to aircraft by means of the harness	1	Pilot not fully attached to aircraft	Pilot can fall out of the aircraft causing (fatal) injuries to pilot Weight of the aircraft not distributed evenly over body causing injuries Aircraft touches the ground at takeoff or landing causing damage to aircraft	1.1	Structural failure of equipment (clasps or straps)	Landing gears designed such that pilot does not necessarily need to carry weigh of the aircraft. Attached with 4 clasps and 4 straps for redundancy	C	1
					1.2	Not attached properly due to inattention of the pilot	Attachments double checked: by pilot and operator	D	1
2	Front landing gears prevent propellor to touch ground	2	Landing gears fails to prevent propellor touching the ground	Propellor hits the ground causing damage or failure of the propellor	2.1	Structural failure during landing	Safety margin used on design of landing gears	D	3
3	Wing provides lift	3	Wing not able to produce enough lift to lift weight of the aircraft	Aircraft starts losing height If lift not restored, crashes into the ground causing (fatal) injuries and damage to aircraft	2.1	Wing skin rips	Wing skin spanned compartmentwise between spars	C	2
					3.2	Airfoil shape changes	Stringers added at trailing and leading edge. Also Rib spacing was decreases	A	1
					3.3	Structural damage	Safety factor used to ensure structural safety. Maintenance prescription	E	4
					3.3	Aircraft exceeds stall angle	Flight envelope protection prevents aircraft from stalling (see 12)		
<b>Power and Propulsion system</b>									
4	Engines drive propellers	4A	Both engines fail to provide power	Aircraft cannot maintain height without the use of thermals	4.1	Battery failure (see 6)	If one engine fails, the other will automatically be switched off	E	2
		4B	One engine fails to provide power	Yawing moment induced on aircraft	4.2	Short circuit in power system	Rudder can compensate for Yawing moment partly, but not known what the exact effects will be	D	3
5	Propellers provides thrust	5	Propellers provide no or less thrust due to damage	Damaged propellor can injure pilot No thrust provided (see 4) Propellor becomes unbalanced inducing vibrations and unsymmetrical thrust (this effect should be investigated further)	5.1	Blades break due to structural failure	Periodic inspection	D	3
					5.2	Loose bolts and nuts due to vibrations and temperature changes	Periodic inspection	A	2
					5.3	Bird strike	Pilot wearing protective clothing	B	3
					5.4	Structural damage due to crosswind		C	2
					5.5	No power provided (see 4)			
6	Batteries provide power for engine	6a	Battery fails to provide power	Engine does not work (see 2)	6a.1	Short circuit due to overheating cables	Test when system gets overloaded	E	2
					6a.2	Short circuit due to water damage	Seal electrical system to make it watertight	D	2
					6a.3	Short circuit due to damage of cables	Periodic maintenance	E	2
					6a.4	Battery drainend	Test battery charging before flight Indicate battery level during flight	B	2
		6b	Battery caught fire and explodes	Explosion can cause severe injuries to pilot and damage to the aircraft	6b.1	Battery overpowered during full power flight	Test if batteries do not get overloaded when all systems are used at full power settings	E	4
					6b.2	Battery overcharged	Always use compatible battery charger	E	2
					6b.3	Battery damages due to crash		E	4
7	Batteries provide power for control system	7	Battery fails to provide power (10A4)	Control system fails (see 10)	7.1				
8	Pedal system charges battery	8	Pedal system does not charge battery while pedalling	No additional battery power gained to extend flight time	8.1	Dynamo fails	Not a problem since additional power due to pedalling is insignificant with respect to battery power	C	1
9	Pedal system provides input for throttle control	9	Throttle can not be controlled by pedal system	No throttle control if no other control sysem is available	8.1	Sensor fails	Throttle can be controlled with other control system, located at control stick	C	1
<b>Control system</b>									
10	FBW converts pilot input to control surface deflections	10a	FBW fails to move control surfaces	Aircraft becomes uncontrollable	10a.1	Actuator fails	Redundant actuators present	E	4
					10a.2	Sensor fails	Redundant sensors present	E	4
					10a.3	Flight computer fails	Redundant flight computer present	E	4
					10a.4	Cables are damaged	Redundant cables present	D	3
					10a.5	Battery of control system empty	FBW connected to propulsion batteries for redundancy	E	4
		10b	FBW does not give desired control surface deflection	Aircraft is difficult to control / uncontrollable	10b.1	Computer not callibrated correctly	Periodic maintenance	D	3
11	FBW provides forced feedback to ease flying	11	No forced feedback given	Aircraft is difficult to control	11.1	Forced feedback actuator fails	Forced feedback failure indicator	C	1
12	Flight envelope protector prevents aircraft to exceed flight envelope limitations	12a	Control systems fails to convert input from flight computer to control surface deflection	See 10a					
		12b	Sensors give faulty or no input to flight envelope protection system	Flight conditions can not be determined correctly leading to incorrect corrective measurements Aircraft can exceeds flight envelope limitations	12b.1	Sensor failure	Redundant sensors present Flight envelope protection shall be switched off if all sensors fail	D	3
		12c	Warning system that aircraft enters limits does not work	Pilot is not aware of entering dangeres flying conditions	12c.1	Earplug failure		C	1
<b>Flight instrumentation</b>									
13	Head-Up-Display shows data	13a	Sensors provide wrong feedback	Flight conditions can not be determined correctly Pilot makes wrong decision based on faulty information	13a.1	Sensor failure	Redundant sensors present	E	3
		13b	HUD gives no feedback	Pilot needs to fly without help of flight instruments	13b.1	Battery empty	HUD Battery checked before flight	D	2
					13b.2	HUD failure		E	3
					13b.3	Flight computer failure	See 10a.3		
14	Communication	14a	The transponder does not work correctly	Air Traffic Control cannot determine the Velo-E-Raptor's location	14a.1	Transponder failure	Periodic maintenance	E	1
		14b	The emergency signal EPRIB fails	No update given on emergency condition	14b.1	EPRIB failure	Periodic maintenance	E	2

